

C165 kpr. 11

PL ISSN 0028-3894



ASSOCIATION OF POLISH
NEUROPATHOLOGISTS

and

MEDICAL RESEARCH CENTRE,
POLISH ACADEMY OF SCIENCES

NEUROPATHOLOGIA POLSKA

VOLUME 29

1991

NUMBER 3-4

WROCLAW · WARSZAWA · KRAKÓW
ZAKŁAD NARODOWY IM. OSSOLIŃSKICH
WYDAWNICTWO POLSKIEJ AKADEMII NAUK

<http://rcin.org.pl>

NEUROPATHOLOGIA POLSKA

QUARTERLY

VOLUME 29

1991

NUMBER 3-4

EDITORIAL COUNCIL

Maria Dąbbska, Jerzy Dymecki, Krystyna Honczarenko, Danuta
Maślińska, Mirosław J. Mossakowski, Halina Weinrauder

EDITORS

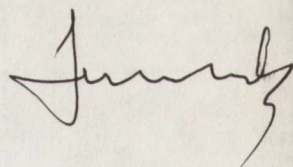
Editor-in-Chief: Irmina B. Zelman
Co-editors: Wiesława Biczyskova, Halina Kroh, Mirosław J. Mossakowski, Mieczysław Wender
Secretary: Anna Taraszewska
Technical Secretary: Teresa Miodowska

EDITORIAL OFFICE

Medical Research Centre
Dworkowa 3, 00-784 Warszawa, Poland, Phone: 49-54-10

The typescript of the present issue was delivered to the publisher 25.06.1991

Zakład Narodowy im. Ossolińskich — Wydawnictwo. Wrocław 1992.
Objętość: ark. wyd. 7,40; ark. druk. 6,75; ark. A₁ -9.
Wrocławska Drukarnia Naukowa. Zam. 1257/91.



EWA SAWICKA, UVE P. KETELSEN*

CYTOCHEMISTRY OF MUSCLE Ca^{++} ATPASE IN MUSCULAR DYSTROPHY

Department of Neurology, School of Medicine, Warsaw; Neuromuscular Unit, Medical Research Centre, Polish Academy of Sciences, Warsaw, Poland; *Department of Pediatric Muscle Diseases, Albert-Ludwigs University, Freiburg, Germany

The ultrastructural picture of Ca^{++} ATPase was examined in muscle biopsies taken from ten cases of Duchenne muscular dystrophy, five cases of limb-girdle muscular dystrophy, four cases of spinal muscular atrophy and four controls. In the Duchenne and in limb-girdle muscular dystrophy a decrease of the reaction product within the terminal cisternae of the sarcoplasmic reticulum (SR), a pronounced reaction of the sarcolemma and T system and an accumulation of the reaction product in the mitochondria were observed. The decreased accumulation of the reaction product within the terminal cisternae of SR seems to suggest a decreased Ca^{++} ATPase activity of SR in the dystrophic muscle, *per se* or due to degradation by Ca^{++} protease. The distinct Ca^{++} ATPase activity of the sarcolemma and T system reflecting an efflux of calcium provides evidence of a high sarcoplasmic calcium level. Possibly, the proliferation of the T system is specifically directed to accelerate the efflux of calcium. In spinal muscular atrophy, an increase in the reaction product accumulation was observed only within the terminal cisternae of SR, probably due to fibrillations in the denervated muscle fibers.

Key words: Duchenne muscular dystrophy, Ca^{++} ATPase, sarcolemma, sarcoplasmic reticulum, T system.

The myofibril damage in muscular dystrophy is probably caused by Ca^{++} -mediated proteases activated by an increased sarcoplasmic calcium (Dayton et al. 1976; Sugita et al. 1980; Pemrick 1981). The excessive calcium level in the sarcoplasm can result in cell death (Duncan 1978, 1987; Schanne et al. 1979). Since Ca^{++} ATPase is responsible for the transport of calcium through the sarcolemma (Malouf, Meissner 1979), the T system (Scales, Sabbadini 1979; Bianchi, Narayan 1982; Hidalgo et al. 1983), sarcoplasmic reticulum (Ikemoto et al. 1968; Meissner 1973) and inner mitochondrial membrane (Lehninger 1970), the cytochemical picture of Ca^{++} ATPase should indicate where precisely the pathology occurs in the calcium transport.

The cytochemical picture of Ca^{++} ATPase was examined in skeletal muscle biopsies taken from Duchenne muscular dystrophy (DMD) and limb-girdle

muscular dystrophy (lgMD) cases. The dystrophic muscle was compared with normal muscle and the muscle in spinal muscular atrophy (SMA).

MATERIAL AND METHODS

Muscle biopsies taken from ten DMD, five lgMD, four SMA and four normal cases provided the material. In all dystrophic cases the electromyography was myopathic and light microscopy revealed a primary myogenic character of the muscle atrophy, in SMA cases the electromyography showed a typical pattern of anterior horn cell lesion and under the light microscope atrophy of grouped muscle fibers was observed.

Quadriceps femoris and biceps brachii muscle biopsies were performed under local anesthesia. These were then: immediately cut into small pieces; incubated either 30 min or 60 min at pH either 7.0 or 9.4 and 37°C in medium containing either 18 mM or 0.1 mM CaCl_2 , 2.7 mM ATP and Iris buffer; rinsed in 0.1 M cacodylate buffer at pH 7.4; fixed 2 hr at pH 7.4 and 4°C in 3% glutaraldehyde; rinsed in 0.1 M cacodylate buffer at pH 7.4; dehydrated in an ethanol and acetone series and Epon-embedded for sectioning of the upper layers of blocks in an ultramicrotome. The ultrathin sections were stained on grids with uranyl acetate and lead citrate. Control muscles were incubated in buffers with or without CaCl_2 and no ATP.

For routine electron microscopy muscle specimens were fixed in 5% glutaraldehyde with 1 hr postfixation in 1% OsO_4 .

RESULTS

The ultrahistochemical pictures of $\text{Ca}^{++}\text{ATPase}$ in normal muscle and in unaffected muscle fibers in dystrophic cases demonstrate: 1) an accumulation of the reaction product within the terminal cisternae of SR, 2) lack of activity within the mitochondria or a slight amount of the reaction product between the inner and the outer membrane and within the cristae, 3) absent or slight activity of the sarcolemma (Figs 1 and 2). A higher concentration of CaCl_2 in the incubation medium and longer time of incubation caused more pronounced accumulation of the reaction product within the mitochondria, excessive sarcomere contraction, dissolution of the Z line and denaturation of the nuclear chromatin. There were no discernible differences in $\text{Ca}^{++}\text{ATPase}$ activities between pH 9.4 and 7.0.

In dystrophic muscle in many muscle fibers an accumulation of the reaction product within the terminal cisternae of SR was decreased, while in the mitochondria it was more visible as compared with normal muscle and muscle in SMA (Figs 3, 4 and 5). The reaction product in the mitochondria was deposited as small particles between the outer and the inner membrane and within the cristae, in the matrix it was visible as granules averaging 30–110 nm in diameter (Figs 3, 4 and 5). The crystalline, i.e. apatite phase of calcium



Fig. 1. Normal quadriceps femoris muscle. Ca^{++} ATPase. Muscle incubated 30 min at pH 9.4 in Tris buffer with Na_2ATP and 0.1 mM CaCl_2 , after incubation fixed in glutaraldehyde (but not osmium tetroxide), stained on grids. The reaction product within the terminal cisternae of SR (arrows) and between the outer and the inner mitochondrial membranes (m). Note absence of activity of the sarcolemma (sl). x 42 000

phosphate, was found only once in the area close to the mitochondria and possibly within the mitochondrial matrix in the muscle incubated for 60 min in medium containing 18 mM CaCl_2 . Routine electron microscopy demonstrated granules within the mitochondrial matrix, resembling calcium phosphate accumulation only once, in a case of IgMD, in muscle fibers rich in mitochondria (Fig. 6). In dystrophic muscle fibers showing the reaction product within the mitochondria, especially in fibers undergoing degeneration,

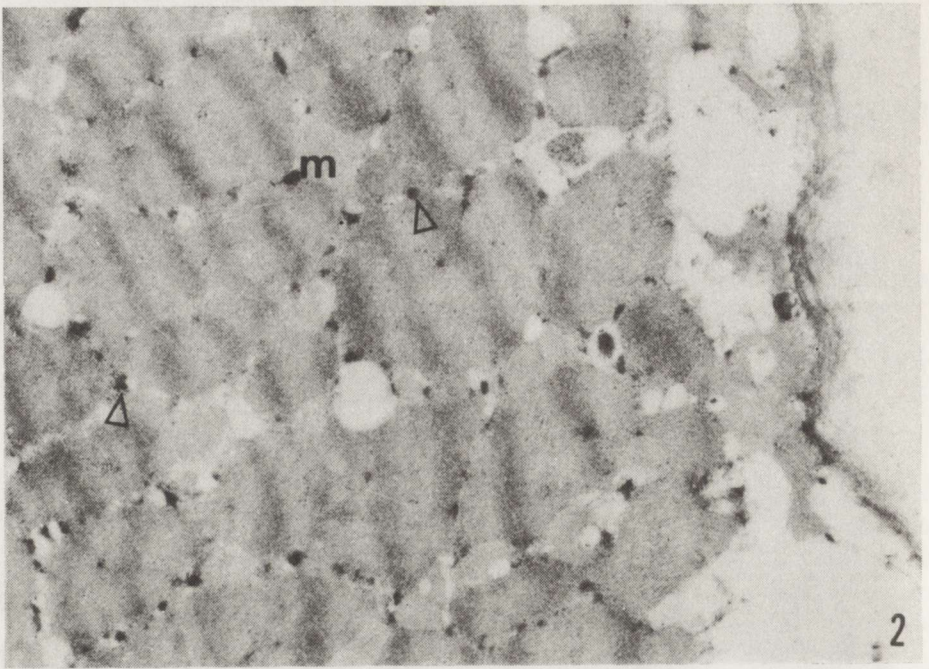


Fig. 2. Normal quadriceps femoris muscle. $\text{Ca}^{++}\text{ATPase}$. Muscle incubated 30 min at pH 7.0 in Tris buffer with Na_2ATP and 0.1 mM CaCl_2 , after incubation fixed in glutaraldehyde (but not osmium tetroxide), stained on grids. The reaction product within SR (arrows). The mitochondria (m) do not show any reaction. x 16 700

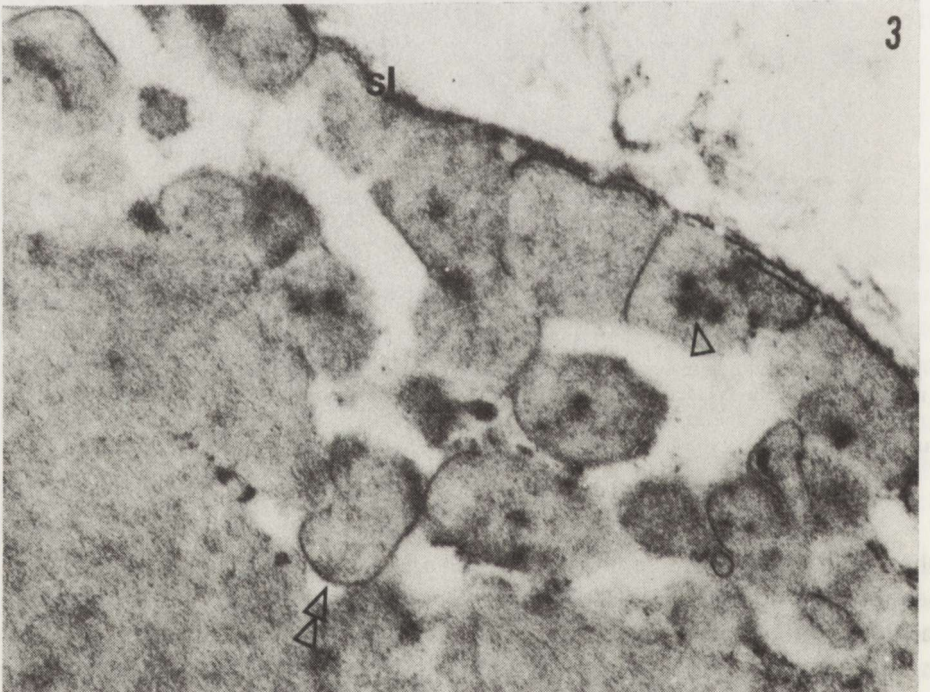


Fig. 3. Duchenne muscular dystrophy. $\text{Ca}^{++}\text{ATPase}$. Quadriceps femoris muscle incubated 60 min at pH 7.0 in Tris buffer with Na_2ATP and 0.1 mM CaCl_2 , after incubation fixed in glutaraldehyde (but not osmium tetroxide), stained on grids. The reaction product within the mitochondrial matrix (arrow) and between the outer and the inner mitochondrial membranes (double arrow). Activity of the sarcolemma (sl). x 42 000

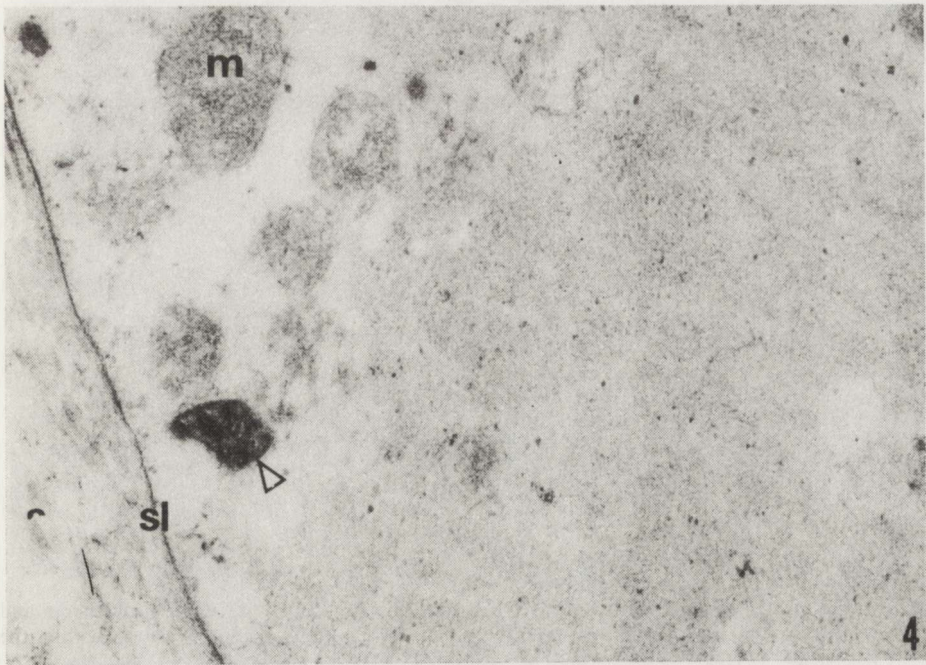


Fig. 4. Duchenne muscular dystrophy. Ca^{++} ATPase. Quadriceps femoris muscle incubated 30 min at pH 9.4 in Tris buffer with Na_2ATP and 18 mM CaCl_2 , after incubation fixed in glutaraldehyde (but not osmium tetroxide), stained on grids. The reaction product visible in some mitochondria (m) only (arrow). Activity of the sarcolemma (sl). x 42 000

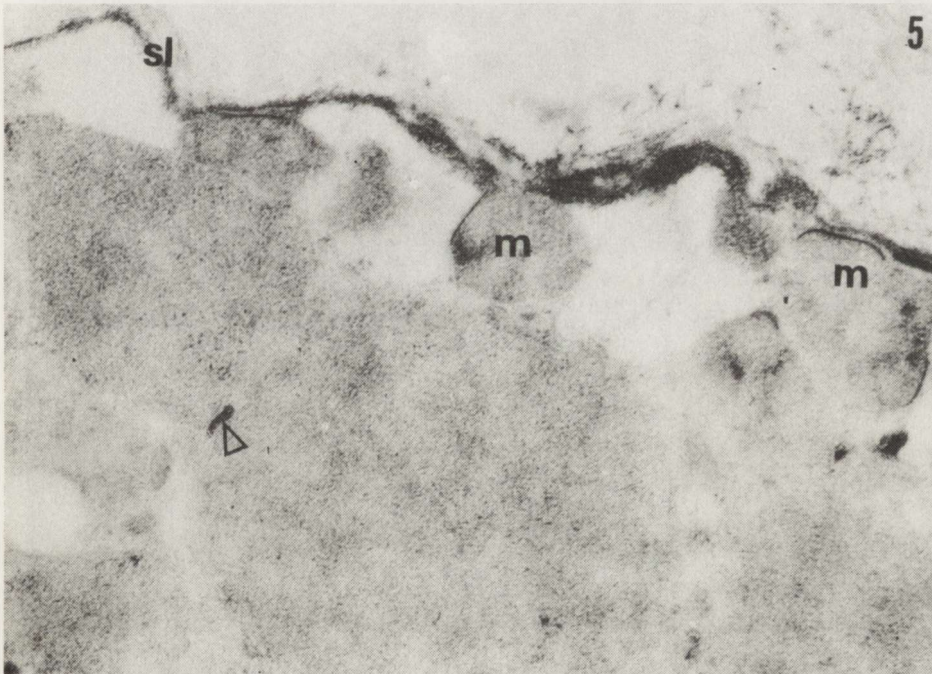


Fig. 5. Duchenne muscular dystrophy. Ca^{++} ATPase. Quadriceps femoris muscle incubated 30 min at pH 9.4 in Tris buffer with Na_2ATP and 0.1 mM CaCl_2 , after incubation fixed in glutaraldehyde (but not osmium tetroxide), stained on grids. Slight accumulation of the reaction product within the mitochondria (m) and SR (arrow). Activity of the sarcolemma (sl). x 42 000

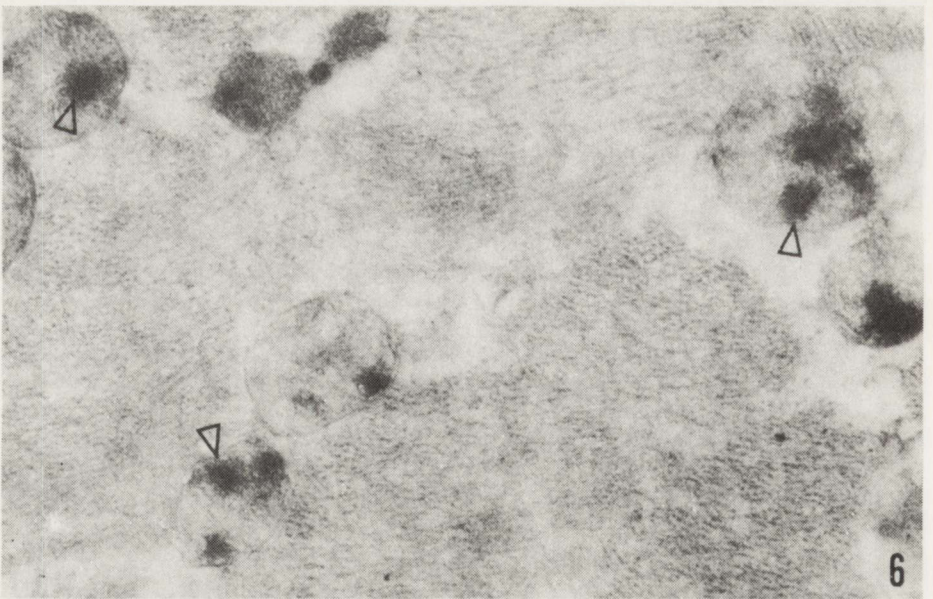


Fig. 6. Limb-girdle muscular dystrophy. Biceps brachii muscle fixed in glutaraldehyde and osmium tetroxide, stained on grids. Intensely electron-opaque granules (arrows) within the mitochondria. x 42 000

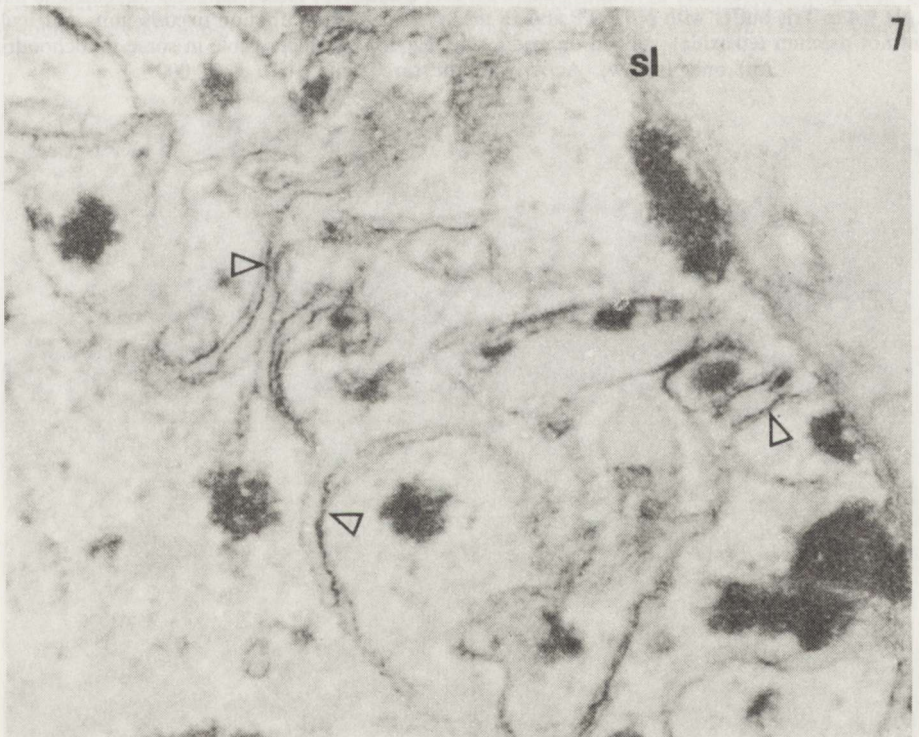


Fig. 7. Duchenne muscular dystrophy. $\text{Ca}^{++}\text{ATPase}$. Quadriceps femoris muscle incubated 30 min at pH 7.0 in Tris buffer with Na_2ATP and 18 mM CaCl_2 , after incubation fixed in glutaraldehyde (but not osmium tetroxide), stained on grids. Irregular whorls of membranes originating possibly from the T system show $\text{Ca}^{++}\text{ATPase}$ activity (arrows). x 48 000

the reaction product was seen also in the sarcolemma (Figs 3, 4 and 5) and sometimes the T system. Irregular whorls of membranes originating probably from the T system and representing Ca^{++} ATPase activity were occasionally observed under the sarcolemma (Fig. 7). A longer incubation time (60 min) and a higher CaCl_2 concentration (18 mM) in the incubation medium resulted in a greater accumulation of the reaction product, especially within the mitochondria, severe sarcomere contraction, Z line clearing and denaturation of the nuclear chromatin. These changes were much more distinct in the dystrophic than in the normal muscle. All the changes observed, particularly

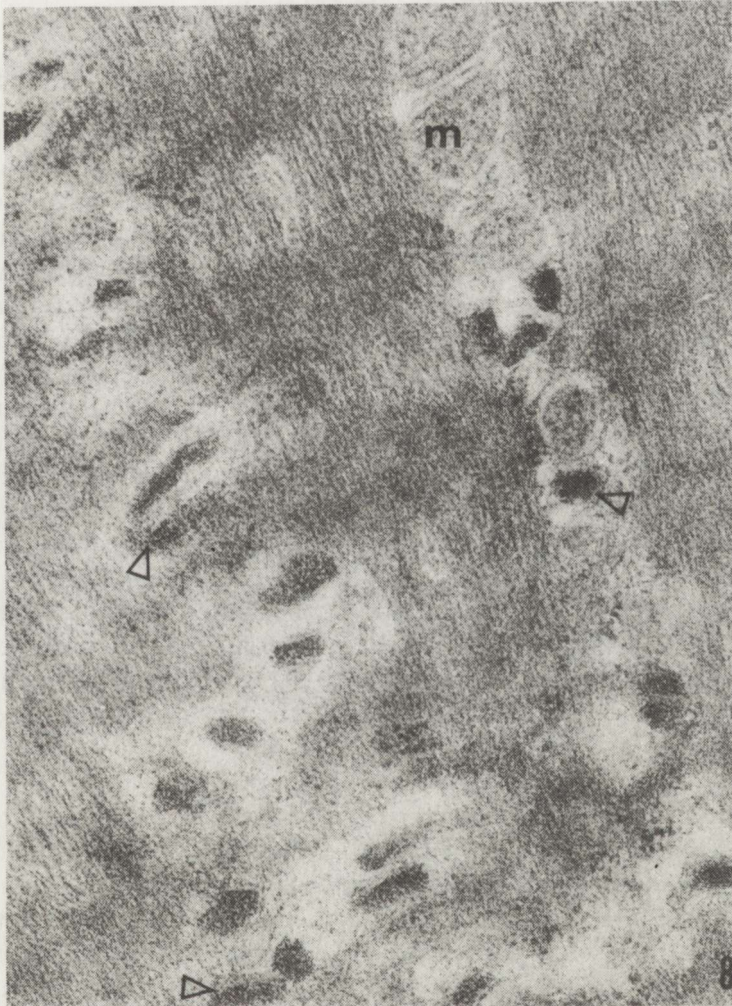


Fig. 8. Spinal muscular atrophy. Ca^{++} ATPase. Quadriceps femoris muscle incubated 30 min at pH 7.0 in Tris buffer with Na_2ATP and 18 mM CaCl_2 , after incubation fixed in glutaraldehyde (but not osmium tetroxide), stained on grids. Abundant SR filled with the reaction product (arrows). The mitochondria (m) do not accumulate any reaction product. x 42 000

a decrease in the reaction product accumulation within the terminal cisternae of SR, were more intense in DMD than in limb-girdle dystrophy.

The ultrahistochemical picture of $\text{Ca}^{++}\text{ATPase}$ in SMA was different, as a higher or at least normal reaction product accumulation within the terminal cisternae of SR and no reaction of the mitochondria and sarcolemma were observed (Fig. 8).

In controls, i.e. muscles incubated in buffers with or without CaCl_2 and no ATP, the reaction pattern although essentially the same, was clearly less well expressed and involved fewer of the ultrastructural elements concerned. Without the substrate, the reaction product was more in evidence than without both the substrate and calcium.

DISCUSSION

Calcium phosphate precipitate as a product of $\text{Ca}^{++}\text{ATPase}$ activity is believed to point to localization of the enzyme activity. Glutaraldehyde fixation alone without osmium postfixation made the electron-opaque reaction product appear against a background of a less electron-dense membrane. The distinct ultrastructural differences between the muscle incubated with ATP and CaCl_2 and the control specimens seem to indicate that the observed intensely electron-opaque material is a product of this very reaction (Sawicka 1977).

Muscle was incubated at pH 9.4 according to the histochemical myofibrillar ATPase Padykula-Herman method (1955) adopted for electron microscopy (Vye et al. 1969; Sawicka 1977, 1978). Since alkaline pH causes calcium release from SR (Dawson 1982) and its accumulation in the mitochondria (Lehninger 1970), the results of this incubation were compared with incubation at pH 7.0. The cytochemical differences between both pH of incubation were not discernible.

Different concentrations of CaCl_2 in the incubation medium (18 mM and 0.1 mM), and different periods of incubation (30 min and 60 min), were used to show the ultrastructural reaction due to a higher calcium concentration. More prominent sarcomere contraction, greater accumulation of calcium in the mitochondria and also clearing of the Z line and denaturation of the nuclear chromatin were observed after 60 min incubation with 18 mM CaCl_2 , this being in agreement with previous reports on the high calcium level resulting in troponin (Bush et al. 1972; Reville et al. 1976) and DNA (Darzynkiewicz et al. 1976) denaturation. The degree of the changes observed due to a higher concentration of calcium in the incubation medium was more distinct in dystrophic than in normal and atrophic muscle. These findings suggest that the plasma membrane of a dystrophic muscle fiber is less resistant to the damaging effect of a high concentration of extracellular calcium with a resulting increase in calcium influx. A high calcium level in the incubation medium under normal conditions affects first of all the calcium concentration in the basement membrane (Borle 1968). Thus, the cytochemical picture observed in dystrophic

muscle seems to be due to its basement membrane pathology. Heparan sulfate proteoglycan appearing in the basement membrane due to many anionic sites ready to form the loose link with Ca^{++} (Kanwar, Farquar 1979; Heathcote, Grant 1981) plays a crucial role in calcium filtration through the sarcolemma. We have not found any reports on heparan sulfate proteoglycan content in the dystrophic muscle basement membrane.

Distinct differences between Ca^{++} ATPase cytochemical pictures in DMD, SMA and normal muscle were observed. In DMD in many muscle fibers the reaction product accumulation was decreased within the terminal cisternae of SR, while it increased in the mitochondria, sarcolemma and T system.

Calcium accumulates to a lesser degree or does not accumulate at all in the terminal cisternae of SR in a dystrophic muscle fiber. This finding is consistent with stereological analysis of SR in dystrophic muscle indicating its decrease (Crowe, Baskin 1979; Watkins, Cullen 1987) as well as with many biochemical data in DMD (Rowland 1980) and experimental MD (Scales, Sabbadini 1979; Mrak 1984). Nevertheless, there are also abundant biochemical data indicating normal Ca^{++} ATPase activity of SR in DMD (Sugita et al. 1966) and experimental MD (Scales et al. 1977; Neymark et al. 1980), or normal Ca^{++} ATPase activity of SR but a decreased ability of calcium to accumulate within SR (Verjovski-Almeida, Inesi 1979). The inconsistent findings were probably due to the inability to isolate the T system from a microsomal fraction. It is also necessary to note that a rise in sarcoplasmic calcium above physiological levels can cause a further Ca^{++} -induced release of Ca^{++} from the SR (Duncan 1978). Nagy and Samaha (1986) found that a decrease in Ca^{++} ATPase of SR was due to the degrading effect of Ca^{++} -activated neutral protease being increased in DMD. In muscle fibers in SMA, an increase in the reaction product accumulation was observed only within the terminal cisternae of SR, probably due to fibrillations in denervated muscle and SR proliferation (Muscatello et al. 1965; Salvatori et al. 1989).

A distinct Ca^{++} ATPase activity of the sarcolemma and T system reflecting an efflux of calcium provides evidence of a high sarcoplasmic calcium level. This is consistent with the data concerning high muscle calcium in DMD (Bertorini et al. 1982) and increased Ca^{++} ATPase of the sarcolemma (Malouf et al. 1981) and the T system (Scales, Sabbadini 1979; Mrak 1984) in experimental dystrophy, although the Ca^{++} ATPase of the sarcolemma in DMD has been found to diverge (Rowland 1980). It seems possible that the proliferation of the T system, observed by us in DMD and earlier described in experimental dystrophy (Malouf, Sommer 1976; Costello, Shafiq 1979; Crowe, Baskin 1979), is specifically directed to accelerate an efflux of calcium. The same could hypothetically occur during muscle fiber splitting, consisting in a division of muscle fiber by proliferating invaginations of the sarcolemma and T system (Sawicka 1988).

Calcium accumulation in the mitochondrial matrix is also evidence of a high sarcoplasmic calcium level, since the mitochondria are forced to

accumulate calcium, when other mechanisms, e.g. calcium accumulation in SR, are for some reason ineffective (Bygrave 1978). The accumulation of calcium in the mitochondria seen only occasionally on routine examination of dystrophic muscle biopsies seems to be due to a low energy-pool of substrates in dystrophic muscle (Stengel-Rutkowski, Barhelmai 1973). Incubation in a medium containing ATP shows the ability of some mitochondria to accumulate calcium and sometimes even release it as hydroxyapatite (Lehninger 1970). The question remains whether the low energy-pool in dystrophic muscle is due to the demands activating different ways of calcium transport or if it results from pathology of the mitochondria themselves (Wrogeman et al. 1973; Scholte, Bush 1980). It is also possible that both factors are implicated.

Thus, a low accumulation of calcium within SR in a dystrophic muscle fiber suggests a decrease in $\text{Ca}^{++}\text{ATPase}$ of SR, *per se* or due to degradation by Ca^{++} protease (Nagy, Samaha 1986). The calcium cannot be stored in the mitochondria because of the low energy pool. The efflux of calcium via $\text{Ca}^{++}\text{ATPase}$ of the sarcolemma and the T system seems to be insufficient. An activation of Ca^{++} proteases, in both the cytoplasm (Nagy, Samaha 1986) and the sarcolemma (Dayton, Schollmeyer 1981; Jackson et al. 1984), may accelerate the calcium-induced cell death (Duncan 1987). Our results do not quite square with the electron-microscopic results of Oberc and Engel (1977) obtained using the calcium pyroantimonate precipitate method. They found that calcium in degenerated muscle fibers accumulated in the mitochondria, SR, nuclei and myofilaments independently of the character of the disease. It remains an open question whether prolonged fixation used in their method increases the plasma membrane permeability and influx of calcium from the extracellular space.

The results of our analysis explain the similarity of the histopathological pictures in DMD and limb-girdle MD rather than elucidate the pathogenesis of DMD. It is believed now that the lack of dystrophin, the protein localized in the sarcolemma and/or triads (Hoffman et al. 1987; Bonilla et al. 1988), i.e. structures responsible for calcium homeostasis, can result in pathological influx of calcium.

Acknowledgement: The author gratefully acknowledge Professors I. Hausmanowa-Petrusewicz and J. Groniowski for critical evaluation of data.

OBRAZ ULTRASTRUKTURALNY $\text{Ca}^{++}\text{ATPAZY}$ W MIĘŚNIU SZKIELETOWYM W POSTĘPUJĄCEJ DYSTROFII MIĘŚNIOWEJ

Streszczenie

Obraz ultrastrukturalny $\text{Ca}^{++}\text{ATPAzy}$ oceniano w biopsjach mięśniowych pobranych w 10 przypadkach postępującej dystrofii mięśniowej (pdm) typu Duchenne, 5 przypadkach pdm typu dwuobrczowego, 4 przypadkach rdzeniowego zaniku mięśni (rdzmm) i 4 mięśniach zdrowych. W pdm stwierdzono zmniejszenie odkładania produktu reakcji w obrębie cystern końcowych siatki sarkoplazmatycznej, wyraźniejszą reakcję sarkolemy i systemu T i zwiększenie odkładania

produktu reakcji w mitochondriach. Zmniejszone gromadzenie produktu reakcji w cysternach końcowych siatki sarkoplazmatycznej w pdm świadczy o obniżonej aktywności Ca^{++} ATPazy siatki sarkoplazmatycznej dystroficznego włókna mięśniowego, aczkolwiek nie można wyłączyć możliwości, że została ona zniszczona przez aktywowaną wysokim stężeniem wapnia Ca^{++} proteazę. Obecność produktu reakcji w sarkolemii i systemie T dystroficznego włókna mięśniowego świadczy o nadmiernie wysokim poziomie wapnia w sarkoplazmie i o konieczności usuwania go z komórki drogą Ca^{++} ATPazy systemu T i sarkolemy. Wydaje się prawdopodobne, że obserwowana w pdm proliferacja systemu T jest celowym działaniem komórki umożliwiającym szybszy odpływ wapnia do przestrzeni pozakomórkowej. W rdzmm obserwowano jedynie zwiększone gromadzenie produktu reakcji w cysternach końcowych siatki sarkoplazmatycznej spowodowane zapewne fibrylacjami odnerwionego mięśnia.

REFERENCES

1. Bertorini TE, Bhattacharya SK, Palmieri GMA, Chesney CM, Pifer D, Baker B: Muscle calcium and magnesium content in Duchenne muscular dystrophy. *Neurology*, 1982, 32, 1088–1092.
2. Bianchi CP, Narayan S: Muscle fatigue and the role of transverse tubules. *Science*, 1982, 215, 295–296.
3. Bonilla E, Samitt CE, Miranda AF, Hays AP, Salviati G, Di Mauro S, Kunkel LM, Hoffman EP, Rowland LP: Duchenne muscular dystrophy: deficiency of dystrophin at the muscle cell surface. *Cell*, 1988, 54, 4447–4452.
4. Borle AB: Calcium metabolism in Hela cells and the effects of parathyroid hormone. *J Cell Biol*, 1968, 36, 567–581.
5. Bush WA, Stromer MH, Goll DE, Suzuki A: Ca^{++} -specific removal of Z lines from rabbit skeletal muscle. *J Cell Biol*, 1972, 52, 367–381.
6. Bygrave FL: Mitochondria and the control of intracellular calcium. *Biol Rev*, 1978, 53, 43–79.
7. Costello BR, Shafiq SA: Freeze fracture study of muscle plasmalemma in normal and dystrophic chickens. *Muscle Nerve*, 1979, 2, 191–201.
8. Crowe LM, Baskin RJ: Stereological analysis of dystrophic chicken muscle. *Am J Pathol*, 1979, 95, 295–316.
9. Darzynkiewicz Z, Traganos F, Sharpless T, Melamed MR: DNA denaturation *in situ*. Effect of divalent cations and alcohols. *J Cell Biol*, 1976, 68, 1–10.
10. Dawson AP: Kinetic properties of the Ca^{2+} -accumulation system of a rat liver microsomal fraction. *Biochem J*, 1982, 206, 73–79.
11. Dayton WR, Goll DE, Zeece MG, Robson RM, Reville WJ: Ca^{++} -activated protease possibly involved in myofibrillar protein turnover. Purification from porcine muscle. *Biochemistry*, 1976, 15, 2150–2158.
12. Dayton WR, Schollmeyer JV: Immunocytochemical localization of a calcium-activated protease in skeletal muscle cells. *Exp Cell Res*, 1981, 136, 423–433.
13. Duncan CJ: Role of intracellular calcium in promoting muscle damage: a strategy for controlling the dystrophic condition. *Experientia*, 1978, 34, 1531–1535.
14. Duncan CJ: Role of calcium in triggering rapid ultrastructural damage in muscle: a study with chemically skinned fibers. *J Cell Sci*, 1987, 87, 581–589.
15. Heathcote JG, Grant ME: The molecular organization of basement membrane. *Int Rev Connect Tissue Res*, 1981, 9, 192–264.
16. Hidalgo C, Gonzales ME, Lagos R: Characterization of the Ca^{2+} - Mg^{2+} -ATPase transverse tubule membranes rabbit skeletal muscle. *J Biol Chem*, 1983, 258, 13937–13945.
17. Hoffman EP, Knudson CM, Campbell KP, Kunkel LM: Subcellular fractionation of dystrophin to the triads of skeletal muscle. *Nature*, 1987, 330, 754–758.
18. Ikemoto N, Sreter FA, Nakamura A, Gergely J: Tryptic digestion and localization of calcium

- uptake and ATPase activity in fragments of sarcoplasmic reticulum. *J Ultrastruct Res*, 1968, 23, 216–232.
19. Jackson MJ, Jones DA, Edwards RH: Increased intracellular Ca^{2+} levels could initiate myofibre death by the activation of phospholipase A, resulting in sarcolemmal dissolution. *Eur J Clin Invest*, 1984, 13, 369–374.
 20. Kanwar Y, Farquhar MG: Anionic sites in the glomerular basement membrane. *In vivo* and *in vitro* localization to the *laminae rarae* by cationic probes. *J Cell Biol*, 1979, 81, 137–153.
 21. Lehninger AL: Mitochondria and calcium ion transport. *Biochem J*, 1970, 119, 129–138.
 22. Malouf NN, Meissner G: Localization of a Mg^{2+} or Ca^{2+} activated (“basic”) ATPase in skeletal muscle. *Exp Cell Res*, 1979, 122, 233–250.
 23. Malouf NN, Samsa D, Allen R, Meissner G: Biochemical and cytochemical comparison of surface membranes from normal and dystrophic chickens. *Am J Pathol*, 1981, 105, 223–231.
 24. Malouf NN, Sommer JR: Chicken dystrophy: the geometry of the transverse tubules. *Am J Pathol*, 1976, 84, 229–316.
 25. Meissner G: ATP and Ca^{2+} binding by the Ca^{2+} pump protein of sarcoplasmic reticulum. *Biochim Biophys Acta*, 1973, 298, 906–926.
 26. Mrak RE: Isolation and characterization of transverse tubule from normal and dystrophic mice. *Biochim Biophys Acta*, 1984, 774, 35–42.
 27. Muscatello U, Margreth A, Aloisi M: On the differential response of sarcoplasm and myoplasm to denervation in frog muscle. *J Cell Biol*, 1965, 27, 1–24.
 28. Nagy B, Samaha FJ: Membrane defects in Duchenne dystrophy: Protease affecting sarcoplasmic reticulum. *Ann Neurol*, 1986, 20, 50–56.
 29. Neymark MA, Kopacz SJ, Lee Ch: Characterization of ATPase in sarcoplasmic reticulum from two strains of dystrophic mice. *Muscle Nerve*, 1980, 3, 316–325.
 30. Oberc MA, Engel WK: Ultrastructural localization of calcium in normal and abnormal skeletal muscle. *Lab Invest*, 1977, 36, 566–577.
 31. Padykula H, Herman E: The specificity of the histochemical method for adenosine triphosphatase. *J Histochem Cytochem*, 1955, 3, 170–183.
 32. Pemrick SM: Evidence that the actin site is impaired by Ca^{++} -activated degradation of the heavy chain of dystrophic myosin. *Biochem Biophys Res Commun*, 1981, 102, 877–884.
 33. Reville WJ, Goll DE, Stromer MH, Robson RM, Dayton WR: A Ca^{++} -activated protease possibly involved in myofibrillar protein turnover. Subcellular localization of the protease in porcine skeletal muscle. *J Cell Biol*, 1976, 70, 1–8.
 34. Rowland LP: Biochemistry of muscle membranes in Duchenne muscular dystrophy. *Muscle Nerve*, 1980, 3, 3–20.
 35. Salvatori S, Damiani E, Zorzato F, Volpe P, Pierobon S, Quagliano D, Salviati G, Margreth A: Denervation-induced proliferative changes of triads in rabbit skeletal muscle. *Muscle Nerve*, 1989, 11, 1246–1259.
 36. Sawicka E: The ultrahistochemical picture of the so-called reversed ATPase in the gastrocnemius muscle of the rat. *Histochemistry*, 1977, 53, 327–339.
 37. Sawicka E: Ultrahistochemical picture of rat muscle fiber types in myofibrillar and “reserved” ATPase reaction. *Acta Med Pol*, 1978, 18, 357–360.
 38. Sawicka E: Ultrastructural analysis of the muscle fiber splitting. *Patol Pol*, 1988, 39, 153–163.
 39. Scales D, Sabbadini R, Inesi G: The involvement of sarcotubular membranes in genetic muscular dystrophy. *Biochem Biophys Acta*, 1977, 465, 535–549.
 40. Scales DJ, Sabbadini RA: Microsomal T system. A stereological analysis of purified microsomes derived from normal and dystrophic skeletal muscle. *J Cell Biol*, 1979, 83, 33–46.
 41. Schanne FAX, Kane AB, Young EE, Farber JL: Calcium dependence of toxic cell death: a final common pathway. *Science*, 1979, 206, 700–702.
 42. Scholte HE, Bush HFM: Early changes of muscle mitochondria in Duchenne dystrophy. Partition and activity of mitochondrial enzymes in fractionated muscle of unaffected boys and adults and patients. *J Neurol Sci*, 1980, 45, 217–234.

43. Stengel-Rutkowski L, Barhelmai W: Über den Muskel-energie-stoffwechsel bei Kindern mit progressiver Muskeldystrophie Typ Duchenne. *Klin Wochenschr*, 1973, 51, 957-961.
44. Sugita H, Ishiura S, Suzuki H, Imahori K: Ca-activated neutral protease and its inhibitors: *in vitro* effect on intact myofibrils. *Muscle Nerve*, 1980, 3, 335-339.
45. Sugita H, Okimoto K, Ebashi S, Okinaka S: Biochemical alterations in progressive muscular dystrophy with special reference to the sarcoplasmic reticulum. In: *Exploratory Concepts of Muscular Dystrophy and Related Disorders*, Ed: AT Milhorat. Excerpta Medica, Amsterdam, 1966, p 321.
46. Verjovski-Almeida S, Inesi G: Rapid kinetics of calcium ion transport and ATPase activity in the sarcoplasmic reticulum of dystrophic muscle. *Biochim Biophys Acta*, 1979, 558, 119-125.
47. Vye MV, Fischman DA, Hansen JL: Ultrastructural localization of adenosinetriphosphatase activity in skeletal muscle by calcium precipitation at high pH. *Virchows Arch Zell Pathol*, 1969, 3, 307-323.
48. Watkins SC, Cullen MJ: A qualitative and quantitative study of the ultrastructure of regenerating muscle fibers in Duchenne muscular dystrophy and polymyositis. *J Neurol Sci*, 1987, 82, 181-192.
49. Wrogemann K, Jacobson BE, Blanchaer MC: On the mechanism of a calcium-associated defect of oxidative phosphorylation in progressive muscular dystrophy. *Arch Biochim Biophys*, 1973, 159, 267-278.

Author's address: Department of Neurology, School of Medicine, 1A Banacha Str, 02-097 Warsaw, Poland

MORPHOLOGY OF PERIPHERAL NERVE IN SOME CASES OF CONGENITAL DEMYELINATING POLYNEUROPATHY*

Department of Neurology, School of Medicine, Warsaw; and Neuromuscular Unit, Medical Research Centre, Polish Academy of Sciences, Warsaw, Poland

Sural nerve taken at biopsy from three subjects aged 8 months, 7 years and 16 years was examined. In all cases congenital motor sensory neuropathy was diagnosed. Morphological examination in case 1 revealed the absence of normally myelinated fibers and the presence of the atypical onion-bulb formations. Proliferation of the Schwann cells with features of the activity of their cytoplasm, lack of the products of myelin breakdown and the presence of large axons with normal appearance might suggest congenital defective myelination connected with the failure of the Schwann cells to form normal myelin sheath. It seems to be justified to include case 1 to the group of hypomyelination neuropathy. Case 2 and case 3 were morphologically similar. The process of demyelination-remyelination, abnormally arranged and abundant in number myelin loops, products of myelin breakdown and features of its degeneration were found. It seems that abnormalities in these cases are connected with failure of the Schwann cells and its relation with axon. This two cases were included to type I hereditary motor sensory neuropathy.

Key words: *Polyneuropathy, hypomyelination polyneuropathy, hypermyelination polyneuropathy, hereditary motor sensory neuropathy.*

Hereditary motor sensory neuropathy with defective myelination is a heterogeneous condition from the clinical, genetical, morphological viewpoint. Among congenital demyelinating neuropathies the place of hypertrophic neuropathy of Dejerine-Sottas is not clear. This autosomal recessive disorder, starting in early childhood, which fulfils criteria of hypertrophic neuropathy is included in type III hereditary motor sensory neuropathy (Harding, Thomas 1984) together with cases of hypomyelinating neuropathy similar to that described by Lyon (1969) and neuropathy with absence of myelin in peripheral nerve. It is also known that total lack of myelin can be associated with congenital arthrogryposis (Charnas et al. 1988). Classification of congenital neuropathy with failure of myelination is unclear from the clinical and morphological viewpoint. In the relevant literature one can come across the

* Work supported by project CPBP, No 06.02.II.9.5.

description of coexistence in the peripheral nerve of fibers with very thin and very thick myelin sheath (Vallat et al. 1987; Vital et al. 1987).

Our material confirms that the morphological features of the nerve in cases of congenital demyelinating neuropathy are not uniform and can differ from the typical descriptions reserved for cases called type I hereditary motor sensory neuropathy according to Harding and Thomas (1980).

MATERIAL AND METHODS

Sural nerves taken at biopsy from 3 subjects aged 8 months, 7 years and 16 years were examined. Basing upon the case history, clinical and electrophysiological examination, congenital motor sensory demyelinating neuropathy was diagnosed in all cases (Tab. 1). Control consisted of sural nerve excised from age-matched subjects without clinical evidence of peripheral nerves system involvement (K.I., 8 mo old, died of pneumonia; W.Z., 6 yr old, with cerebral palsy; P.S., 17 yr old, died of road accident). Paraffin sections, thick Epon- and ultrathin sections and teased fibers were assessed. In each case the sural nerve was removed from above the lateral malleolus. A part of the nerve for routine histology was fixed in Baker's solution and then paraffin sections were stained with cresyl violet and according to Klüver-Barrera and Bielschowsky methods. The second part of the specimen was fixed in 5% glutaraldehyde, postfixed in 1% osmium tetroxide, dehydrated and embedded in Epon. Thick Epon sections (1–1.5 μm) were cut with an LKB ultratome and stained with toluidine blue (modified Pal-Kultschitzky method) or thionine and acridine orange. For histologic measurements (density of myelinated fibers per 0.1 sq mm) sections were photographed under the light microscope and magnified up to 1000 times. Thin Epon sections were stained with uranyl

Table 1. Clinical data in cases of polyneuropathy

Case No.	Case		Onset of the disease	Heredity	CSF protein level (mg%)	Conduction velocity m/sec			Motor condition on examination
	Initials	Age				Median nerve	Sensory fibers	Sural nerve	
1	W.E.	8 mo	At birth	Sporadic ¹	180	2.3 (N-32)	Not recorded	Not done	Severe impairment of motor function
2	P.A.	7 yr	Infancy	Autosomal dominant ²	75	15.6	15.5	21.9	Profound impairment of motor function
3	Ž.A.	16 yr	Early childhood	Sporadic ³	55	2.7	Not recorded	Not done	Mild impairment of motor function

¹ Parents and siblings negative on clinical examination. ² Autosomal dominant (father and brother diseased). ³ Parents and older sister negative on clinical examination.

acetate and lead citrate and examined under a JEM 100 B electron microscope. The third part of the specimen was fixed in 5% glutaraldehyde, postfixed in 1% osmium tetroxide, washed in buffer and passed through glycerine in increasing concentrations (from 5–40%). Single fibers (30–250) were isolated without preselection from each available fascicle, (routinely we assess 30 fibers consisting of at least 4 internodes) for evaluation of the percentage of demyelinated or remyelinating fibers.

RESULTS

Case 1 differed morphologically from cases 2 and 3 hence will be discussed separately. In case 1 on the hematoxylin-eosin stain marked hypercellularity of endoneurium was discerned. In cases 2 and 3 on the van Gieson stain small onion-bulb formations were seen. On Klüver-Barrera stain in case 1 poorly myelinated axons and numerous nuclei were observed. In cases 2 and 3 in this method myelinated fibers were not numerous and had thin myelin sheaths. In many fibers the myelin sheath was discontinuous and partly greatly thickened. Bielschowsky stain revealed the presence of axons which in cases 2 and 3 were thicker than in case 1. Cresyl violet stain in all cases was negative.

Density of the myelinated fibers in all cases was lower than in control ones (Tab. 2). On thick Epon sections in case 1 poorly myelinated thin axons were visible (Fig. 1 a–b). In cases 2 and 3 a smaller than in control cases number of myelinated fibers, onion-bulb formations and abnormally myelinated fibers were seen. Defective myelination was expressed by the presence of fibers with myelin deficiency and axons with abnormally arranged myelin loops with infolding and outfolding (Fig. 2 a–b). It was not possible to isolate a fiber with visible myelin sheath in case 1. In cases 2 and 3 nearly all fibers exhibited extensive demyelination with small myelinated segments; thickenings of myelin were visible in most fibers (Fig. 3). Thickenings of myelin in isolated fibers

Table 2. Quantitative and qualitative data in sural nerve

Case		Density of myelinated fibers 0.1 mm ²	Number of isolated fibers	Fibers with demyelination/ remyelination %
No.	Age			
Polyneuropathy				
1	8 mo	380	40	No fibers with myelin sheath isolated
2	7 yr	500	35	100
3	16 yr	350	64	93.8
Control				
4	8 mo	2058	100	0.0
5	6 yr	1285	150	0.0
6	17 yr	694	150	3.3

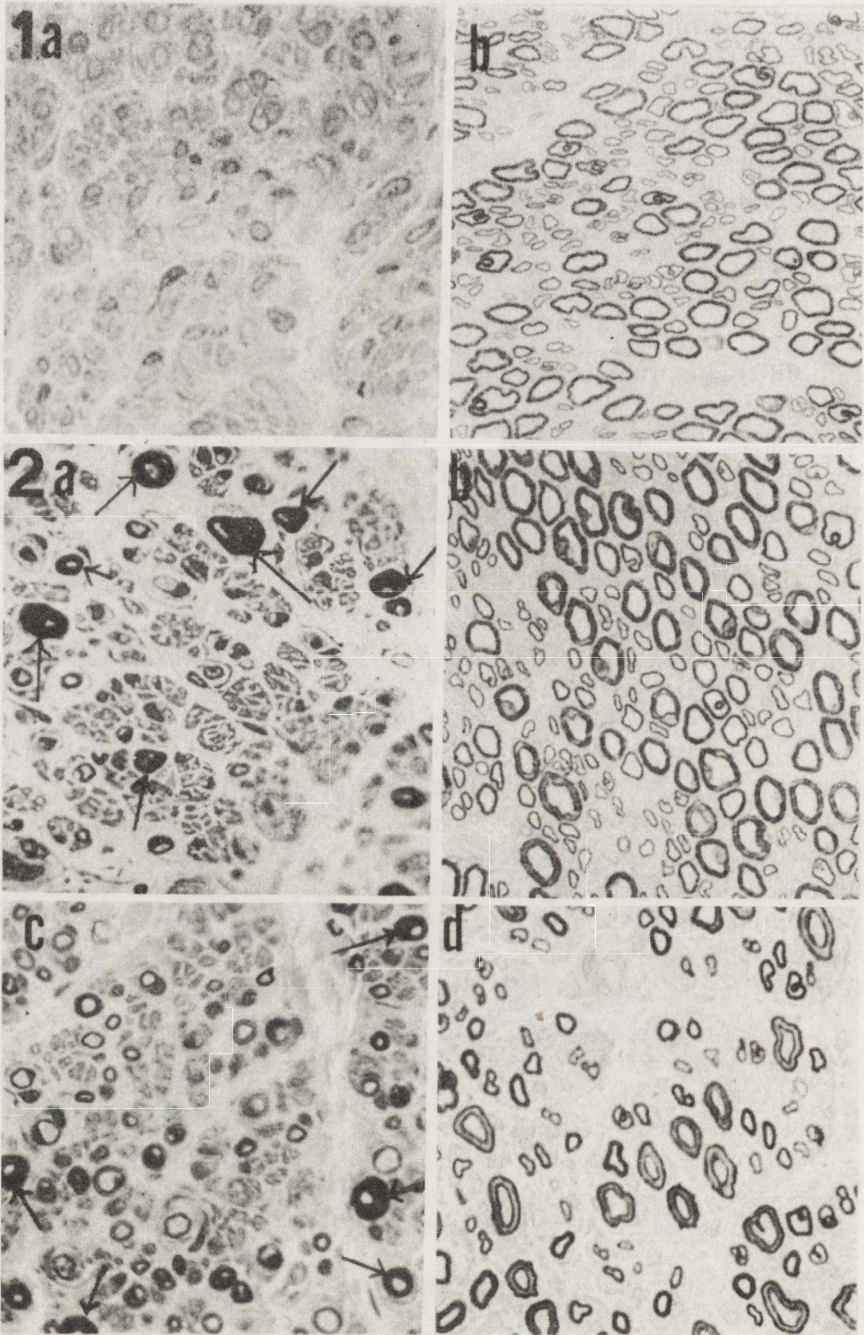


Fig. 1. *a* — case 1. Poorly myelinated fibers, *b* — control. Thick Epon section. x 640
Fig. 2. *a* — case 2; *c* — case 3, *b* — control, *d* — control. In cases 2 and 3 fibers with abnormally arranged myelin sheath (arrows). Thick Epon sections. x 640

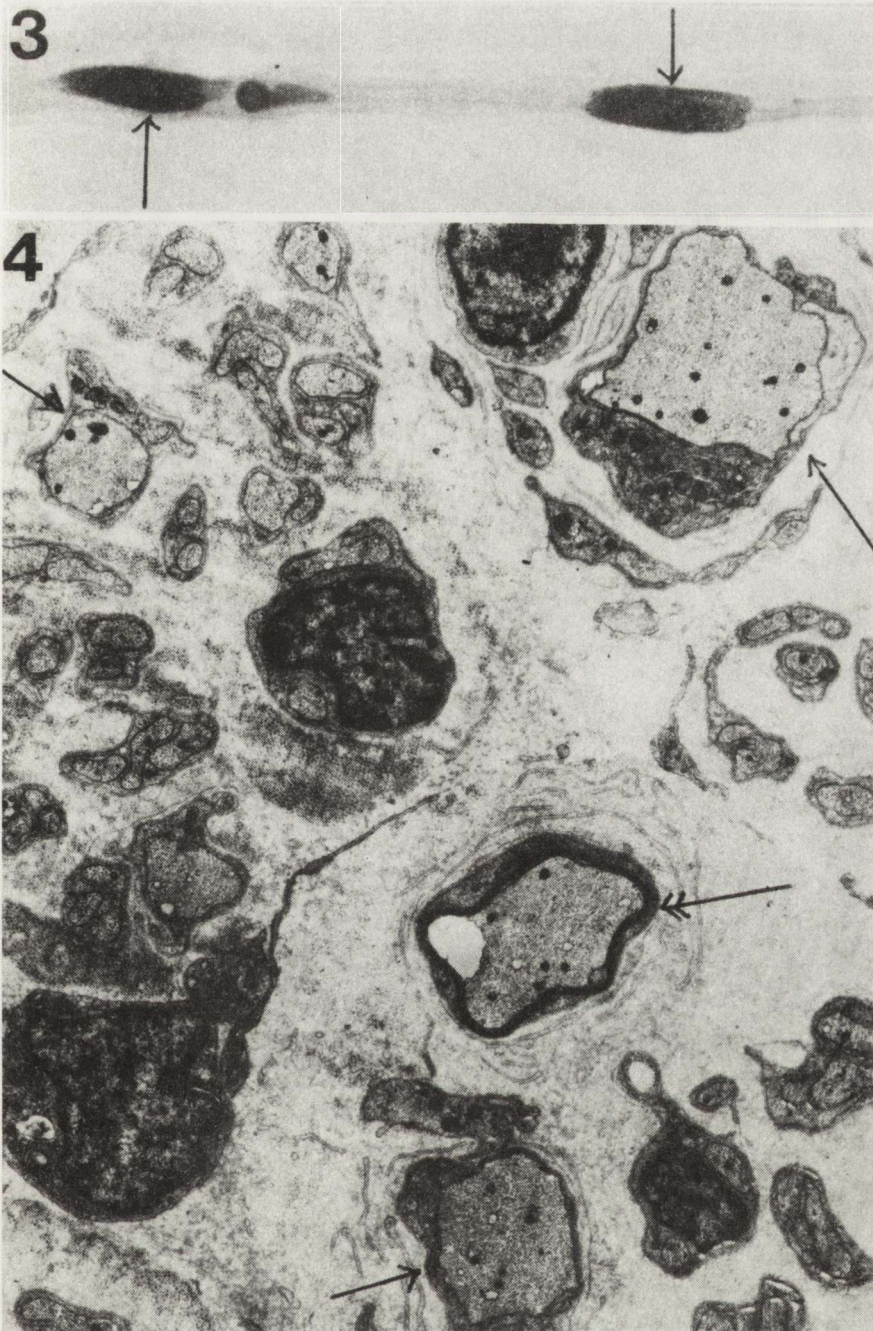


Fig. 3. Case 3. Thickenings of myelin (arrows) within poorly myelinated teased fiber. x 680

Fig. 4. Case 1. Unmyelinated (arrows) and poorly myelinated fibers (double arrows) enclosed by double layered basement membranes of Schwann cell. x 7200

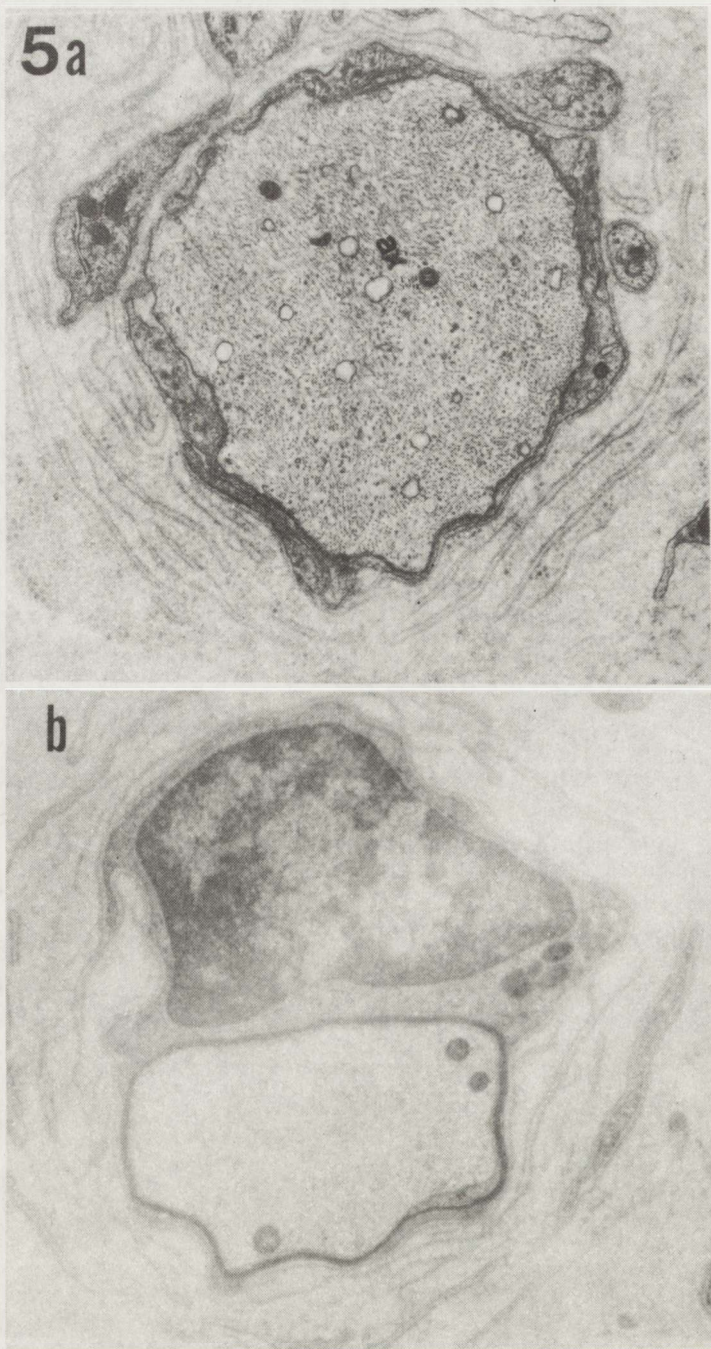


Fig. 5. Case 1. Unmyelinated (*a*) and poorly myelinated (*b*) axons with diameter exceeding $3\ \mu\text{m}$ enclosed by onion-bulb formation composed of concentrically arranged multiple, partly connected lamellae of double layered basement membrane. ax — axon, *a* — $\times 9000$, *b* — $\times 14\ 400$

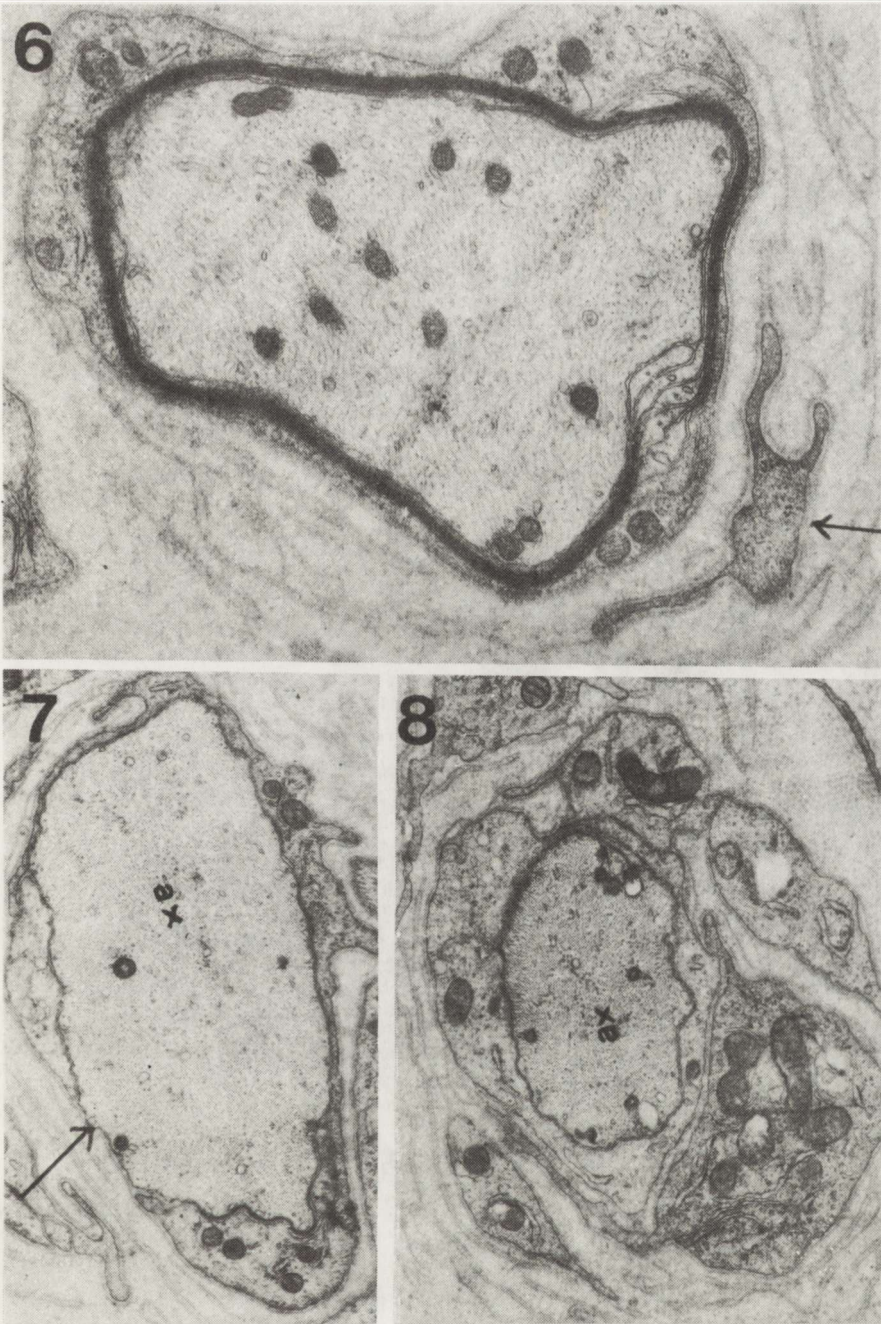


Fig. 6. Case 1. Poorly myelinated fiber. Schwann cell process entrapped between double layered basement membrane (arrow) x 2770

Fig. 7. Case 1. Axon (ax) of diameter above 3 μ m partly immediately enveloped by basement membrane (arrow). x 12 000

Fig. 8. Case 1. Unmyelinated axon (ax) surrounded by Schwann cell processes exhibiting features of increased activity. x 12 000



Fig. 9. Case 2. Onion-bulb formations (arrows) composed of Schwann cell processes and their basement membrane. x 3600



Fig. 10. Case 2. Axon (ax) with abnormally arranged myelin folds. x 11 000

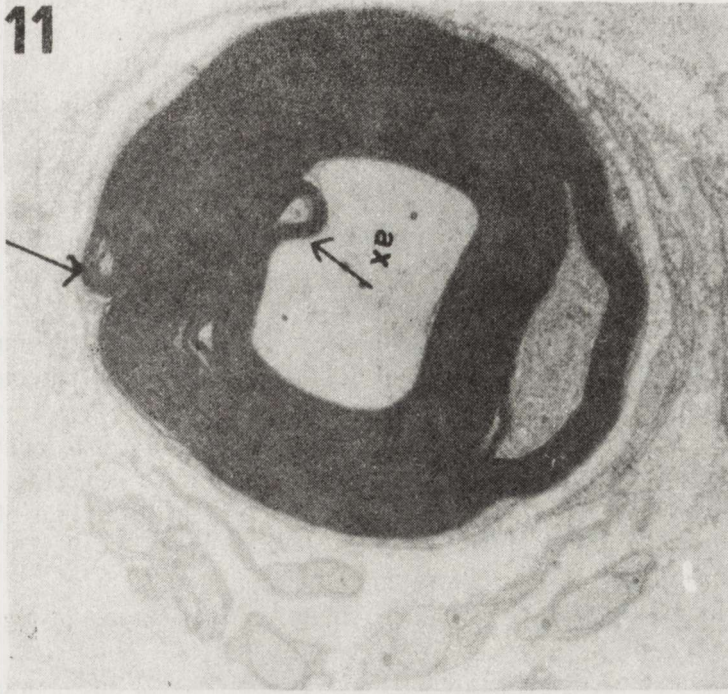


Fig. 11. Case 3. Axon (ax) with myelin sheath disproportionately thick relative to its caliber. Note foldings of myelin (arrows). x 6000

Fig. 12. Case 2. Axon (ax) with excessive myelin outfolding exhibiting degenerative changes. x 11 000

corresponded to the axons with disproportionately thick myelin relative to axon caliber seen on thick Epon sections.

Electron microscopic examination in case 1 revealed:

1. Poorly myelinated fibers enclosed by double layered basement membranes (Fig. 4);
2. Unmyelinated or poorly myelinated fibers enclosed by onion-bulb formation composed of concentrically arranged multiple, undulating partly connected lamellae of double layered basement membrane (Fig. 5 a-b). Cytoplasmic extension of a Schwann cell between double layered basement membrane was sometime visible (Fig. 6);
3. Very rarely axons of diameter above 3 μm were partly immediately enveloped by basement membrane (Fig. 7). Double layered basement membranes were present in the nearest vicinity;
4. Unmyelinated or poorly myelinated axons surrounded by Schwann cell processes exhibiting features of increased activity were seen (Fig. 8);
5. There were no unmyelinated fibers involved in formation of atypical onion-bulb structures;
6. No products of myelin degredation were found;
7. The axons were well preserved. There were no features of regeneration of fibers.

Electron microscopic picture of the nerve in cases 2 and 3 was similar:

1. Myelinated fibers were more numerous than in case 1;
2. Most myelinated fibers formed a centre of onion-bulb formation;
3. Onion-bulb formations were composed of Schwann cell processes and their basement membrane (Fig. 9);
4. A striking feature of fibers was the abnormally arranged myelin sheath (Fig. 10);
5. Numerous fibers with disproportionately thick myelin relative to axonal caliber were found. Frequently it was a result of numerous and complex foldings of myelin (Fig. 11);
6. Degenerative changes of the myelin sheath were observed (Fig. 12);
7. A few fibers were normally myelinated;
8. The unmyelinated fibers seemed to be unaltered;
9. There were no features of regeneration.

To summarize, in all three nerves in all applied methods abnormality of myelination was ascertained; moreover, in cases 2 and 3 features of myelin degeneration were found.

DISCUSSION

Examination of the sural nerve taken from three subjects with congenital motor sensory neuropathy revealed a very pronounced abnormality of myelination. Morphological features of the nerve, taken from case 1 differed from those of nerves taken from cases 2 and case 3.

Basic features in case 1 were: lack of normally for age myelinated fibers and presence of atypical onion-bulb structures composed of multiple, concentrically arranged double-layered basement membranes with sporadically entrapped Schwann cell cytoplasm. Lack of myelin breakdown products and normal appearance of axons suggest that most of the naked or poorly myelinated axons with caliber exceeding 3 μm are the result of hypomyelination. The presence of atypical onion-bulb formations excludes case 1 from the category of congenital hypomyelination described by some authors (Karch, Ulrich 1975; Kasman et al. 1976; Palix, Coiquet 1978; Hakamada et al. 1983). Our case is similar to the cases presented by other authors (Lyon 1969; Anderson et al. 1973; Joosten et al. 1974; Kennedy et al. 1977; Moss et al. 1979; Towfighi 1981; Guzzetta et al. 1982; Ono et al. 1982; Harati, Butler 1985).

It seems that hypomyelination in case 1 is the result of failure of the Schwann cell population (total or part) to form a normal myelin sheath in spite of apparently present activity of Schwann cell cytoplasm. The primary defect of Schwann cell could be supported by some similarity of hypomyelinating neuropathy to that observed in trembler mouse (Ayers, Anderson 1973). The significance of the Schwann cell abnormality was confirmed by the experiment of Aquayo et al. (1977 a, b). Segments of sciatic nerve from trembler mice were grafted into sciatic nerves of normal mice and *vice versa*. In each instance the regenerated axons took on the morphological appearance of the donor nerve. On the other hand, support for the hypomyelination hypothesis in case 1 comes also from the unaltered morphological state of axons similar to the observation of Kennedy et al. (1977). The authors described a case of congenital hypomyelination neuropathy which was biopsied twice (at 9 months and 5 1/2 years of age). The axons of the intramuscular nerve and also of the sural nerve were well preserved and physiologically functional in spite of the absence of myelin sheaths. Schwann cells like in the here presented case 1 were unable to form or maintain normal myelin in response to axonal influence, they did, however, retain the capacity to proliferate and form cell processes.

Lack of evidence of active breakdown of myelin, lack of demyelination-remyelination process, lack of typical onion-bulb structures described by Weller (1967) and Zacks et al. (1968) indicate that case 1 differs from cases called Dejerine-Sottas neuropathy which by some authors is classified as hypomyelinating neuropathy type III (Dyck 1975; Harding, Thomas 1984). It seems, however, reasonable to place case 1 in type III hereditary motor sensory neuropathy, underscoring the heterogeneity of type III neuropathy.

Basic morphological features in case 2 and case 3 were: extensive demyelination-remyelination, abnormally arranged, very often abundant in number myelin loops, degenerative changes of myelin. The morphology of these cases probably corresponds to "globular neuropathy" (Dayan et al. 1969). Morphological features similar to case 2 and case 3 were found by Vallat et al. (1987) in two cases of neuropathy. The authors defined their cases as hypo- and hypermyelination neuropathy. It was Nordborg et al. (1984) who

pointed out such morphological features in autosomal recessive and sporadic cases of hereditary motor sensory neuropathy. Onishi et al. (1986) pose the question whether hereditary motor sensory neuropathy type I with excessive myelin folding is a new finding or new disorder. If one assumes that type I hereditary motor sensory neuropathy is not a uniform disorder, but a syndrome with definite clinical, electrophysiological and morphological characteristics – case 2 and case 3 with some reservation (much pronounced changes) could be included to type I neuropathy. The dominant type of hereditary motor sensory neuropathy with onset in early infancy (like presented case 2) was described by Vanasse and Dubovitz (1981) and also observed in our Department (Badurska et al. 1986).

It does not seem justified to treat the above described changes as very specific *in toto*. Abnormally arranged myelin loops were found sporadically in different neuropathies, but abnormal fibers seen in case 2 and case 3 seem to differ from the “sausages” which are present in hereditary pressure neuropathy comprehensively described by some authors (Behse et al. 1972; Madrid, Bradley 1975; Meier, Moll 1982). Up to date studies do not answer which mechanisms are really responsible for such abnormality in myelination and demyelination. Biochemical examination in hereditary motor sensory neuropathy in recent years has not revealed any abnormality in lipids (Turpin, Haun 1981; Yao, Dyck 1981; Hagberg, Westerberg 1983). It seems justified to assume the complexity of the putative mechanism in these cases including: abnormal relation between axon and Schwann cell – sending false signals by axon with involvement of the feedback mechanism for adjustment of the myelin sheath to the size of the axon; disorder of Schwann cell expressed by formation of an excess of myelin of little value which wraps around the axon and partly undergoes breakdown; aberrant myelination connected with altered physico-chemical properties of membranes resulting in impeding their adherence and causing excessive wrapping around. Our feeling is that all the mentioned above factors play a part in forming morphological abnormalities in case 2 and case 3.

In conclusion our material confirms the variability of the nerve morphology and of the putative mechanism in cases of congenital demyelinating neuropathy.

Acknowledgement: The author is grateful to Professor I. Hausmanowa-Petrusewicz for critical review of the manuscript.

ZMIANY W NERWACH OBWODOWYCH W NIEKTÓRYCH PRZYPADKACH WRODZONYCH POLINEUROPATII DEMIELINIZACYJNYCH

Oceniano nerw łydkowy pobrany biopsyjnie od chorych w wieku 8 miesięcy, 7 lat i 16 lat. We wszystkich przypadkach na podstawie wywiadu, badania klinicznego, badania elektrofizjologicznego i badania płynu mózgowo-rdzeniowego rozpoznano wrodzoną ruchowo-czuciową polineuropatię. Oceniano skrawki parafinowe, poprzeczne półcienkie skrawki eponowe, włókna izolowane oraz preparaty mikroskopowo-elektronowe. Przeprowadzone badania nerwów wykazały we

wszystkich przypadkach znacznego stopnia nieprawidłowości. Podstawową zmianą w przypadku I był brak prawidłowo zmielinizowanych włókien oraz obecność nietypowych struktur cebulopodobnych składających się głównie z licznych warstw błon podstawnych komórki Schwanna bardzo rzadko zawierających wypustki cytoplazmy komórki Schwanna. Nieobecność rozpadu mieliny, proliferacja komórek Schwanna wykazujących niekiedy cechy pobudzenia, prawidłowy wygląd aksonów nasuwa przypuszczenie, iż duże aksony pozbawione mieliny lub z bardzo cienką osłonką mielinową były wynikiem procesu hypomielinizacji najprawdopodobniej związanego z defektem komórki Schwanna. Przypadek nr I zaliczono do grupy neuropatii hypomielinizacyjnych – typ III. Przypadki 2 i 3 wykazywały znaczne podobieństwo morfologiczne. Podstawowymi zmianami w tych przypadkach były: rozległa demielinizacja w znacznie mniejszym stopniu remielinizacji włókien, nieprawidłowy układ niekiedy bardzo licznych pętli mieliny, cechy czynnego rozpadu mieliny. Wydaje się, że w tych przypadkach zmiany związane były zarówno z defektem komórki Schwanna jak i aksonu. Przypadki te zaliczono do typu I dziedzicznej ruchowo-czuciowej neuropatii.

REFERENCES

1. Aguayo AJ, Kasarjian J, Skamene E, Kongsharn P, Bray GM: Abnormal myelination in transplanted Trembler mouse Schwann cells. *Nature*, 1977, 265, 73–74.
2. Aguayo AJ, Bray G, Perkins S, Duncan I: Myelination of mouse axons by Schwann cells transplanted from normal and abnormal human nerves. *Nature*, 1977, 268, 735–755.
3. Anderson RM, Dennett X, Hopkins IJ, Shield LK: Hypertrophic interstitial polyneuropathy in infancy: Clinical and pathological features in two cases. *J Pediatr*, 1973, 82, 619–624.
4. Ayers MM, Anderson R: Onion-bulb neuropathy in the Trembler mouse: a model for hypertrophic interstitial neuropathy (Dejerine-Sottas) in man. *Acta Neuropathol (Ber)*, 1973, 25, 54–70.
5. Badurska B, Jędrzejowska H, Drac H, Ryniewicz B: Ruchowo-czuciowa neuropatia dziedziczna. I. Podstawy klasyfikacji, obraz kliniczny. *Neurol. Neurochir Pol*, 1986, 20, 24–28.
6. Behse F, Buchthal F, Carlsen F, Knappeis GG: Hereditary neuropathy with liability to pressure palsies. Electrophysiological aspects. *Brain*, 1972, 95, 777–794.
7. Charnas L, Trapp B, Griffin J: Congenital absence of peripheral myelin: Abnormal Schwann cell development causes lethal arthrogryposis multiplex congenital. *Neurology*, 1988, 36, 966–974.
8. Dayan AD, Graveson GS, Robinson PK, Woodhouse MA: Globular neuropathy. A disorder of axons and Schwann cells. *J Neurol Neurosurg Psychiatry*, 1969, 31, 552–560.
9. Dyck PJ: Inherited neuronal degeneration and atrophy affecting peripheral motor, sensory and autonomic neurons. In *Peripheral neuropathy*. Eds: PJ Dyck, PK Thomas, EH Lambert. Saunders, Philadelphia 1975, pp 825–867.
10. Guzzetta F, Ferriere G, Lyon G: Congenital hypomyelination polyneuropathy. *Brain*, 1982, 105, 395–416.
11. Hagberg B, Westerberg B: The nosology of genetic peripheral neuropathies in Swedish children. *Develop Med Child Neurol*, 1983, 25, 3–18.
12. Hakamada S, Kumagai T, Hara K, Miyazaki S, Miyazaki K, Watanabe K: Congenital hypomyelination neuropathy in a newborn. *Neuropediatrics*, 1983, 14, 182–183.
13. Harati J, Butler IJ: Congenital hypomyelinating neuropathy. *J Neurol Neurosurg Psychiatry*, 1985, 48, 1269–1276.
14. Harding AE, Thomas PK: The clinical features of hereditary motor and sensory neuropathy type I and II. *Brain*, 1980, 103, 259–285.
15. Harding AE, Thomas PK: Genetically determined neuropathies. In *Peripheral Nerve Disorders*. Eds: AK Asbury, RW Gilliatt, Butterworths, London, 1984, 205–286.
16. Joosten E, Gabreëls F, Gabreëls-Festen A, Vrensen G, Karten J, Votermans S: Electron-microscope heterogeneity of onion-bulb neuropathies of the Dejerine-Sottas type. Two

- patients in one family with the variant described by Lyon (1969). *Acta Neuropathol (Berl)*, 1974, 27, 105–118.
17. Karch SB, Urich H: Infantile polyneuropathy with defective myelination: an autopsy study. *Med Child Neurol*, 1975, 17, 504–551.
 18. Kasman M, Bernstein L, Schulman S: Chronic polyradiculopathy of infancy: a report of three cases with familial incidence. *Neurology*, 1976, 26, 565–573.
 19. Kennedy WR, Sung JH, Berry JF: A case of congenital hypomyelination neuropathy: clinical morphological and chemical studies. *Arch Neurol*, 1977, 34, 337–345.
 20. Lyon G: Ultrastructural study of a nerve biopsy from a case of early infantile chronic neuropathy. *Acta Neuropathol (Berl)*, 1969, 13, 131–142.
 21. Madrid R, Bradley WG: The pathology of neuropathies with focal thickening of the myelin sheath (tomaculous neuropathy) studies on the formation of the abnormal myelin sheath. *J Neurol Sci*, 1975, 25, 415–488.
 22. Meier C, Moll C: Hereditary neuropathy with liability to pressure palsy. *J Neurol*, 1982, 73–95.
 23. Moss RB, Sriram S, Kelts KA, Forno LS, Lewiston NJ: Chronic neuropathy presenting as a floppy infant with a respiratory distress. *Pediatrics*, 1979, 64, 459–464.
 24. Nordborg C, Conradi N, Sourander P, Hagberg B, Westerberg B: Hereditary motor and sensory neuropathy of demyelinating and remyelinating type children. *Acta Neuropathol (Berl)*, 1984, 65, 1–9.
 25. Onishi A, Murai J, Frjita T, Furuya H, Kuruoiwa J: Hereditary motor sensory neuropathy type I with excessive myelin-folding: new finding or new disorder? *Peripheral Neuropathy Association of America, Hilton Head Island, SC (USA)* 1986.
 26. Ono J, Senba E, Okada S, Abe J, Futagi J, Shimizu H, Sugita T, Hashimoto S, Yabuuchi H: A case report of congenital hypomyelination. *Eur J Pediatr*, 1982, 138, 265–270.
 27. Palix C, Coignet J: Un cas de polyneuropathie périphérique neo-natale par amyélinisation. *Pédiatrie*, 1978, 33, 201–207.
 28. Towfighi J: Congenital hypomyelination neuropathy: glial bundles in cranial and spinal nerve roots. *Ann Neurol*, 1981, 10, 570–573.
 29. Turpin JC, Haun JJ: Lipid analysis in nerve biopsy specimens of hypertrophic neuropathy. *Arch Neurol*, 1981, 38, 436–438.
 30. Vallat JM, Gil R, Leboutet MJ, Hugon J, Moulies D: Congenital hypo- and hypermyelination neuropathy. *Acta Neuropathol (Berl)*, 1987, 74, 197–201.
 31. Vanasse M, Dubowitz V: Dominantly inherited peroneal muscular atrophy (hereditary motor and sensory neuropathy type I) in infancy and childhood. *Muscle Nerve*, 1981, 55, 39–46.
 32. Vital A, Vital C, Riviere JP, Brechenmacher C, Marot J: Variability of morphological features in early infantile polyneuropathy with defective myelination. *Acta Neuropathol (Berl)*, 1987, 73, 295–300.
 33. Weller RO: On electron microscopic study of hypertrophic neuropathy of Dejerine and Sootas. *J Neurol Neurosurg Psychiatry*, 1967, 30, 111–125.
 34. Yao JK, Dyck PJ: Lipid abnormalities in hereditary neuropathy. Endoneural and liver lipids of HMSN III (Dejerine-Sootas disease). *J Neurol Sci*, 1981, 52, 179–190.
 35. Zacks SJ, Lipshutz H, Elliott F: Histochemical and electronmicroscopic observation on “onion-bulb” formation in a case of hypertrophic neuritis of 25 years duration with onset in childhood. *Acta Neuropathol (Berl)*, 1968, 11, 157–173.

Author's address: Department of Neurology, School of Medicine, 1A Banacha St., 02–097 Warsaw, Poland

PAWEŁ P. LIBERSKI^{1,2}, RICHARD YANAGIHARA¹, CLARENCE J. GIBBS JR¹,
D. CARLETON GAJDUSEK¹

TUBULOVESICULAR STRUCTURES IN EXPERIMENTAL CREUTZFELDT-JAKOB DISEASE AND SCRAPIE: A PUTATIVE VIRUS OR A PATHOLOGICAL PRODUCT OF THE DISEASE

¹Laboratory of Central Nervous System Studies, National Institute of Neurological Disorders and Stroke, National Institutes of Health, Bethesda, USA. ²Electron Microscopic Laboratory, Department of Oncology and Department of Neurology, School of Medicine, Łódź, Poland

Tubulovesicular structures, measuring 20 to 50 nm in diameter, were found in dilated pre- and postsynaptic neuronal processes in mice infected with the Fujisaki strain of the Creutzfeldt-Jakob disease virus and hamsters infected with the 263K strain of virus. The consistent presence of these structures in naturally occurring and experimentally induced subacute spongiform virus encephalopathies, irrespective of the host species or virus strain, argue for their representing either aggregates or individual components of the infectious virus itself, or the pathological product of the disease.

Key words: *tubulovesicular structures, experimental Creutzfeldt-Jakob disease, experimental scrapie*

The definite structure of viruses causing Creutzfeldt-Jakob (CJD) and other subacute spongiform virus encephalopathies is unknown (Gajdusek 1977). The tubulovesicular structures have been reported in postsynaptic processes (dendrites) in brains of scrapie-affected mice and sheep (David-Ferreira et al. 1968; Bignami, Parry 1971; Lampert et al. 1971 b; Field, Narang 1972; Narang 1973, 1974, 1987; Lamar et al. 1974; Baringer, Prusiner 1978; Baringer et al. 1979; Gibson, Doughty 1989; Liberski et al. 1988, 1990 a) and experimental CJD in chimpanzees (Lampert et al. 1971 a). We report here tubulovesicular structures (TVS) in brains of mice experimentally infected with the Fujisaki strain of CJD virus and hamsters infected with the 263K strain of scrapie virus.

MATERIAL AND METHODS

Weanling, 4- to 6-week-old NI Swiss mice (Animal Production Area, Frederic Cancer Research Facility, Frederick, MD) were inoculated intracerebrally with 0.03 ml of 10% brain homogenate obtained from mice

infected with the Fujisaki strain of CJD virus or intraocularly with 0.01 ml of the same homogenate (Liberski et al. 1989 c). The animals were killed by intracardiac perfusion with 180 ml of 1% paraformaldehyde and 1.5% glutaraldehyde prepared in phosphate buffer (pH 7.4). Sham-inoculated animals were used as controls.

6-week-old Syrian hamsters (Department of Oncology, School of Medicine, Łódź) were inoculated intracerebrally with 0.05 ml of 10% suspension of hamster brain infected with the 263K strain of scrapie virus (Liberski et al. 1989 b). The hamsters were perfused with 100 ml of 1% paraformaldehyde and 1.5% glutaraldehyde prepared in cacodylate buffer (pH 7.4) followed by 50 ml of 4% paraformaldehyde and 5% glutaraldehyde prepared in the same buffer.

The incubation period lasted 18 weeks for mice infected with CJD virus intracerebrally, 25 to 51 weeks for mice infected with CJD virus intraocularly and 8 weeks for scrapie-infected hamsters.

After perfusion the animals were kept at 4° for 2 to 4 hours, then the brains were removed and several tissue blocks 1 mm³ from different anatomical regions were dissected. This report is confined only to the parietal cortex of mice and subcortical gray matter (brain stem at the level of inferior olivae) in hamsters. Samples were postfixed in 1% osmium tetroxide, dehydrated through graded ethanols and propylene oxide and embedded in Epon 812 (hamsters) or Embed (mice) (Electron Microscopy Sciences, Ft. Washington, PA, USA). Semithin sections were stained with methyl blue. Ultrathin sections stained with lead citrate and uranyl acetate, were examined in Hitachi 11A, Philips 300 and Zeiss (Opton) EM 109 transmission electron microscope.

RESULTS

More than 4000 electron micrographs were analyzed. Loosely arranged TVS, measuring 20 to 50 nm in diameter were found in distended pre- and postsynaptic processes in the parietal cortex of mice terminally affected with CJD, regardless of the route of inoculation (Figs 1–4). In the affected neurites mitochondria, multivesicular bodies and clear vesicles approximately 100 nm in diameter were occasionally found. TVS were also detected in the subcortical gray matter of hamsters terminally ill with scrapie (Figs 5–6). When TVS were found in presynaptic processes they were intermingled with synaptic vesicles (Fig. 6). At higher magnifications TVS appeared as spheres or short tubules, occasionally with a dense core (Fig. 7). It seems that TVS were more numerous and more densely packed in mice infected with the Fujisaki strain of CJD virus than in hamsters infected with the 263K strain of scrapie virus. They were clearly absent in sham-inoculated mice and hamsters.

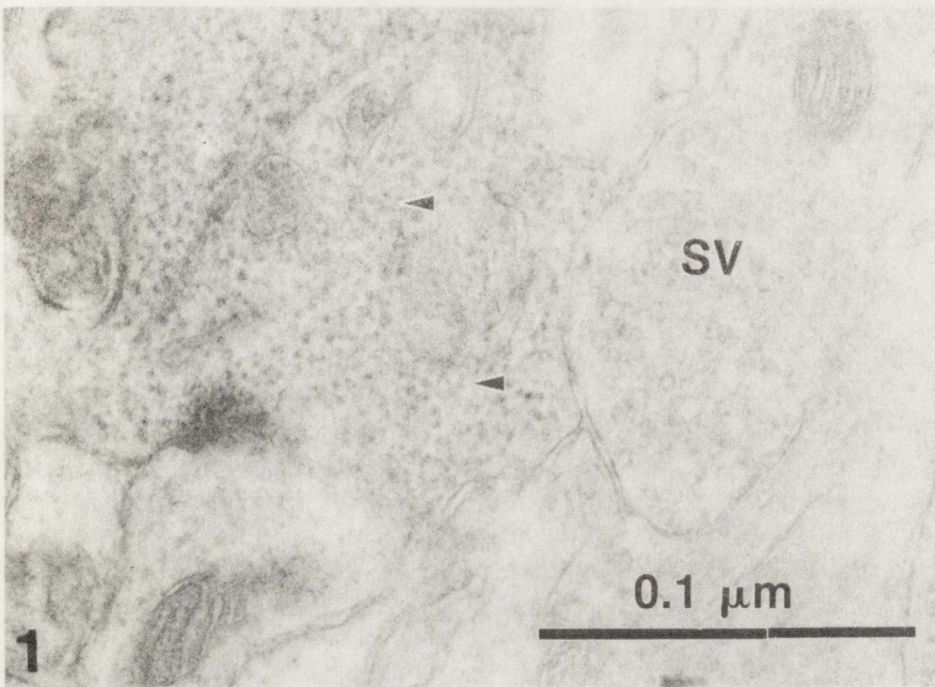


Fig. 1. Tubulovesicular structures (TVS) (arrowheads) in a presynaptic terminal in parietal cortex of mouse 47 weeks after intraocular inoculation with the Fujisaki strain of CJD virus. Compare the size of TVS to that of synaptic vesicles (SV). Bar = 0.1 μm

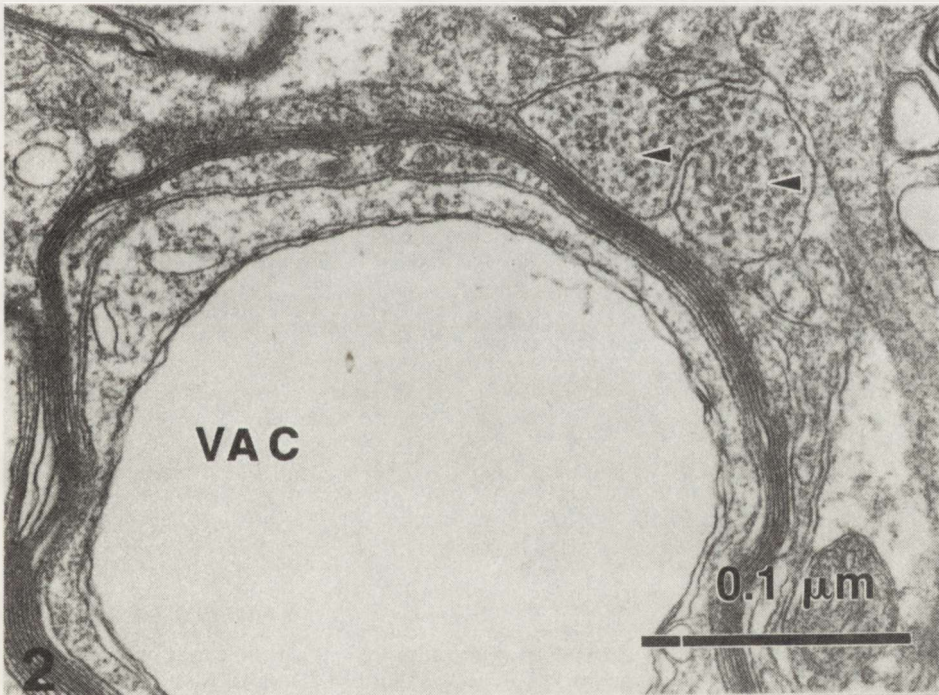


Fig. 2. Unidentified neuronal process containing TVS (arrowheads) in parietal cortex of a mouse 18 weeks after intracerebral inoculation with the Fujisaki strain of CJD virus. Note intraaxonal vacuole (VAC) in the vicinity. Bar = 0.1 μm

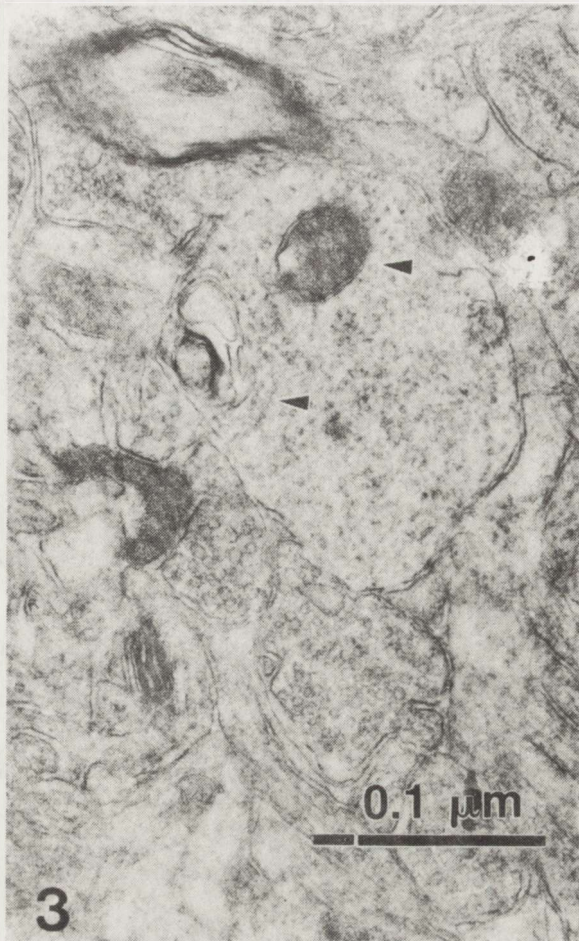
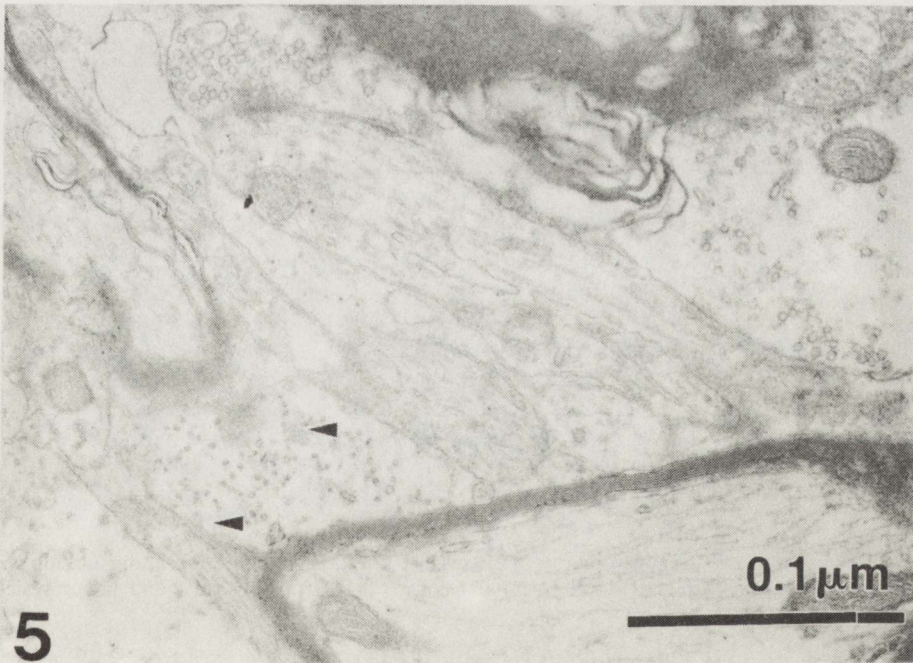
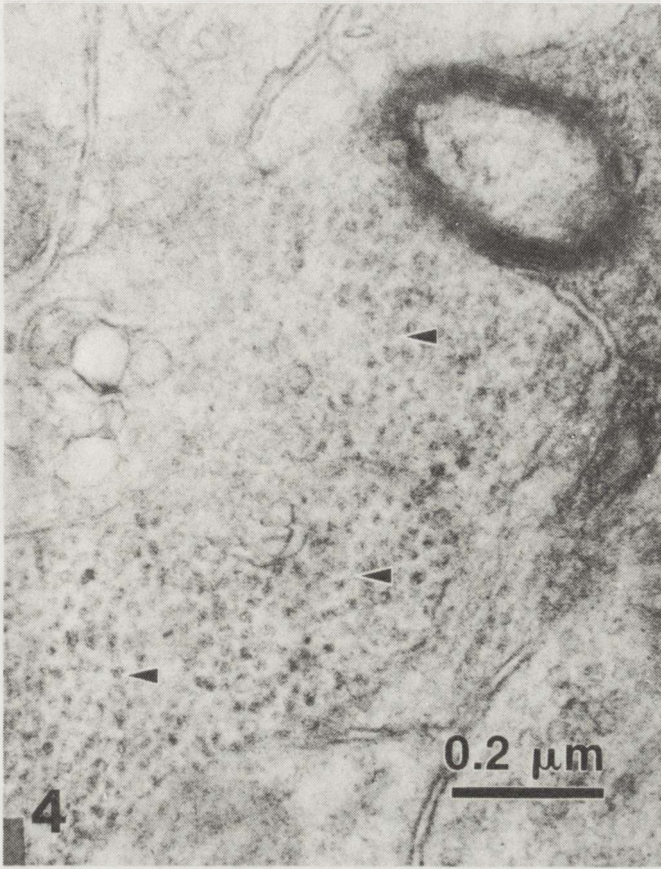


Fig. 3. TVS (arrowheads) within presynaptic terminal in parietal cortex of a mouse 47 weeks after intraocular inoculation with the Fujisaki strain of CJD virus. Bar = 0.1 μm

Fig. 4. TVS (arrowheads) within unidentified neuronal process in parietal cortex of a mouse 47 weeks after intraocular inoculation with the Fujisaki strain of CJD virus. Note the some TVS contain a dense core. Bar = 0.2 μm

Fig. 5. TVS (arrowheads) within unidentified neuronal process in subcortical gray matter of hamster 8 weeks after intracerebral inoculation with the 263K strain of scrapie virus. Compare the size of TVS with that of synaptic vesicles. Bar = 0.1 μm



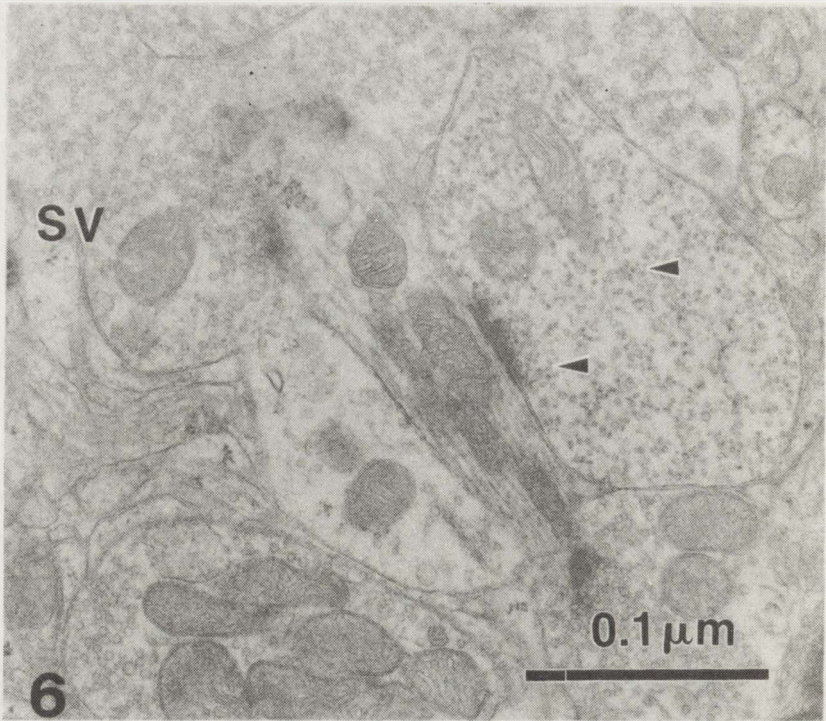


Fig. 6. TVS within presynaptic terminal of hamster 8 weeks after intracerebral inoculation with the 263K strain of scrapie virus. Compare the size of TVS with that of synaptic vesicles (SV). Bar = 0.1 μm

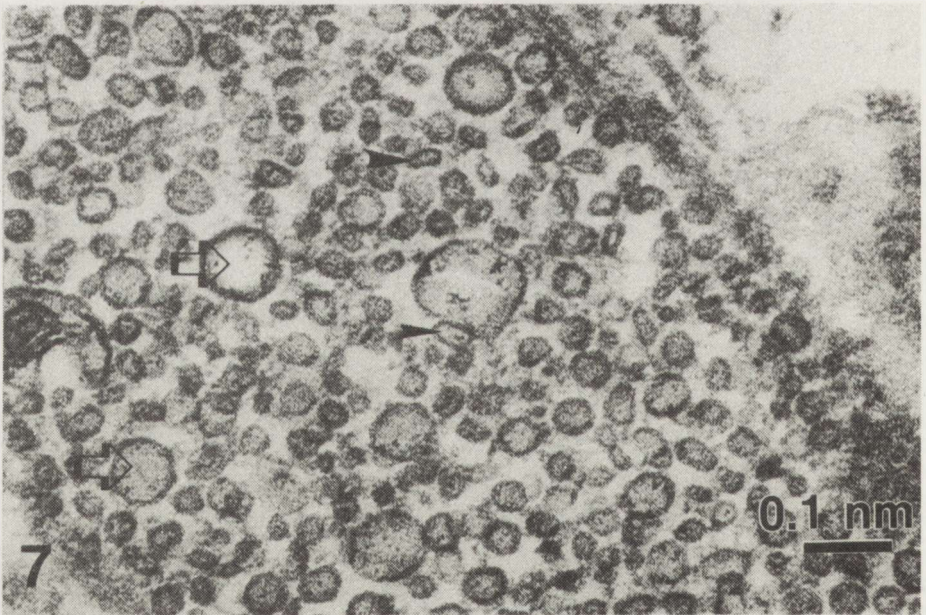


Fig. 7. TVS within undetermined process of hamster 8 weeks after intracerebral inoculation with the 263K strain of scrapie virus. Note tubular form of TVS (arrowheads) and larger vesicles (arrows). Bar = 0.1 μm

DISCUSSION

TVS reported here in mice infected with the Fujisaki strain of CJD virus and hamsters infected with the 263K strain of scrapie virus closely resembled those structures measuring 23–36 nm in diameter first described in scrapie-affected mice by David-Ferreira et al. (1968). Similar structures have been detected in natural scrapie in sheep and goats (Bignami, Parry 1971; Field, Narang 1972; Narang 1973, 1974), experimental scrapie in mice and rats (Lampert et al. 1971 b; Lammar et al. 1974; Narang et al. 1980; Baringer, Prusiner 1978; Baringer et al. 1979; 1981; Gibson, Doughty 1989), experimental CJD in chimpanzees (Lampert et al. 1971 a) and recently in novel bovine spongiform encephalopathy (Liberski et al. 1990 b). The apparent lack of TVS in scrapie-affected hamster brains, presenting the highest titer of infectivity, raised doubts concerning their biological significance (Baringer, Prusiner 1978; Baringer et al. 1979; Liberski 1987). The reported observation along with those published previously by Narang et al. (1987 a, b) called for critical re-evaluation of the subject. Furthermore, when "scrapie tubules" (interpreted as TVS detected in touch preparations – Narang et al. 1987 b) were subjected to detergent extraction, they revealed an inner core resembling scrapie-associated fibrils (Merz et al. 1981).

The diameter of TVS, ranging approximately from 20 to 35 nm, is larger than the size of the CJD or scrapie virus estimated on the basis of irradiation experiments (Alper et al. 1966; Bellinger-Kawahara et al. 1987; Gibbs et al. 1978; Latarjet 1979). However, the older data based on ultrafiltration studies suggested an unconventional virus size larger than that based exclusively on the target theory (Gibbs et al. 1965) and re-evaluation of published data suggested that the scrapie virus could be 10 to 20 times larger than that previously recognized (Rohwer 1984). If we consider that some estimations of the size of scrapie virus are erroneously underestimated (Diringer, Kimberlin 1983), then the size of TVS may reflect the size of the putative scrapie virus. However, the true nature of TVS, whether they represent an aggregate or a part of the virus itself, or the yet to be characterized pathological product of the disease is still unclear.

Acknowledgement: Dr Paweł P. Liberski is the recipient of a fellowship from the Fogarty International Center, Bethesda, USA and a grant from the Ministry of Health and Social Care, Poland. The authors acknowledge the skillful technical assistance of Mr K. Nagashima, Ms K. Pomeroy and Ms L. Romanska.

STRUKTURY TUBULOPECHERZYKOWE W DOŚWIADCZALNEJ CHOROBIE
CREUTZFELDTA-JAKOBA I SCRAPIE: POTENCJALNY WIRUS
CZY PATOLOGICZNY PRODUKT CHOROBY

Streszczenie

Wykazano obecność struktur tubulopęcherzykowych, o średnicy 20–50 nm, w rozdętych zakończeniach pre- i postsynaptycznych u myszy zakażonych szczepem Fujisaki wirusa choroby Creutzfeldta-Jakoba oraz u chomików zakażonych szczepem 263K wirusa scrapie. Ich stała

obecność we wszystkich dotychczas badanych, zarówno występujących naturalnie jak i indukowanych eksperymentalnie encefalopatiach gąbczastych, niezależnie od gatunku gospodarza i szczepu wirusa, sugeruje, iż struktury te są bądź agregatem lub indywidualnym komponentem wirusa, bądź patologicznym produktem choroby.

REFERENCES

1. Alper T, Haig DA, Clarke MC: The scrapie agent: evidence against its dependence for replication on intrinsic nucleic acid. *J Gen Virol*, 1966, 22, 278–284.
2. Baringer JR, Prusiner SB: Experimental scrapie in mice. Ultrastructural observations. *Ann Neurol*, 1978, 9, 205–211.
3. Baringer JR, Prusiner SB, Wong J: Scrapie-associated particles in postsynaptic processes. Further ultrastructural studies. *J Neuropathol Exp Neurol*, 1981, 40, 281–288.
4. Baringer JR, Wong J, Prusiner SB: Further observations on the neuropathology of experimental scrapie in mouse and hamster. In: *Slow transmissible diseases of the nervous system*. Eds: SB Prusiner, WJ Hadlow. Academic Press, New York, 1979, vol 2, pp 111–121.
5. Bellinger-Kawahara C, Cleaver JE, Diener TO, Prusiner SB: Purified scrapie prions resist inactivation by UV irradiation. *J Virol*, 1987, 61, 159–166.
6. Bignami A, Parry HB: Aggregations of 35-nanometer particles associated with neuronal cytopathic changes in natural scrapie. *Science*, 1971, 171, 389–390.
7. David-Ferreira JF, David-Ferreira KL, Gibbs CJ Jr, Morris AJ: Scrapie in mice: ultrastructural observations in cerebral cortex. *Proc Soc Exp Biol Med*, 1968, 28, 313–320.
8. Diringier H, Kimberlin RH: Infectious scrapie agent is apparently not as small as recent claims suggest. *Biosci Rep*, 1983, 3, 563–568.
9. Field EJ, Narang HK: An electron-microscopic study of scrapie in the rat: further observations on "inclusion bodies" and virus-like particles. *J Neurol*, 1972, 17, 347–364.
10. Gajdusek DC: Unconventional viruses and the origin and disappearance of kuru. *Science*, 1977, 197, 943–960.
11. Gibbs CJ Jr, Gajdusek DC, Latarjet R: Unusual resistance to ionizing radiation of the viruses of kuru, Creutzfeldt-Jakob disease and scrapie. *Proc Natl Acad Sci USA*, 1978, 75, 6268–6270.
12. Gibbs CJ Jr, Gajdusek DC, Morris JA: Viral characteristics of the scrapie agent in mice. In: *Slow, latent and temperate virus infections*. Eds: DC Gajdusek, CJ Gibbs Jr, MP Alpers. U.S. Dept. Health, Education, Welfare, Washington, 1965, pp 195–202.
13. Gibson PH, Doughty LA: An electron microscopic study of inclusion bodies in synaptic terminals of scrapie-affected animals. *Acta Neuropathol (Berl)*, 1989, 77, 429–425.
14. Lamar CH, Gustafson DP, Krasovich M, Hinsman EJ: Ultrastructural studies of spleen, brain and brain cell cultures of mice infected with scrapie. *Vet Pathol*, 1974, 11, 13–19.
15. Lampert P, Gajdusek DC, Gibbs CJ Jr: Experimental spongiform encephalopathy (Creutzfeldt-Jakob disease) in chimpanzees. *J Neuropathol Exp Neurol*, 1971 a, 30, 20–32.
16. Lampert P, Hooks J, Gibbs CJ Jr, Gajdusek DC: Altered plasma membranes in experimental scrapie. *Acta Neuropathol (Berl)*, 1971 b, 19, 81–93.
17. Latarjet R: Inactivation of the agents of scrapie, Creutzfeldt-Jakob disease and kuru by radiation. In: *Slow transmissible diseases of the nervous system*. Eds: SB Prusiner, WJ Hadlow. Academic Press, New York, 1979, vol 2, pp 387–407.
18. Liberski PP: Charakterystyka morfologiczna modelu 263K scrapie u chomików ze szczególnym uwzględnieniem badań mikroskopowo-elektronowych. Habilitation doctor's thesis. School of Medicine, Łódź, 1987, pp 1–123.
19. Liberski PP, Plucienniczak H, Hrabec E, Bogucki A: Isolation and purification of scrapie-associated fibrils and prion protein from scrapie-infected hamster brain. *J Comp Pathol*, 1989 a, 100, 178–185.

20. Liberski PP, Yanagihara R, Gibbs CJ Jr, Gajdusek DC: Tubulovesicular structures in experimental Creutzfeldt-Jakob disease and scrapie. *Intervirology*, 1988, 29, 115-119.
21. Liberski PP, Yanagihara R, Gibbs CJ Jr, Gajdusek DC: Scrapie as a model for neuroaxonal dystrophy. *Exp Neurol*, 1989 b, 106, 133-141.
22. Liberski PP, Yanagihara R, Gibbs CJ Jr, Gajdusek DC: White matter ultrastructural pathology in experimental Creutzfeldt-Jakob disease. *Acta Neuropathol (Berl)*, 1989 c, 79, 1-9.
23. Liberski PP, Yanagihara R, Gibbs CJ Jr, Gajdusek DC: Appearance of tubulovesicular structure in experimental Creutzfeldt-Jakob disease and scrapie precedes the onset of clinical disease. *Acta Neuropathol (Berl)*, 1990 a (in press).
24. Liberski PP, Yanagihara R, Wells GAH, Gibbs CJ Jr, Gajdusek DC: Comparative ultrastructural studies of bovine spongiform encephalopathy, scrapie and Creutzfeldt-Jakob disease. *J Comp Pathol*, 1990 b (submitted).
25. Merz PA, Somerville RA, Wiśniewski HM, Iqbal K: Abnormal fibrils from scrapie-infected brains. *Acta Neuropathol (Berl)*, 1981, 65, 63-74.
26. Narang HK: Virus-like particles in natural scrapie of the sheep. *Res Vet Sci*, 1973, 14, 108-110.
27. Narang HK: An electron microscopic study of natural sheep brain: further observations on virus-like particles and paramyxovirus-like tubules. *Acta Neuropathol (Berl)*, 1974, 28, 317-329.
28. Narang HK: Scrapie, an unconventional virus: the current views. *Proc Soc Exp Biol Med*, 1987, 184, 375-388.
29. Narang HK, Asher DM, Gajdusek DC: Tubulofilaments in negatively stained scrapie-infected brains: relationship to scrapie-associated fibrils. *Proc Natl Acad Sci USA*, 1987 a, 84, 7730-7735.
30. Narang HK, Asher DM, Pomeroy KL, Gajdusek DC: Abnormal tubulovesicular particles in brains with scrapie. *Proc Soc Exp Biol Med*, 1987 b, 184, 504-509.
31. Narang HK, Chandler RL, Anger HS: Further observations on particulate structures in scrapie-affected brain. *Neuropathol Appl Neurobiol*, 1980, 6, 23-28.
32. Rohwer R: Scrapie infections agent is virus-like in size and susceptibility to inactivation. *Nature*, 1984, 308, 658-662.

Address for correspondence: PP Liberski, MD, PhD. Department of Neurology, School of Medicine, 22 Kopcińskiego Str, 90-153 Łódź, Poland

ANNA TARASZEWSKA, IRMINA B ZELMAN, ANDRZEJ SZMIELEW

DEVELOPMENT OF SELECTIVE NEURONAL LOSS
IN THE RAT HIPPOCAMPUS AFTER INJECTION OF
QUINOLINIC ACID.
LIGHT- AND ELECTRON MICROSCOPIC STUDIES

Department of Neuropathology, Medical Research Centre, Polish Academy of Sciences, Warsaw

Neurotoxic action of quinolinic acid (QUIN) on rat hippocampus was studied by light and electron microscopy to determine the structural characteristics and dynamics of development of selective neuronal necroses. QUIN in a single dose (60 nmoles) was injected into the dorsal rat hippocampus. Early changes (at 1 h) characterized by chromatolysis in pyramidal cell perikarya were followed by advanced postsynaptic lesions after 3 and 24 h. Subsequent selective loss of pyramidal neurons in CA1 and hilar regions was observed after 7 days, accompanied by proliferation and hypertrophy of astrocytes. Two types of irreversible neuronal damage corresponding to acute excitotoxic swelling of cell body and slower progressing electron dense cell necrosis are described. A very rapid course of events led to complete disappearance of cell body without any cellular phagocytosis during the first 24 h. Dark type of neuronal necrosis progressing to 7th day was associated with involvement of astrocytes in neuronal cytorrhesis. Our studies suggest a biphasic mechanism in the development of QUIN-induced neuronal death.

Key words: *quinolinic acid, selective neuronal necrosis, rat hippocampus*

Excessive activation of the excitatory amino acid (EAA) neurotransmitter systems, especially of NMDA receptors, is believed to play an important role in the pathophysiology of some acute and chronic neurological disorders (Jørgensen, Diemer 1982; Schwarcz et al. 1984; Rothman, Olney 1987; Choi, Rothman 1990). A range of exogenous analogues of glutamate and aspartate was used for *in vitro* and *in vivo* studies of EAA-mediated neurotoxicity. Intracerebral injection of EAA receptor agonists produces dose-dependent lesions characterized by "axon-sparing" postsynaptic degeneration of neurons and selective neuronal vulnerability in the proximity to the injection site.

Quinolinic acid (QUIN) is the verified endogenous agonist of the NMDA receptors exhibiting powerful excitatory and neurotoxic properties (Stone, Perkins 1981; Schwarcz et al. 1983). This compound received special attention as a putative endogenous excitotoxin involved in such neurodegenerative

disorders in humans as temporal lobe epilepsy, Huntington's disease or senile brain atrophy (Schwarcz et al. 1984; Stone et al. 1987). In both human and rat normal brain, QUIN is present in a low concentration, but its increased content was found in aging rat brain (Wolfensberger et al. 1983; Moroni et al. 1984). Hippocampus and striatum are structures most sensitive to the excitatory and neurotoxic action of QUIN (Perkins, Stone 1983; Schwarcz, Köhler 1983; Schwarcz et al. 1983). It has been demonstrated, that intrahippocampal or intrastriatal QUIN injection produces in rat typical excitotoxic lesions (Foster et al. 1983; Schwarcz et al. 1983, 1984). However, data concerning detailed morphological aspects of these lesions are very scarce in the previously reported *in vivo* studies. Recently, ultrastructural characteristics of QUIN neurotoxicity have been studied in organotypic and dissociated hippocampal cultures (Kida et al. 1988; Khaspekov et al. 1989; Kida, Matyja 1990).

In this report we present light and electron microscopic observations on the development of neuronal cell necrosis induced by QUIN in the rat hippocampus.

MATERIAL AND METHODS

Adult male Wistar rats, 280–320 g b.w. were used. The rats were anesthetized intraperitoneally with chloral hydrate (36 mg/100 g b.w.). In stereotaxic apparatus, QUIN was injected by means of a Hamilton syringe into the right dorsal hippocampus, through a hole burred in the calvarium (coordinates: 0.5 mm posterior to bregma, 2 mm from midline and 4 mm below the dura). QUIN was administered in a single dose of 60 nmoles in a volume of 1 μ l of phosphate buffer over a period of 2 min. After the operation, the skin was closed with wound clips and the animals were allowed to recover from anesthesia. Control rats were injected in the same way with 1 μ l of phosphate buffer. Experimental and control animals were sacrificed by intracardiac perfusion with 3% glutaraldehyde in cacodylate buffer (pH 7.4) 15 min, 1, 3, 24 hours and 7 days after operation.

Material for electron microscopic examination was taken from 2–3 experimental and 1–2 control animals in each group of survival time. Small sections of hippocampus were dissected approximately 1–2 mm caudally from the injection site and placed overnight in the perfusion solution, then postfixed for 1 h in buffered 2% osmium tetroxide, dehydrated and embedded in Epon 812. Semithin sections were stained with 1% toluidine blue and viewed in the light microscope. Ultrathin sections counterstained with uranyl acetate and lead citrate were photographed in a JEM 1500XB electron microscope. Moreover, the frontal brain slices through the remaining part of the dorsal hippocampus were embedded in paraffin and stained with HE.

RESULTS

Light microscopy

Fifteen minutes and 1 h after the operation in both experimental and control material dark hyperchromatic neurons were seen, disseminated in the whole pyramidal layer and among the interneurons. In the control rats surviving 3 and 24 h, all neurons were normal, whereas at the same times in the QUIN-injected animals severe lesions of pyramidal cells in restricted CA1 and hilar regions were encountered. Two types of pyramidal cell alterations were distinguished. The first was characterized by neurons with extremely swollen perikaryal cytoplasm and condensed nucleus as well as marked swelling of their dendrites (Fig. 1). The second one, more numerous 24 h after QUIN application, comprised neurons with shrunken dark cytoplasm and pyknotic nucleus (Figs 2, 3). This type of degeneration corresponded to acidophilic neurons commonly seen after 24 h on HE-stained sections. After 7 days an almost total loss of pyramidal cells and numerous hypertrophic astrocytes were observed in CA1 and hilar regions. Only single intact nerve cells corresponding to interneurons were preserved (Fig. 4), whereas all neurons of CA2 – CA3 regions and of the granule cell layer were unaffected (Fig. 5).

Electron microscopy

Fifteen minutes after QUIN injection the changes in pyramidal cells consisted in condensation of cytoplasm and nucleoplasm and were similar to transient neuronal injury in control animals. After 1 h, depolymerization of polyribosomes and increased vesicular profiles occurred in the condensed perikaryal cytoplasm of some CA1 pyramidal cells (Fig. 6). At this time swollen perikarya were not observed and swollen dendrites in *stratum radiatum* were only rarely found. Advanced alterations of pyramidal neurons and ultrastructural signs of their irreversible damage appeared 3 h after QUIN application. According to the light microscopic picture, two types of necrotic cells were present. Type 1 was characterized by massive swelling of neuronal perikarya with loss of cell body configuration, disappearance of cytoplasmic organelles and aggregation of nuclear chromatin (Fig. 7). The cytoplasm devoid of ribosomes, contained floccular and fine granular material, vesicular profiles of fuzzy membranes and damaged mitochondria exhibiting condensed matrix flocculent densities (Fig. 8). Together with these changes, remains of degenerated cell bodies formed by aggregations of uniformly fine granular material were noted (Fig. 9). Subsequent loss of this material within surroundings of extended astrocytic watery processes was also observed (Fig. 10). Besides such severely injured neurons, some pyramidal cells exhibited moderate swelling of perikaryal cytoplasm with preserved integrity of organelles (Fig. 7).

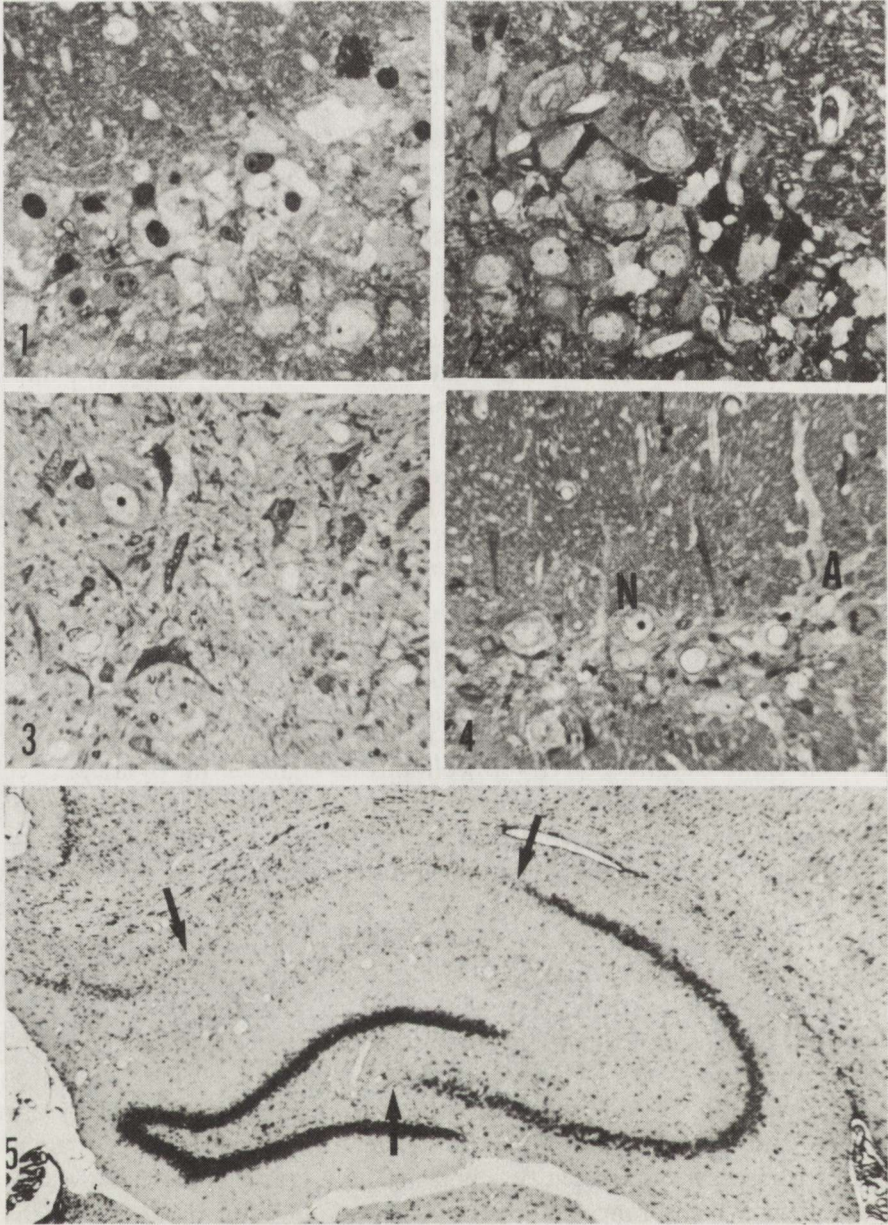


Fig. 1. Extremely swollen perikarya and dark nuclei of CA1 pyramidal neurons. 3 h after QUIN injection. Epon section. Toluidine blue. x 400

Fig. 2. Shrunken dark cells with pyknotic nuclei in the neighborhood of swollen (on the right) and unaffected (on the left) neurons. 3 h after QUIN injection. Epon section. Toluidine blue. x 400

Fig. 3. Dark degenerated neurons in hilar region. 24 h after QUIN injection. Epon section. Toluidine blue. x 400

Fig. 4. Severe loss of CA1 pyramidal neurons. N – interneuron, A – hypertrophic astrocyte. 7 days after QUIN injection. Epon section. Toluidine blue. x 400

Fig. 5. Selective neuronal loss in CA1 and hilar regions (arrows). 7 days after QUIN injection. HE. x 40

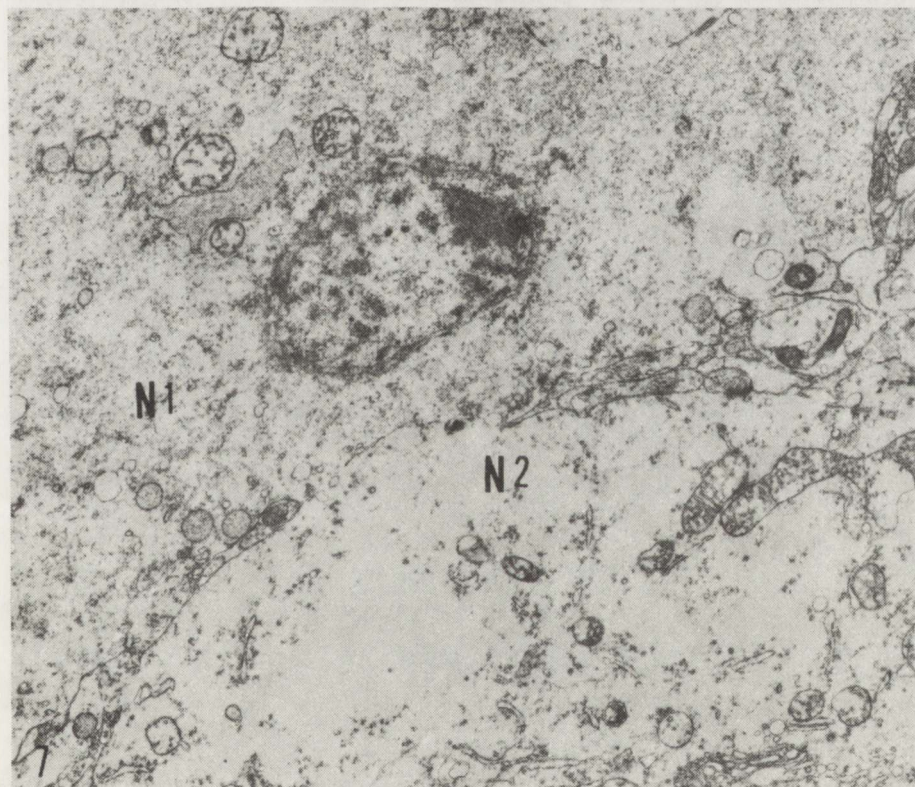
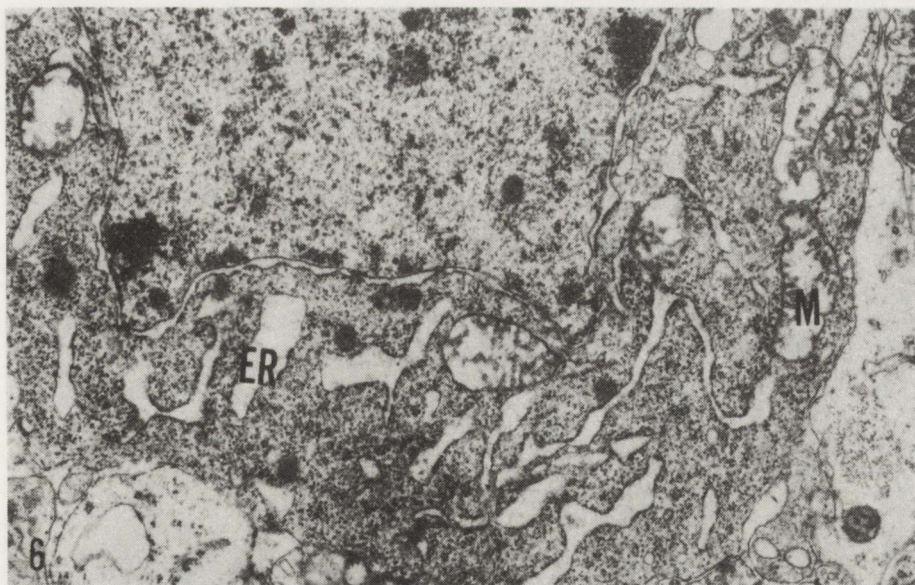


Fig. 6. Slightly condensed cytoplasm and nucleoplasm of pyramidal cell. In cytoplasm numerous free dispersed ribosomes, enlarged channels of endoplasmic reticulum (ER) and swollen mitochondria (M). 1 h after QUIN injection. x 15 000

Fig. 7. Neuron (N1) with structural disintegration of enlarged perikaryal cytoplasm and condensation of nuclear chromatin. In the other – N2 moderately swollen cytoplasm with preserved organelles. 3 h after injection. x 10 000

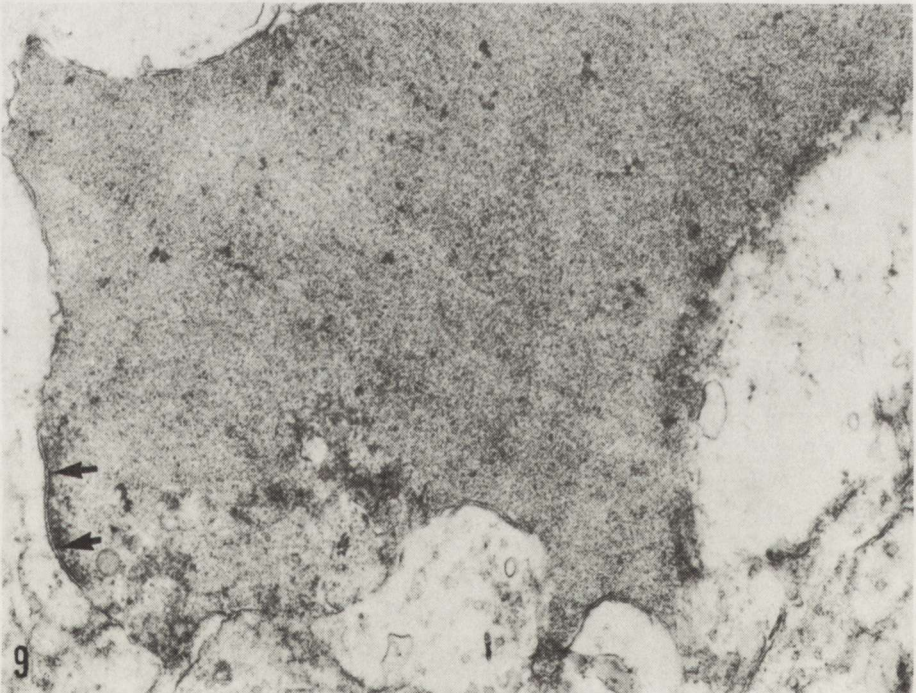
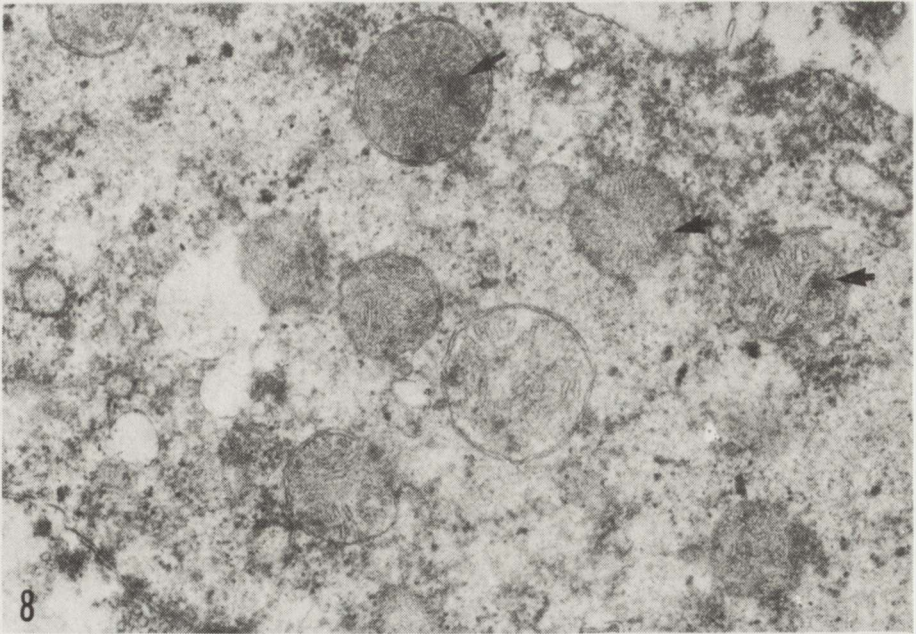


Fig. 8. Fragment of pyramidal cell. Cytoplasm containing floccular and fine granular material and condensed mitochondria with flocculent densities in the matrix (arrows). 3 h after QUIN injection. x 34 500

Fig. 9. Aggregation of homogeneously fine-granular material bounded by cell membrane. Arrows indicate preserved postsynaptic membrane specialization. Remnants of cytoplasmic organelles could be identified. 24 h after QUIN injection. x 28 000

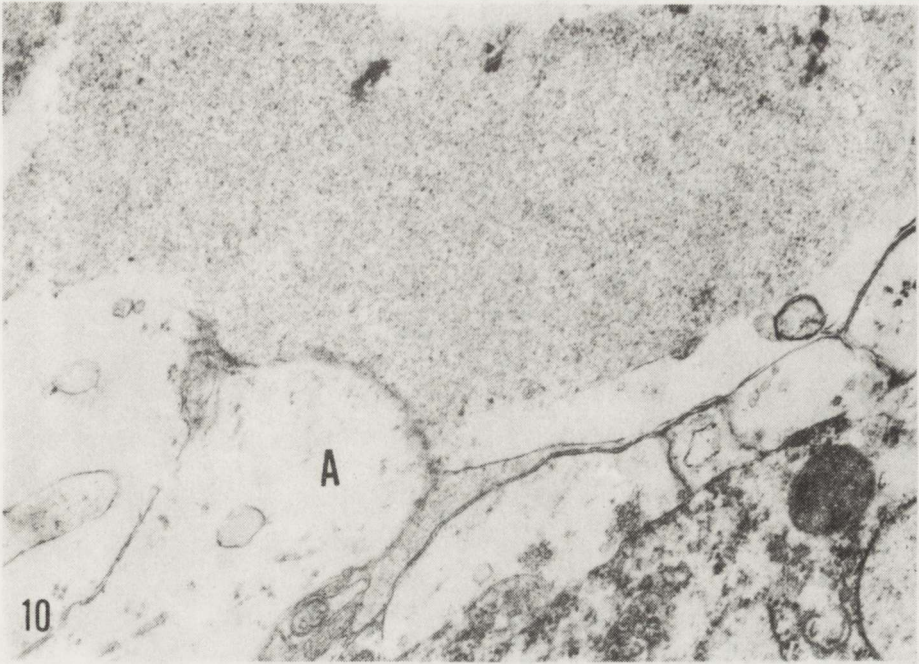


Fig. 10. Free-lying aggregation of fine granular material surrounded by enlarged astroglial processes (A) or directly by cytoplasm of astrocytic processes (arrows). 24 h after QUIN injection. x 45 000

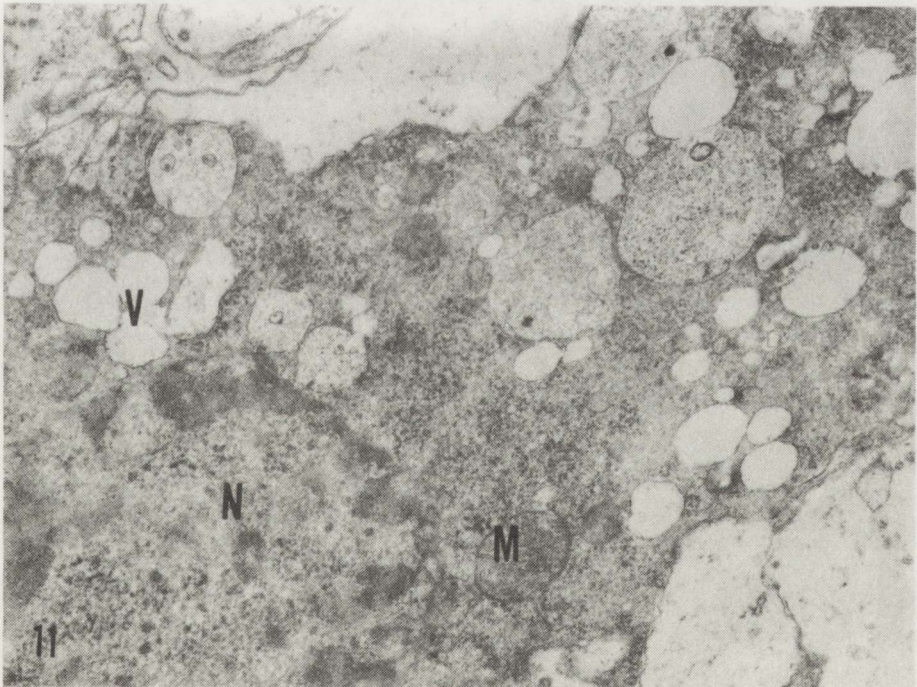


Fig. 11. Pyramidal cell with clumping of nuclear chromatin (N) and dark condensed cytoplasm exhibiting numerous vacuoles (v). M – dark mitochondrion. 24 h after QUIN injection. x 20 000



Fig. 12. Pronounced condensation and vacuolization of neuronal cytoplasm. Some vacuoles (v) interrupt the cell surface. 3 h after QUIN injection. x 37 500

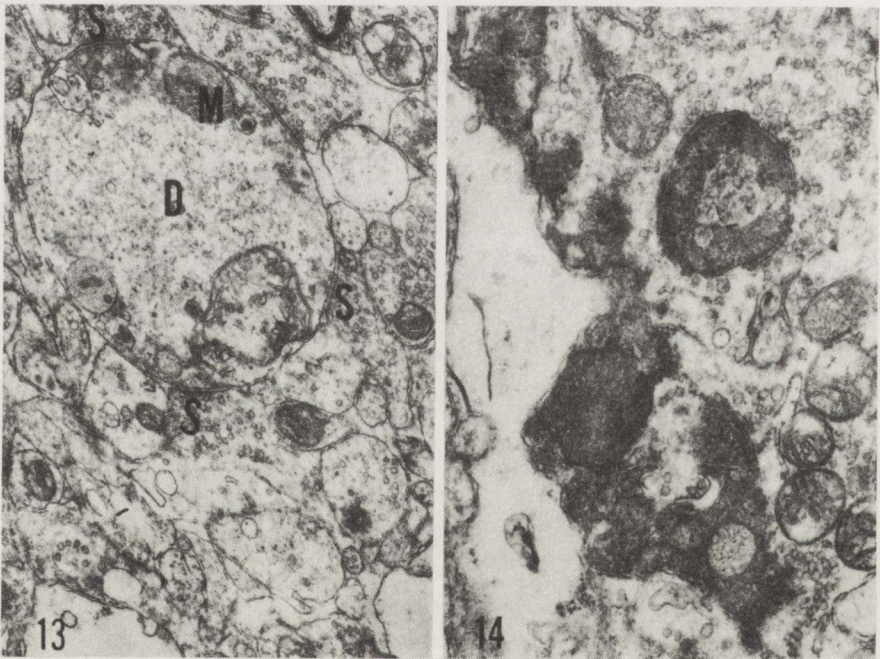


Fig. 13. Dendrite (D) with floccular disintegration of cytoplasm. M – degenerated mitochondria. Axon terminals in synaptic contacts (S) with the dendrite are well preserved. 3 h after QUIN injection. x 19 000

Fig. 14. Clusters of electron-dense material of degenerated postsynaptic dendrites, and unaffected presynaptic terminals. 24 h after QUIN injection. x 24 000

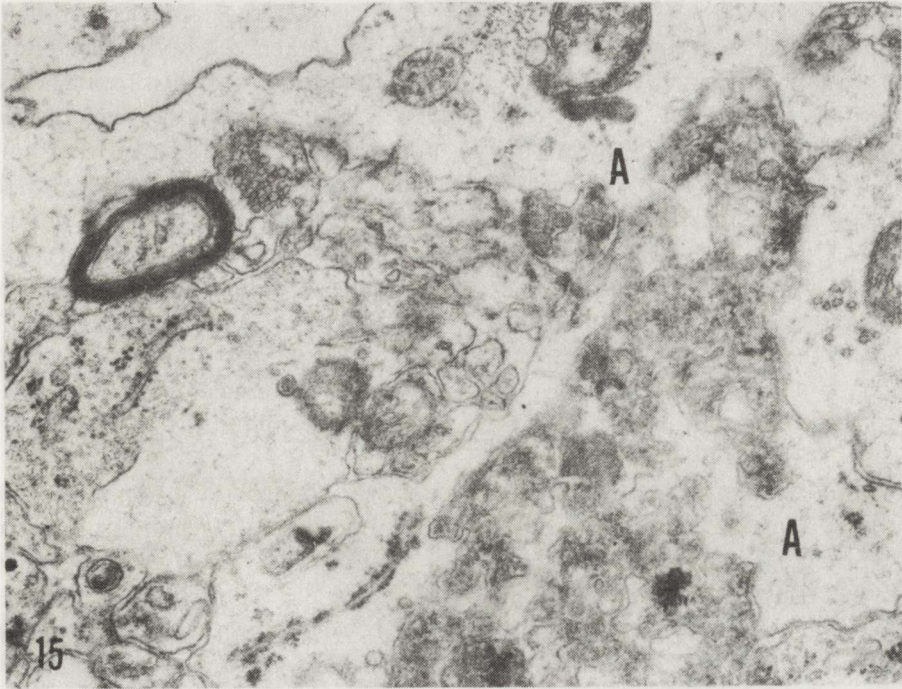


Fig. 15. Electron-dense fragments of degenerated pyramidal cell body closely surrounded by invaginating astroglial cytoplasm (A). 7 days after QUIN injection. x 30 000

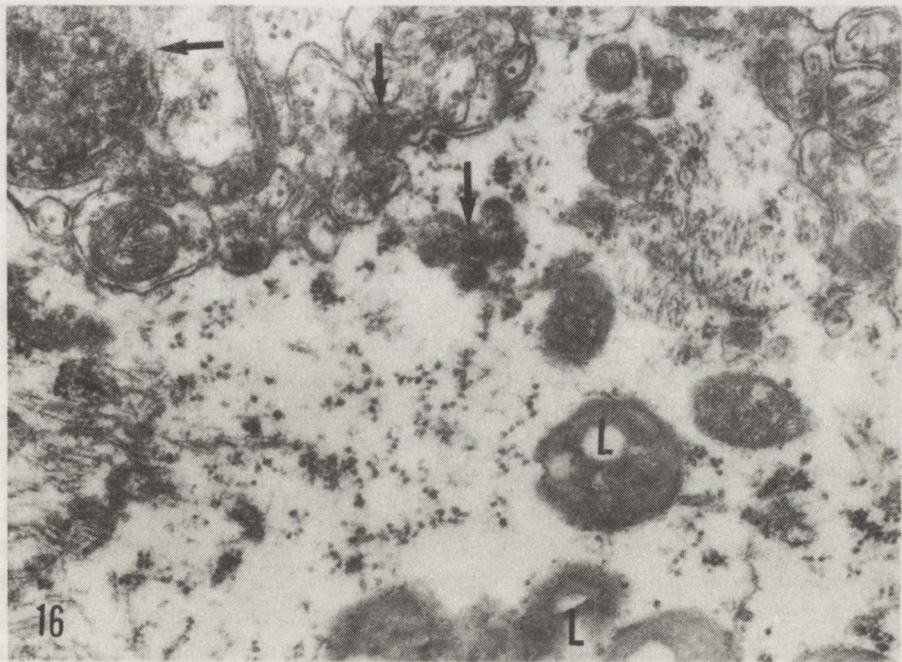


Fig. 16. Astroglial cytoplasm containing numerous lipid droplets (L) and fragments of electron-dense material (arrows). 7 days after QUIN injection. x 30 000

The second type of necrotic neurons was characterized by electron-dense compact cytoplasm and nucleoplasm and by shrunken cell body. Irreversible cell damage, similarly as in type 1, was manifested by disappearance of ribosomes and ER, by dark mitochondria with flocculent matrix densities and disintegration of cytoplasm into fine granular material (Fig. 11). Furthermore, numerous electron-lucent vacuoles or vacuoles with floccular content in the condensed cytoplasm and vacuolar fragmentation of cell body were a common feature (Fig. 12). Degenerated dark neurons were seen simultaneously with necrotic type 1 cells 3 h after QUIN application; they increased in number after 24 h and were still present after 7 days.

Both these types of changes were observed in dendritic processes in *stratum radiatum* and *stratum oriens* (Figs 13, 14). Disseminated clusters of electron-dense degenerated dendrites were particularly ubiquitous after 24 h and 7 days.

Axon terminals in synaptic junctions with degenerated dendrites and neuronal somata seemed normal in both symmetric and asymmetric types of synapses (Figs 13, 14).

Seven days after QUIN application the ultrastructural picture revealed widely extended cytoplasm of hypertrophic astrocyte processes replacing the loss of postsynaptic elements, whereas the axons remained intact. A few profiles of vacuolated dark necrotic pyramidal cell perikarya and degenerated dendrites were also observed (Fig. 15). They were closely surrounded and invaded by astroglial processes. Small fragments of electron-dense material concomitant with lipid droplets were found in the astrocyte cytoplasm (Fig. 16).

DISCUSSION

Two basic mechanisms have been proposed for the excitotoxic neuronal death: the first is early acute cellular swelling due to depolarization-associated influx on Na^+ , Cl^- , and H_2O , followed by osmotic cell lysis, and the other is delayed cell degeneration attributed to excessive influx of Ca^{2+} through voltage-sensitive or receptor-activated channels (Rothman 1985; Rothman et al. 1987; Choi 1988). In our study, the presented two types of irreversible neuronal injury might account in general for this biphasic mechanism of excitotoxicity. It is particularly noteworthy that neuronal necrosis type 1, evolving with acute cellular swelling was observed only in the early period (3 h) after QUIN application, whereas dark degenerated neurons (neuronal necrosis type 2) were seen mostly after 24 h. Occurrence of dark degenerated neurons already after 3 h suggests that the early phase of neurotoxic QUIN action does not lead necessarily to cellular swelling. This is supported by the fact, that the initial structural changes, seen 1 h after QUIN injection were characterized by apparent perikaryal chromatolysis and slight condensation of cytoplasm and

nucleoplasm. On the other hand, swollen neuronal perikarya with structurally preserved organelles such as ER, polyribosomes and mitochondria were seen after 3 h. Thus, swelling of the cytoplasm alone seems to be reversible. The signs of QUIN-induced irreversible neuronal injury were basically the same in both swollen and dark necrotic cells and consisted in clumped aggregation of nuclear chromatin, disintegration of cytoplasmic constituents and degeneration of mitochondria exhibiting condensed matrix with characteristic flocculent densities. Such ultrastructural features suggest a drastic activation of intracellular proteolytic and lipolytic processes, in agreement with the "calcium hypothesis" of excitotoxic neuronal cell death (Choi 1988; Murphy et al. 1988; Ogura et al. 1988).

The neurotoxic effect of QUIN is related to activation of the postsynaptic NMDA receptors (Stone, Connick 1985; Stone et al. 1987) and is calcium-dependent (Kim, Choi 1987). The NMDA receptor/ionic channel complex is highly permeable to Ca^{2+} and is blocked by magnesium ions in a voltage-dependent way (Ascher, Nowak 1987). Ca^{2+} influx through voltage-gated channels or directly through the NMDA-activated channels during excitations is dependent on extracellular Ca^{2+} concentration. Other possible mechanisms which might lead to an increase of free cytosolic calcium content in response to glutamate receptor activation include mobilization of Ca^{2+} from intracellular stores, decrease of Ca^{2+} efflux or Ca^{2+} uptake by organelles (Choi 1988).

The exact mechanism of QUIN neurotoxic action is not yet fully understood. There exist some discrepancies between the excitatory and toxic effects of QUIN. In the rat hippocampus neurotoxic lesions were observed after intrahippocampal administration of QUIN in a dose of 30–60 nmoles (Schwarcz et al. 1983), whereas the recorded neuronal seizures and behavioural convulsant effects were noted with doses as high as 120 and 500 nmoles, respectively (Schwarcz et al. 1983, 1984; Stone, Connick 1985). In our studies, the dose of 60 nmoles of QUIN evoked total loss of pyramidal neurons in restricted CA1 and hilar regions. These results are consistent with the previously reported data indicating selective dose-dependent vulnerability of hippocampal neurons to QUIN, contrary to the other agonists of the NMDA receptor or NMDA itself, which produce wide-spread damage of both pyramidal and granule cells in the hippocampus (Schwarcz et al. 1984). Differences in the regional sensitivity of NMDA and QUIN neurotoxic action led to a proposal that QUIN is a ligand for only one subtype of the NMDA receptor sites (Perkins, Stone 1983). Moreover, regional variations in NMDA receptor density do not closely correlate with the different susceptibility of hippocampal neurons to QUIN. Although the high level of NMDA receptors in the CA1 region could explain the selective vulnerability of CA1 neurons, the hilus represents only a few NMDA recognition sites. On the other hand, the dentate gyrus, which is spared from the QUIN toxicity, is rich in NMDA receptors (Monaghan, Cotman 1985). In addition, the neurotoxic and excitatory effects of QUIN have been shown to be dependent on the synaptic

integrity of the afferent glutaminergic input to the hippocampus (Schwarcz et al. 1984), thus both pre- and postsynaptic sites for QUIN are postulated. Activation of presynaptic QUIN receptors may result in release of glutamate and aspartate or other compounds interacting with the QUIN-specific NMDA receptor sites (Schwarcz et al. 1984; Stone et al. 1987). These data suggest, that several factors may interfere with the mechanism of QUIN excitotoxicity *in vivo* and influence the regional variations in vulnerability of particular neuron populations. Protective effect of kynurenic acid (Foster et al. 1984), Mg^{2+} and Zn^{2+} (Kida, Matyja 1990; Matyja, Kida 1991) against QUIN neurotoxicity has been reported. Their possible role as endogenous modulators of excitotoxicity refers to different sites of QUIN action, since kynurenic acid is a powerful synaptic blocker at the presynaptic QUIN site, whereas Mg^{2+} and Zn^{2+} are antagonists of the postsynaptic NMDA receptor. With regard to relative resistance of the CA3 region, the particularly high Zn^{2+} concentration in the hippocampal mossy fiber system should be emphasized (Ibata, Otsuka 1969). In addition, the cerebral enzyme system of QUIN metabolism seems to participate in the mechanism of QUIN toxicity (Speciale et al. 1987; Whetsell et al. 1988). The recent immunohistochemical study of Whetsell et al. (1990) revealed a high content of QUIN degradative enzyme QPRT (quinolinic acid phosphoribosyltransferase) in granule cells and in CA2 and some CA1 pyramidal neurons which survived after hippocampal injection of QUIN.

The distribution of QUIN-induced lesions in the rat hippocampus closely resembles the pattern of neurodegenerative changes in Ammon's horn in temporal lobe epilepsy or in postischemic and posthypoglycemic states in humans, in which most CA1 and hilar neurons are particularly injured.

In our studies neuronal damage produced by QUIN, corresponds to both acute excitotoxic neuronal death and more slowly progressing electron-dense acidophilic cell necrosis. In both conditions a very rapid course of events leads to complete loss of injured neurons without any cellular phagocytosis during the first 24 h after QUIN administration. Here instead, an electron-dense type of delayed neuronal death, progressing up to 7 days, was associated with involvement of astrocytes in the process of cytorrhesis and phagocytosis. It seems the presented light microscopic and ultrastructural findings provide a model which could be regarded as illustration of selective neuronal loss known to occur in a variety of neurodegenerative processes.

ROZWÓJ WYBIÓRCZYCH ZANIKÓW NEURONALNYCH
W HIPOKAMPIE SZCZURA PO WSTRZYKNIĘCIU KWASU CHINOLINOWEGO.
BADANIA W MIKROSKOPIE ŚWIETLNYM I ELEKTRONOWYM

Streszczenie

Określono charakter i dynamikę rozwoju wybiórczych martwic neuronalnych powstających w hipokampie szczura pod wpływem działania kwasu chinolinowego (QUIN). Neurotoksynę podawano zwierzętom jednorazowo w dawce 60 nmoli do grzbietowego hipokampa. Czas

przeżycia po iniekcji wynosił 15 min, 1, 3, i 24 godziny oraz 7 dni. Wczesne zmiany neuronalne, obserwowane po 1 godz., charakteryzowały się chromatolizą perykarionów komórek piramidowych. Po 3 i 24 godz., stwierdzano typowe zaawansowane uszkodzenia postsynaptyczne, a po 7 dniach rozległe ubytki neuronów piramidowych w obrębie sektora CA1 i wnęki z towarzyszącym im przerostem i rozplemem astrogleju. Wyróżniono dwa typy nieodwracalnych uszkodzeń neuronalnych. Pierwszy z nich, o obrazie odpowiadającym ostremu ekscytotoksycznemu uszkodzeniu komórki nerwowej, prowadził w okresie pierwszych 24 godzin do całkowitego bezodczynowego zaniku neuronu. Drugi typ – rozwijające się wolniej „ciemne” uszkodzenie komórki (dark degeneration), obserwowane jeszcze w 7 dniu po podaniu kwasu chinolinowego, przebiegał z udziałem astrogleju w procesie zaniku neuronu.

Różnice strukturalne, jak również niejednakowa dynamika procesu w obu typach martwic neuronalnych, sugerują dwufazowy mechanizm działania kwasu chinolinowego w rozwoju wybiórczych zaników komórek piramidowych w hipokampie.

REFERENCES

1. Ascher P, Nowak L: Electrophysiological studies of NMDA receptors. *Trends Neurosci*, 1987, 10, 284–288.
2. Choi DW: Calcium-mediated neurotoxicity: relationship to specific channel types and role in ischemic damage. *Trends Neurosci*, 1988, 11, 465–469.
3. Choi DW, Rothman SM: The role of glutamate neurotoxicity in hypoxic-ischemic cell death. *Ann Rev Neurosci*, 1990, 13, 71–82.
4. Foster AC, Collins JF, Schwarcz R: On the excitotoxic properties of quinolinic acid, 2,3-piperidine dicarboxylic acids and structurally related compounds. *Neuropharmacology*, 1983, 22, 1331–1342.
5. Foster AC, Vezzani A, Oldendorf WA, Schwarcz R: Kynurenic acid blocks neurotoxicity and seizures induced in rats by the related brain metabolite quinolinic acid. *Neurosci Lett*, 1984, 18, 273–278.
6. Iyata Y, Otsuka N: Electron microscopic demonstration of zinc in the hippocampal formation using Timm's sulphide silver technique. *J Histochem Cytochem*, 1969, 17, 171–175.
7. Jörgensen MB, Diemer NH: Selective neuron loss after cerebral ischemia in the rat: possible role of transmitter glutamate. *Acta Neurol Scand*, 1982, 66, 536–546.
8. Khaspekov L, Kida E, Victorov J, Mossakowski MJ: Neurotoxic effect induced by quinolinic acid in dissociated cell culture of mouse hippocampus. *J Neurosci Res*, 1989, 22, 150–157.
9. Kida E, Matyja E: Dynamics and pattern of ultrastructural alterations induced by quinolinic acid in organotypic culture of rat hippocampus. *Neuropatol Pol*, 1990, 28, 67–82.
10. Kida E, Matyja E: Prevention of quinolinic acid neurotoxicity in rat hippocampus *in vitro* by zinc. Ultrastructural observations. *Neuroscience*, 1990, 37, 347–352.
11. Kida E, Matyja E, Khaspekov L: The ultrastructure of rat hippocampal formation in organotypic tissue culture after exposure to quinolinic acid. *Neuropatol Pol*, 1988, 26, 507–520.
12. Kim JP, Choi DW: Quinolinic acid neurotoxicity in cortical cell culture. *Neuroscience*, 1987, 23, 423–432.
13. Matyja E, Kida E: Effect of magnesium on quinolinic acid-induced damage of hippocampal formation *in vitro*. *Neuropatol Pol*, 1991, 29, in 169–170.
14. Monaghan DT, Cotman CW: Distribution of N-methyl-D-aspartate-sensitive L-³H-glutamate binding sites in the rat brain. *J Neurosci*, 1985, 5, 2909–2919.
15. Moroni F, Lombardi G, Moneti G, Aldino C: The excitotoxin quinolinic acid is present in the brain of several mammals and its cortical content increases during the aging process. *Neurosci Lett*, 1984, 47, 51–55.
16. Murphy TH, Malouf AT, Sastre A, Schnaar RL, Coyle JT: Calcium-dependent glutamate cytotoxicity in a neuronal cell line. *Brain Res*, 1988, 444, 325–332.

17. Ogura A, Miyamoto M, Kudo Y: Neuronal death *in vitro*: parallelism between survivability of hippocampal neurons and sustained elevation of cytosolic CA^{2+} after exposure to glutamate receptor agonist. *Exp Brain Res*, 1988, 73, 447-458.
18. Perkins MN, Stone TW: Quinolinic acid: regional variations in neuronal sensitivity. *Brain Res*, 1983, 259, 172-176.
19. Rothman SM: The neurotoxicity of excitatory amino acids is produced by passive chloride influx. *J Neurosci*, 1985, 5, 1483-1489.
20. Rothman SM, Olney JW: Excitotoxicity and the NMDA receptor. *Trends Neurosci*, 1987, 10, 299-302.
21. Rothman SM, Thurston JH, Hanhart RE: Delayed neurotoxicity of excitatory amino acids *in vitro*. *Neuroscience*, 1987, 22, 471-480.
22. Schwarcz R, Köhler C: Differential vulnerability of central neurons of the rat to quinolinic acid. *Neurosci Lett*, 1983, 38, 85-90.
23. Schwarcz R, Whetsell WO Jr, Mangano RM: Quinolinic acid: an endogenous metabolite that produces axon-sparing lesions in rat brain. *Science*, 1983, 219, 316-318.
24. Schwarcz R, Brush GS, Foster AC, French ED: Seizure activity and lesions after intrahippocampal quinolinic acid injection. *Exp Neurol*, 1984 a, 84, 1-17.
25. Schwarcz R, Foster AC, French ED, Whetsell WO Jr, Köhler C: Excitotoxic models for neurodegenerative disorders. *Life Sci*, 1984 b, 35, 19-32.
26. Speciale C, Okuno E, Schwarcz R: Increased quinolinic acid metabolism following neuronal degeneration in the rat hippocampus. *Brain Res*, 1987, 436, 18-24.
27. Stone TW, Connick JH: Quinolinic acid and other kynurenines in the central nervous system. *Neuroscience*, 1985, 15, 597-617.
28. Stone TW, Perkins MN: Quinolinic acid: a potent endogenous excitant at amino acids receptors in CNS. *Eur J Pharmacol*, 1981, 72, 411-412.
29. Stone TW, Connick JH, Winn P, Hastings MH, English M: Endogenous excitotoxic agents. In: *Selective neuronal death*. Eds. G Bock, M O'Connor. Ciba Foundation Symposium 126, New York, Wiley and Sons Ltd, 1987, pp 204-214.
30. Whetsell WO Jr, Köhler C, Schwarcz R: Quinolinic acid: a glia-derived excitotoxin in the mammalian central nervous system. In: *The biochemical pathology of astrocytes*. Eds: MD Norenberg, L Hertz, A Schousboe. AR Liss, New York, 1988, pp 191-202.
31. Whetsell WO Jr, Du F, Köhler C, Okuno E, Schwarcz R: Quinolinic acid metabolism in experimental models and in neurodegenerative disease. XIth International Congress of Neuropathology, Kyoto, Japan, September 2-8, 1990, p 172 (Abstr).
32. Wolfensberger M, Amsler U, Cuenod M, Foster AC, Whetsell WO Jr, Schwarcz R: Identification of quinolinic acid in rat and human brain tissue. *Neurosci Lett*, 1983, 41, 247-252.

Authors' address: Department of Neuropathology, Medical Research Centre, Polish Academy of Sciences, 3 Dworkowa Str, Warsaw, Poland

EWA MATYJA, ELŻBIETA KIDA

EFFECT OF MAGNESIUM ON QUINOLINIC
ACID-INDUCED DAMAGE OF HIPPOCAMPAL FORMATION
IN VITRO

Department of Neuropathology, Medical Research Centre, Polish Academy of Sciences, Warsaw,
Poland

The influence of $MgCl_2$ on QUIN neurotoxicity in cultured explants of rat hippocampus was investigated. $MgCl_2$ was added in two concentrations (100 μM and 1mM) simultaneously with QUIN to the culture medium. Magnesium ions at the low concentration were able to prevent typical postsynaptic damages, whereas acute excitotoxic nerve cell injury was reduced only partially. The higher concentration of Mg^{2+} diminished damages of both postsynaptic elements and pyramidal neurons. The protective effect obtained with higher Mg^{2+} concentration might be connected with sufficient block of NMDA-receptors activation necessary to QUIN neurotoxicity.

Key words: *Magnesium ions, QUIN neurotoxicity, tissue culture.*

Quinolinic acid (QUIN) is an endogenous excitatory amino acid that produces cell death *via* activation of the N-methyl-D-aspartate (NMDA) subtype receptor (Perkins, Stone 1983; Stone, Connick 1985; Stone et al. 1987). Recently, the neurotoxic effect of different amino acid agonists have been widely studied but the exact mechanism of these compounds is as yet not well understood.

A great deal of evidence indicates that QUIN could be considered as a possible etiological factor in Huntington's disease and other neurodegenerative diseases and epilepsy (Schwarcz et al. 1984). If so, the neurotoxic properties of QUIN are of considerable interest in understanding the pathogenesis of certain human neurological states and the prevention of its toxicity might be of important therapeutic value. It has been indicated that changes in divalent cations such as Ca^{2+} and Mg^{2+} could be potent modulators of neuronal excitability (Choi 1985; Garthwaite et al. 1986; Kohr, Heinemann 1988). Most noticeably Mg^{2+} exert a regulatory effect on the activation of the glutamate receptor of NMDA-subtype (Adult et al. 1980; Mayer et al. 1984; Nowak et al. 1984; Flatman et al. 1986; Thomson 1986).

The present study was undertaken to investigate the effect of different concentrations magnesium ions on QUIN-induced neuronal damage. The studies were performed on organotypic cell cultures of the hippocampal formation – a structure of high vulnerability to QUIN action probably due to the large amount of NMDA-receptors in the CA₁ sector (Cotman et al. 1987).

MATERIAL AND METHODS

The experiments were performed on 21-day *in vitro* (DIV) organotypic cultures of rat hippocampus, well-differentiated and sensitive to QUIN action (Kida et al. 1988). The cultures prepared from 2-3-day-old Wistar rats were kept in Maximow assemblies at 36.5°C and fed twice weekly. The nutrient medium consisted of 20% fetal bovine serum and 80% Minimal Essential Medium (MEM) supplemented with 600 mg% glucose. The 21-day-old culture were divided into several groups. One group was exposed to nutrient medium supplemented with 100 µM or 1 mM of MgCl₂. The second was exposed to 100 µM of QUIN alone (Sigma, Co). The third one was maintained in medium containing 100 µM or 1 mM of MgCl₂ and 100 µM of QUIN applied simultaneously. Sister cultures were grown in standard conditions in nutrient medium. Twenty four hours, 3 and 7 days after exposure to the test agents, the cultures were fixed for electron microscopy. Briefly, they were fixed in 1.5% cold glutaraldehyde for 1 h, washed in cacodylate buffer pH 7.2–7.4, postfixed in 2% osmium tetroxide, dehydrated in graded alcohols and embedded in Epon 812. Ultrathin sections were counterstained with lead citrate and uranyl acetate and examined in a JEM 1500XB electron microscope.

RESULTS

Hippocampal cultures exposed for 24 hours and 3, 7 days to MgCl₂ independently of concentration revealed no distinct ultrastructural alterations. The neurons of various type (Fig. 1) and the compact, well organized neuropil rich in synaptic contacts (Fig. 2) showed no differences as compared with control cultures, grown in standard conditions.

The cultures, kept in medium supplemented with 100 µM of QUIN alone, displayed characteristic morphological changes, typical for the action of this neurotoxin, manifested by both neuronal and dendritic abnormalities (for details see Kida et al. 1988; Kida, Matyja 1990). Most postsynaptic elements were severely swollen (Fig. 3). The nerve cells, especially large pyramidal neurons, showed clumping of nuclear chromatin and vacuolar degeneration of the cytoplasm (Fig. 4). Seven days after QUIN exposure a lot of large nerve cells were severely damaged exhibiting destruction of both nucleus and cytoplasmic organelles.

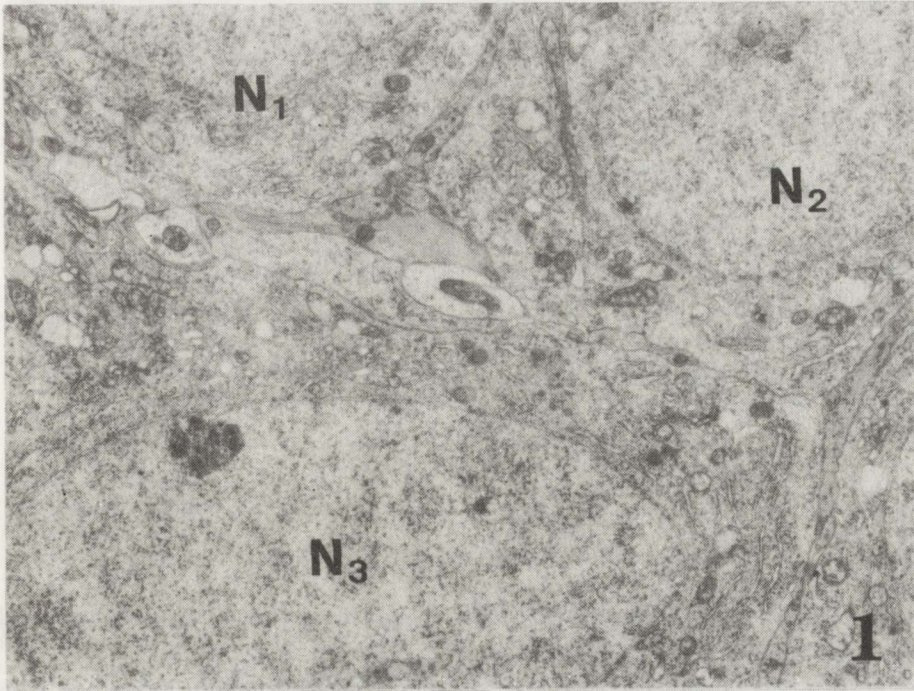


Fig. 1. Hippocampal culture 21 DIV + 3 days after MgCl₂ application. Neurons (N₁, N₂, N₃) display well preserved nucleus and cytoplasmic organelles. x 7500

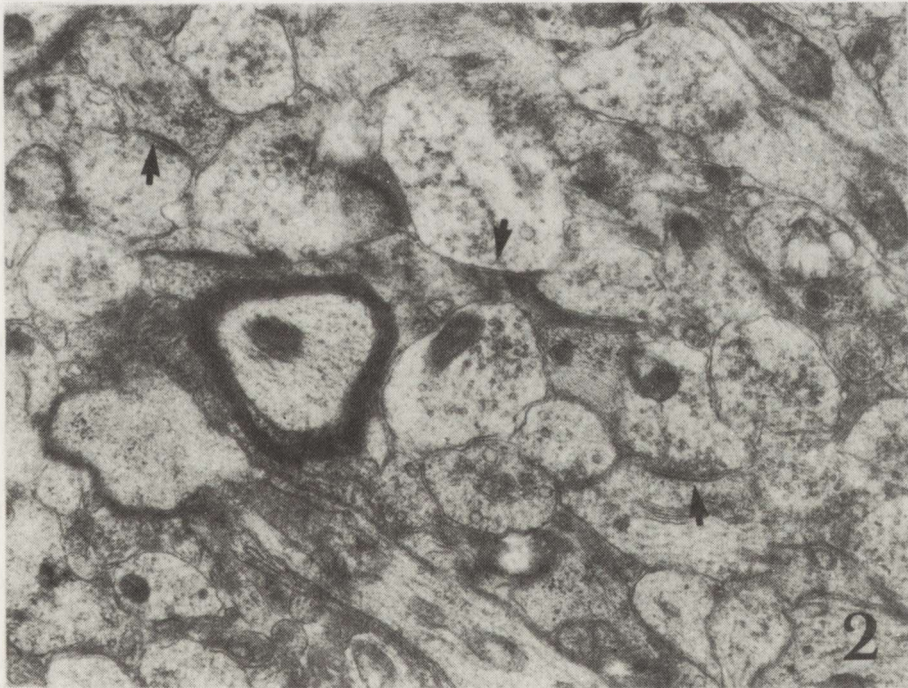


Fig. 2. The same culture. Dense neuropil containing numerous synaptic contacts between normally appearing postsynaptic dendrites and axonal boutons (arrows). x 12 500

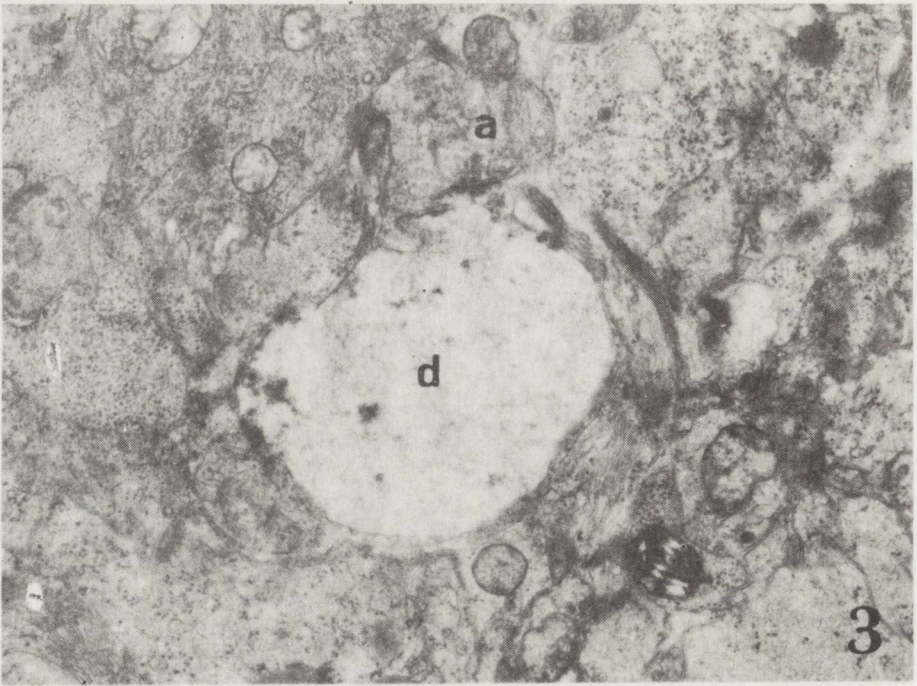


Fig. 3. Hippocampal culture 21 DIV + 3 days after exposure to QUIN. Severely enlarged, electron-lucent postsynaptic dendrite (d) containing only remnants of organelles. Well preserved axonal terminal (a). x 18 500

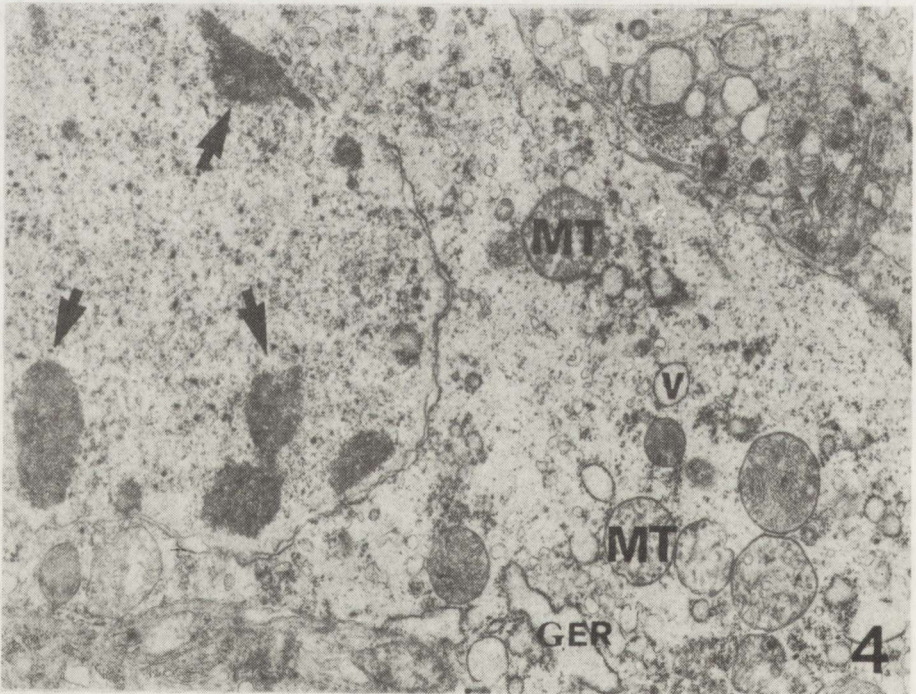


Fig. 4. The same culture. Degenerated pyramidal neurons exhibiting clumping of nuclear chromatin (arrows) and electron-lucent cytoplasm with damaged mitochondria (MT), dilated channels of granular endoplasmic reticulum (GER), vacuoles (v) and vesicles. x 15 000

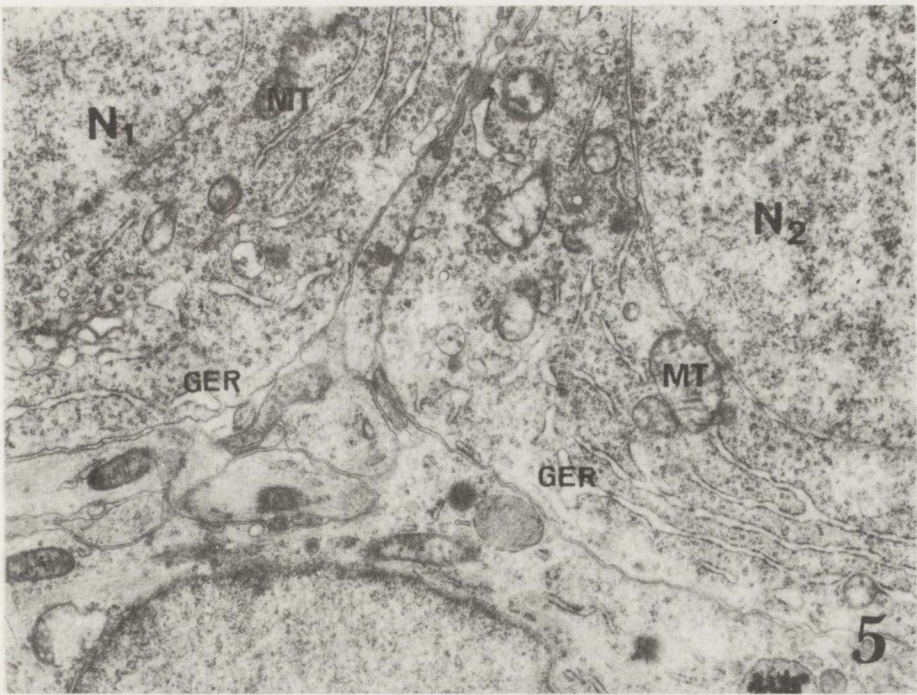


Fig. 5. Hippocampal culture 21 DIV + 24 hours after QUIN and 100 μ M of $MgCl_2$ application. Two normally appearing pyramidal neurons (N_1 , N_2). Unchanged nucleus, relatively well preserved mitochondria and slightly dilated channels of granular endoplasmic reticulum (GER).
x 17 500

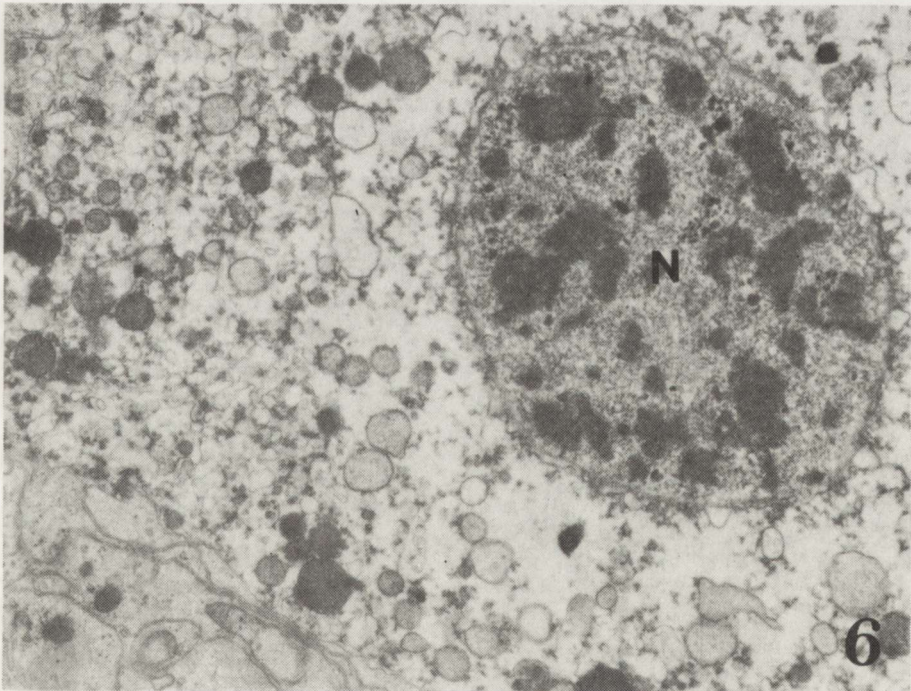


Fig. 6. Hippocampal culture 21 DIV + 7 days after QUIN and 100 μ M of $MgCl_2$ application. Severely damaged nerve cell. Nucleus (N) exhibiting clumping of nuclear chromatin. Numerous damaged organelles, vacuoles of various size and dense bodies. x 15 500

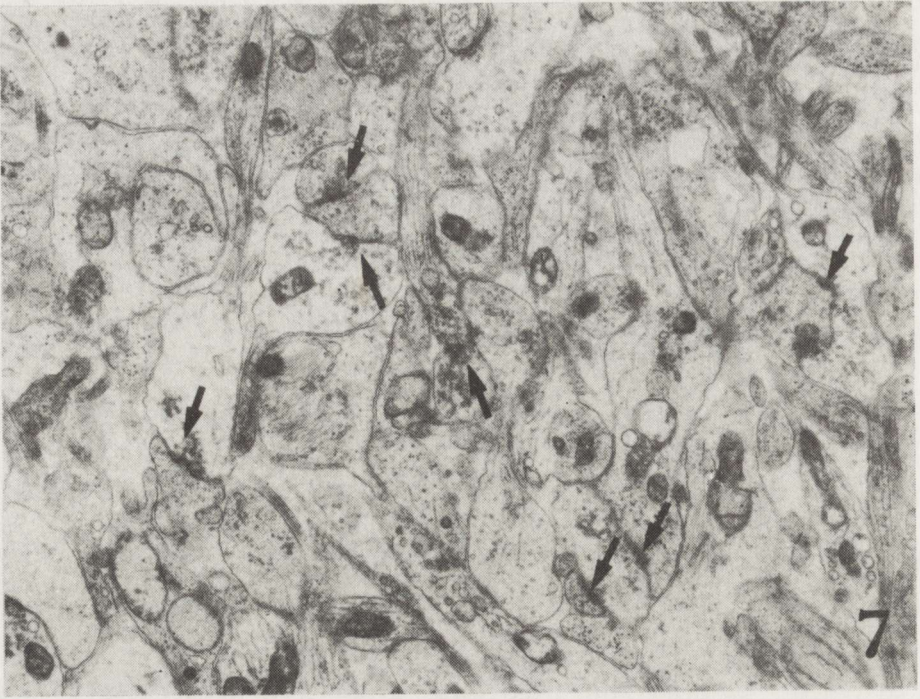


Fig. 7. 24 hours after QUIN and 100 μ M of $MgCl_2$ treatment. Dense neuropil with numerous quite well-preserved synapses (arrows). x 15 000

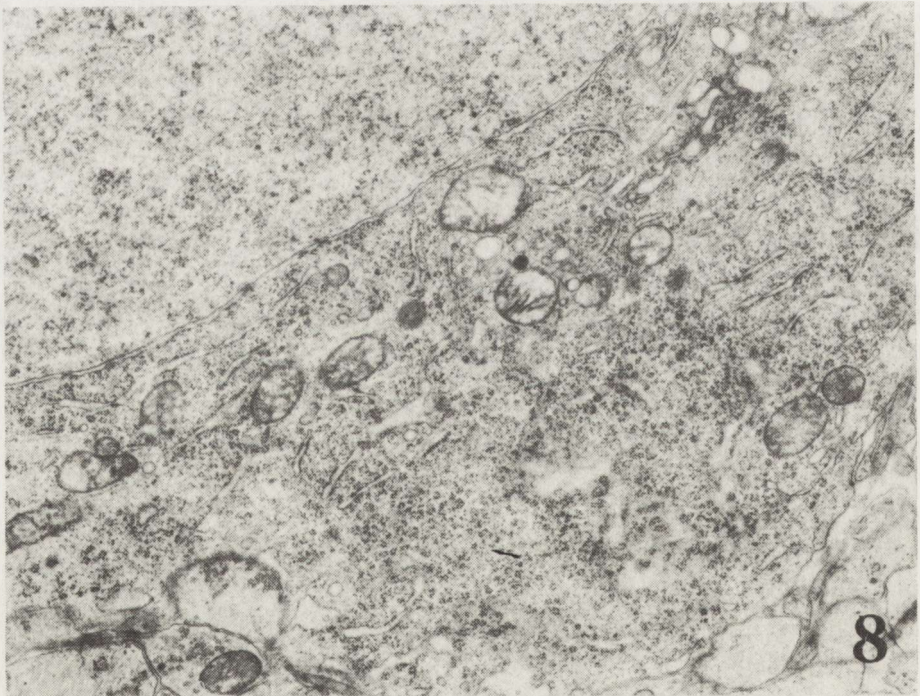


Fig. 8. Hippocampal culture. 3 days after QUIN and 1 mM of $MgCl_2$ exposure. Well-preserved pyramidal neurons. x 19 000

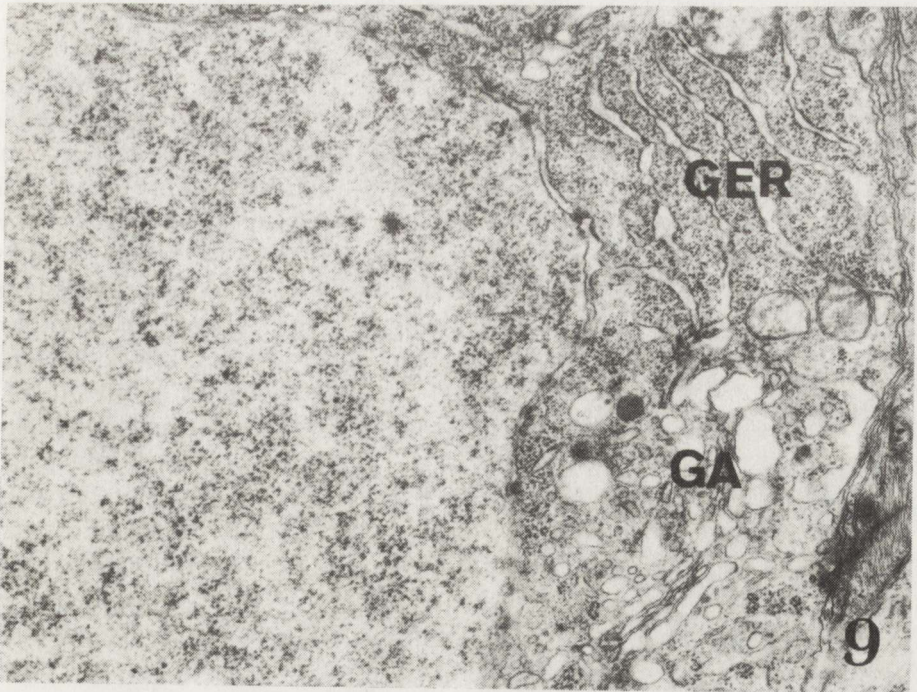


Fig. 9. The same culture. Pyramidal neurons exhibit slightly dilated channels of granular endoplasmic reticulum (GER) and well-developed Golgi apparatus (GA). x 20 000

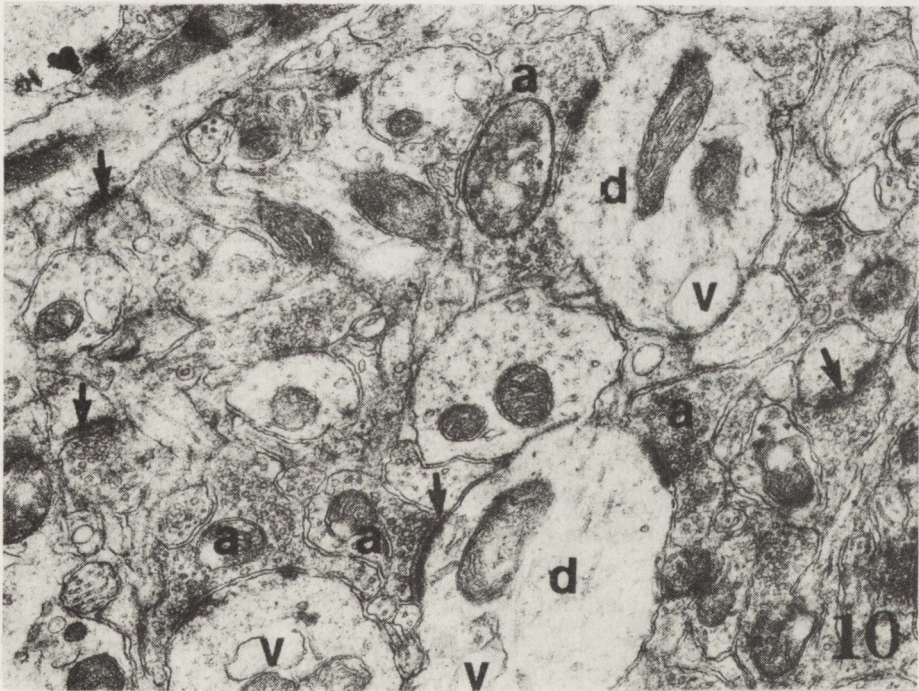


Fig. 10. The same culture. Neuropil with numerous synapses (arrows) Some postsynaptic dendrites (d) containing single vacuoles (v). Intact axonal boutons (a). x 30 000

The cultures exposed simultaneously to QUIN and $MgCl_2$ showed less advanced and rarely encountered degenerative changes in comparison with the cultures treated with QUIN alone. However, the protective effect of Mg^{2+} ions depended on the concentration of $MgCl_2$ in the culture medium. After 24-h exposure to medium containing the lower dose of $MgCl_2$ (100 μM) only some pyramidal neurons were preserved (Fig. 5). Nevertheless, still a large number of nerve cells showed pronounced ultrastructural abnormalities, especially in the later stages of observation. The character of neuronal damage resembled the pattern of QUIN-induced changes, including severe cell swelling and nuclear alterations. The nucleus displayed clumping of nuclear chromatin and disintegration of the nuclear membrane (Fig. 6). However, the main difference consisted of a greater number of preserved, but distinctly damaged organelles visible in the swollen cytoplasm, in contrast to the almost "empty" appearance of the cell cytoplasm observed after QUIN treatment. Neuropil examined after 24 hours post QUIN and $MgCl_2$ treatment was quite well preserved. The axon and dendritic processes were still numerous and showed no evidence of ultrastructural changes (Fig. 7). The cultures examined 3 and 7 days after exposure to QUIN and $MgCl_2$ still revealed the presence of degenerating nerve cells exhibiting severely damaged organelles.

The cultures exposed simultaneously to QUIN and higher (1 mM) concentration of $MgCl_2$ showed less pronounced morphological changes of both dendritic processes and neurons. A lot of pyramidal nerve cells were quite well preserved independently of the time of observation (Fig. 8). However, also in these experiments some large nerve cells displayed ultrastructural abnormalities consisting in mitochondrial changes, enlargement of cisternae of Golgi apparatus and dilatation of granular endoplasmic reticulum (Fig. 9). However, vacuolization of the neuronal cytoplasm due to degenerative changes of mitochondria and cisternae of endoplasmic reticulum, typical for QUIN action, were never seen. The neuropil was quite well preserved and the majority of dendritic endings and axonal boutons did not reveal morphological abnormalities (Fig. 10). A few swollen postsynaptic dendrites forming synaptic contacts with several axonal boutons could be observed occasionally.

DISCUSSION

The results indicate that magnesium applied simultaneously with QUIN is able to diminish typical QUIN-induced tissue damage in hippocampal cultures. This effect seemed to be dose-dependent as it has been found, that the lower concentration of magnesium ions could prevent only acute postsynaptic damage induced by QUIN action, whereas, severe excitotoxic neuronal injury was only partially reduced. Dendritic changes, typical for QUIN, were not found, independently of the time of survival post QUIN and Mg^{2+} exposure. In contrast to the well preserved postsynaptic elements numerous nerve cells were affected even as early as 24 hours after application of the two agents.

Especially, after the low concentration of MgCl₂, large pyramidal neurons displayed advanced morphological changes representing irreversible cell injury.

It has been recently suggested that physiological concentration of magnesium can block ion channels linked to NMDA-receptors (Nowak et al. 1984). The transient decrease in Mg²⁺ may support the development of seizure activity due to removal of the voltage-dependent block, which Mg²⁺ exerts on NMDA-activated ionophores (Köhr, Heinemann 1988). If the action exerted by magnesium ions on NMDA receptors is voltage-dependent, it could be reversed by depolarization of the membrane (Mayers et al. 1984; Nowak et al. 1984). Our experiments showed that, because of the drastic depolarization of NMDA-subtype receptors by QUIN, Mg ions in lower concentration became unable to block NMDA receptors at the hyperpolarized membrane.

It has been documented that activation of a relatively small fraction of the NMDA receptors population might be sufficient to produce substantial neuronal injury (Choi et al. 1988). Moreover, the membrane ionic conductance in the tissue culture might differ markedly from those *in vivo* as it was suggested in cerebellar cultures being more vulnerable to swelling-induced lysis (Garthwaite et al. 1986). Thus, the occurrence of death of some neurons following exposure to QUIN and lower Mg²⁺ concentration in the present experiment suggests that neurons in cell culture might be more vulnerable to QUIN than *in vivo*, similarly to the glutamate toxicity in cerebellum culture demonstrated by Brooks and Burt (1980).

WPLYW MAGNEZU NA USZKODZENIA WYWOŁANE POD WPLYWEM KWASU CHINOLINOWEGO W STRUKTURZE HIPOKAMPA IN VITRO

Streszczenie

Celem badań była ocena wpływu MgCl₂ na neurotoksyczne działanie kwasu chinolinowego (QUIN). Badania przeprowadzono na hodowlach organotypowych hipokampa szczura, do których podawano MgCl₂ w stężeniu 100 μM oraz 1 mM równocześnie z kwasem chinolinowym. Jony magnezu w niskim stężeniu były zdolne do zmniejszania uszkodzeń elementów postsynaptycznych, podczas gdy ostre, toksyczne uszkodzenia komórek nerwowych były tylko częściowo zredukowane. Wyższe stężenie Mg²⁺ powodowało zmniejszenie stopnia uszkodzeń zarówno elementów postsynaptycznych, jak i neuronów piramidowych. Efekt ochronny wyższego stężenia Mg²⁺ może być związany z dostatecznym hamowaniem aktywności receptorów NMDA.

REFERENCES

1. Adult B, Evans RH, Francis AA, Oakes DJ, Watkins JC: Selective depression of excitatory amino acid induced depolarizations by magnesium ions in isolated spinal cord preparations. *J Physiol*, 1980, 307, 413–428.
2. Brooks N, Burt DR: Development of muscarinic receptor binding in spinal cord cultures and its reduction by glutamic and kainic acids. *Dev Neurosci*, 1980, 3, 118–127.
3. Choi DW: Glutamate neurotoxicity in cortical cell culture is calcium dependent. *Neurosci Lett*, 1985, 58, 293–297.

4. Choi DW, Koh J, Peters S: Pharmacology of glutamate neurotoxicity in cortical cell culture. *J Neurosci*, 1988, 8, 185-196.
5. Cotman CW, Monaghan DT, Otterson OP, Storm-Mathisen J: Anatomical organization of excitatory amino acid receptors and their pathways. *Trends Neurosci*, 1987, 10, 273-279.
6. Flatman JA, Schwindt PC, Crill WE: The induction and modification of voltage-sensitive responses in cat neocortical neurons by N-methyl-D-aspartate. *Brain Res*, 1986, 363, 62-77.
7. Garthwaite G, Hajos F, Garthwaite J: Ionic requirements for neurotoxic effects of excitatory amino acid analogues in rat cerebellar slices. *Neuroscience*, 1986, 18, 437-447.
8. Kida E, Matyja E: Dynamics and pattern of ultrastructural alterations induced by quinolinic acid in organotypic culture of rat hippocampus. *Neuropatol Pol*, 1990, 28, 67-82.
9. Kida E, Matyja E, Khaspekov L: The ultrastructure of rat hippocampal formation in organotypic tissue culture after exposure to quinolinic acid. *Neuropatol Pol*, 1988, 26, 507-520.
10. Kohr G, Heinemann U: Differences in magnesium and calcium effects on N-methyl-D-aspartate- and quisqualate-induced decrease in extracerebellar sodium concentration in rat hippocampal slices. *Exp Brain Res*, 1988, 71, 425-430.
11. Mayer ML, Westbrook GL, Guthrie PB: Voltage-dependent block by Mg^{2+} of NMDA responses in spinal cord neurons. *Nature*, 1984, 309, 261-263.
12. Nowak L, Bregestovski P, Ascher P, Herbert A, Prochiantz A: Magnesium gates glutamate-activated channels in mouse central neurons. *Nature*, 1984, 307, 462-465.
13. Perkins MN, Stone TW: Quinolinic acid: regional variations in neuronal sensitivity. *Brain Res*, 1983, 259, 172-176.
14. Schwarcz R, Foster AC, French ED, Whetsell Jr WO, Kohler C: Excitotoxic models for neurodegenerative disorders. *Life Sci*, 1984, 35, 19-32.
15. Stone TW, Connick JH: Quinolinic acid and other kynurenines in the central nervous system. *Neuroscience*, 1985, 15, 597-617.
16. Stone TW, Connick JH, Winn P, Hastings MH, English M: Endogenous excitotoxic agents. In: *Selective neuronal death*. Eds: G Bock and M O'Connor, Ciba Foundation Symposium 126. Wiley a. Sons, Chichester, 1987, pp 204-220.
17. Thomson AM: A magnesium sensitive post-synaptic potential in rat cerebral cortex resembles neuronal responses to N-methylaspartate. *J Physiol*, 1986, 370, 531-549.

Author's address: Department of Neuropathology, Medical Research Centre, Polish Academy of Sciences, 3 Dworkowa Str, 00-784 Warsaw, Poland

JANINA RAFAŁOWSKA¹, EWA DOLIŃSKA¹, DOROTA DZIEWULSKA¹ STANISŁAW
KRAJEWSKI²

ASTROCYTIC REACTIVITY IN VARIOUS STAGES OF HUMAN BRAIN INFARCT IN MIDDLE AND SENILE AGE*

¹Department of Neurology, School of Medicine, Warsaw, ²Department of Neuropathology,
Medical Research Centre, Polish Academy of Sciences, Warsaw, Poland

The examined material comprised 15 cases of ischemic brain infarct in subjects aged from 45 to 101 years (6 brains of the deceased patients aged from 45 to 57 years and 9 brains of aged from 80 to 101 years). Astroglial cell immunoreactivity in both age groups was compared. The technique of the peroxidase-antiperoxidase of Sternberger's et al. (1970) for visualization of GFAP immunoreactivity was used. Results of our investigations revealed that within the first two days after ischemic brain infarct astroglial cell reactivity was very poor in both age groups. In the surroundings of the necrotic lesion immunoreactive astrocytes appeared from the 3rd day after stroke. They were more numerous and their activity was more pronounced in middle-aged cases than in senile ones. It is suggested that age may modify the action of the factors having influence on astrocytic reactivity.

Key words: *Brain infarct, astroglial cell immunoreactivity, middle age, senile age.*

According to the handbooks of neurology and neuropathology, gliosis particularly fibrillary is manifested within the brain cortex, basal ganglia and within the white matter of senile brain. There is a hypothesis that proliferation of astroglial cells is a substitutional reaction in diffuse senile brain atrophy (Seitelberger 1975). However, diffuse brain atrophy is accompanied by an increase of glial cells density which may result from condensation of glial cells, without their proliferation. Morphometric studies of Miyamake et al. (1988) revealed that the number of glial cells in atrophic brain was not increased either in the II-VI cortical layers and in the white matter. Data from experimental brain injury indicate that the astroglial cells reactivity is determined by the animal's age and the astrocytic reaction does not occur in damage of neonatal rats (Janeczko 1988). Also the mature scar with participation of astrocytes and collagen fibers does not appear until the 8-12th day after birth (Berry et al. 1983). It is suggested that the reactivity of the

*Studies supported by the Central Programme of Basic Research within agreement No. 06.02.II.1.

injured brain is a function of its development degree (Janeczko 1986). Thus, the question arises whether advanced involution influences the astroglial cells reactivity during ischemic brain stroke in senile subjects.

MATERIAL AND METHODS

The examined material comprised 15 cases aged from 45 to 101 years, with ischemic brain infarcts. Clinical data, results of general autopsy and gross brain examination in those cases were published previously (Rafałowska et al. 1990). Under investigation were 6 brains of the subjects deceased at age from 45 to 57 years and 9 brains of those deceased at age from 80 to 101 years. Astroglial cell immunoreactivity in both age groups during the first five days and on the 11th and 12th day after stroke was compared. Furthermore, astroglial reactivity in cases of the deceased on the 6th, 15th and 35th day of disease was estimated. In all the cases autopsy was performed within 24 h after death.

Formalin-fixed and paraffin-embedded slices from infarct area and its surroundings were investigated immunocytochemically. The peroxidase-antiperoxidase method of Sternberger et al. (1970) was used for visualization of astroglial cell immunoreactivity to glial fibrillary acidic protein (GFAP). The immunocytochemical reactions were run as follows: 5–8 μm thick sections, deparaffinized and pretreated with 0.0125% trypsin for 1 h, were preincubated with 2% normal swine serum diluted with trisma-base (Sigma, USA) at pH 7.6. Thereafter, they were incubated overnight with primary polyclonal rabbit antibodies against GFAP (1:3000, Dakopatts, RFG). After rinsing the sections with PBS, pH 7.6, they were incubated with the following secondary reagents for 1 h: swine antibodies against rabbit IgG (1:50) and rabbit-PAP-complex (1:200), all antisera from Dakopatts, Denmark. The immune reaction was developed during 15 min incubation in 0.05% Diaminobenzidine tetrachloride (Sigma, USA) with addition of 0.01% H_2O_2 . Afterwards the sections were counterstained with hemalum, dehydrated and mounted with DePeX (Serva FRG).

RESULTS

On the first and second day after stroke, in both middle-aged and senile cases, within the nonreactive necrotic area numerous GFAP-positive particles of various size and shape were visible. A few immunoreactive astrocytes were shrunken and deprived of processes (Figs 1 and 2). Similarly changed astrocytes, somewhat more numerous in middle-aged cases, were seen in the partially necrotic infarct surroundings. On the third day in the middle-aged (49 years) case, within the infarct region festoonlike areas completely immunonegative to GFAP were noted. Less damaged parts of the cerebral cortex adjacent to tissue necrosis revealed proliferation of astrocytes and the presence

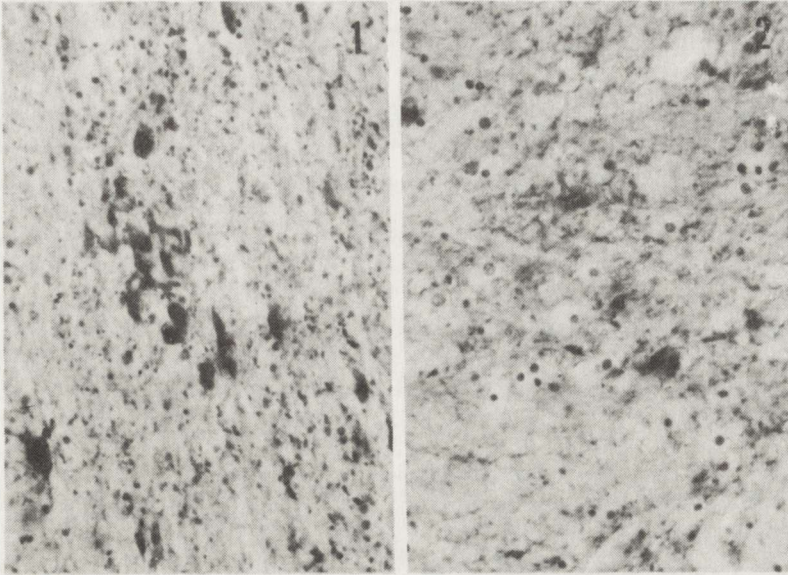


Fig. 1. Middle-aged case (53 years), 2nd day after stroke. Partially necrotic area. Numerous GFAP-positive particles and regressive changes of immunoreactive astrocytes. x 448

Fig. 2. Senile case (80 years) 2nd day after stroke. Partially necrotic area. Regressive changes of non-numerous immunoreactive astrocytes. x 448

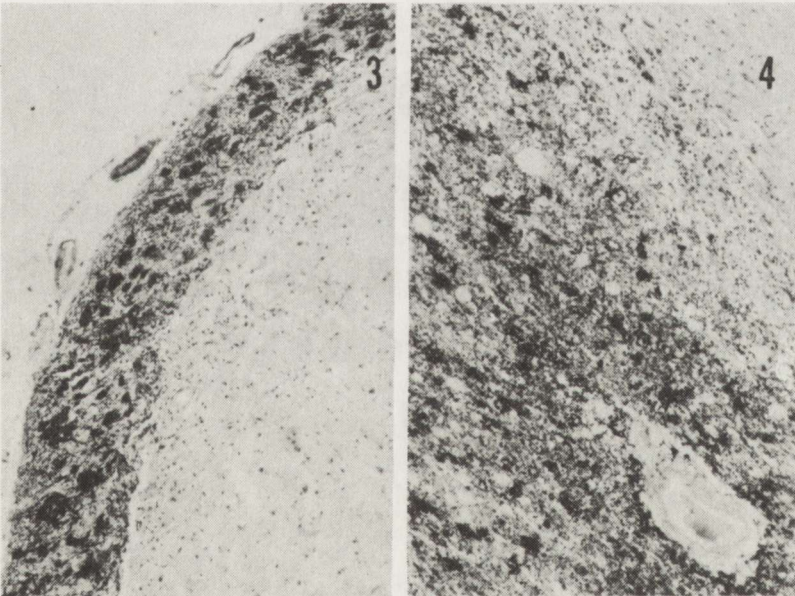


Fig. 3. Middle-aged case (49 years), 3rd day after ischemic incident. Necrotic area immunonegative to GFAP. Hypertrophy and proliferation of astrocytes in relatively well preserved cortical molecular layer. x 112

Fig. 4. The same case as in Fig. 3. Numerous GFAP-positive astrocytes in white matter adjacent to necrotic region. x 112

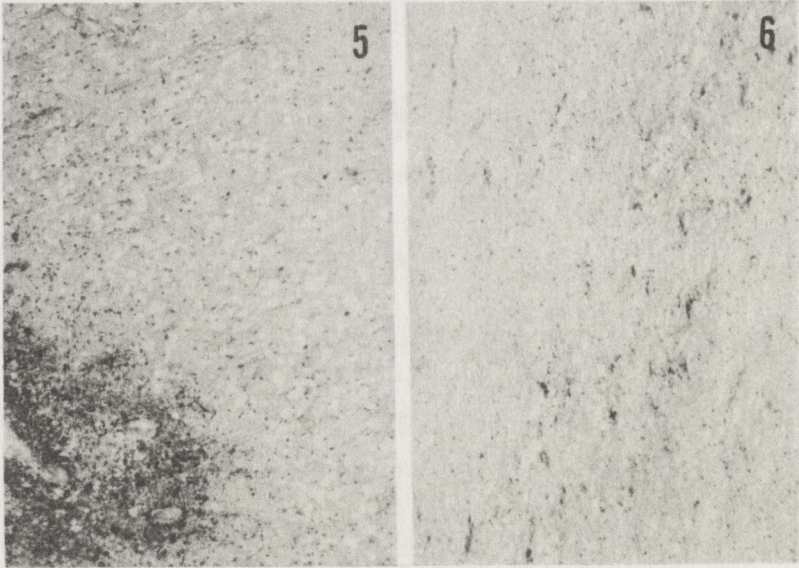


Fig. 5. Senile case (88 years), 3rd day after stroke. Spongy state in cerebral cortex within infarct region. Hypertrophic astrocytes in sulcal area of a better preserved cortical molecular layer. x 112
Fig. 6. Senile case (88 years), 3rd day after infarct. Non-numerous immunoreactive astrocytes in partially necrotic white matter x 112

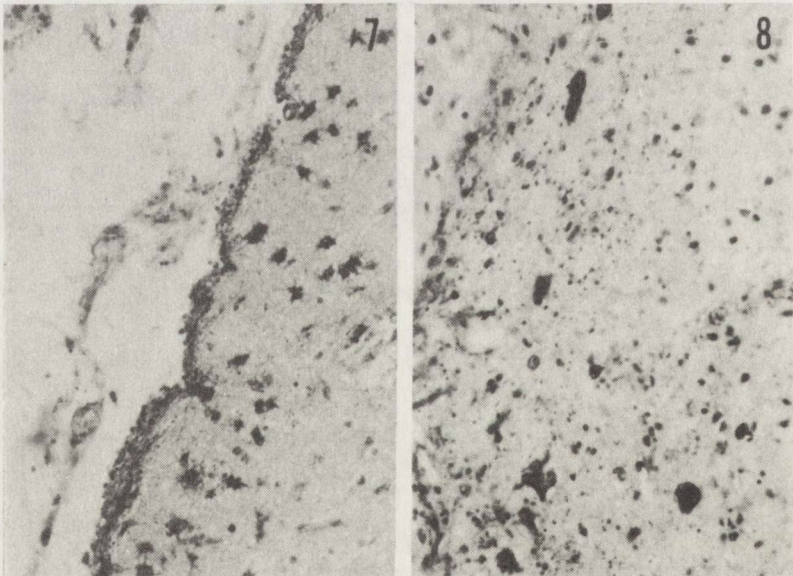


Fig. 7. Middle-aged case (55 years), 4rd day after brain stroke. Hypertrophy and moderate proliferation of astrocytes in cortical molecular layer. x 224
Fig. 8. Senile case (86 years) with the same survival time. Regressive changes of immunoreactive astrocytes in cortical molecular layer. Numerous GFAP-immunopositive particles. x 224

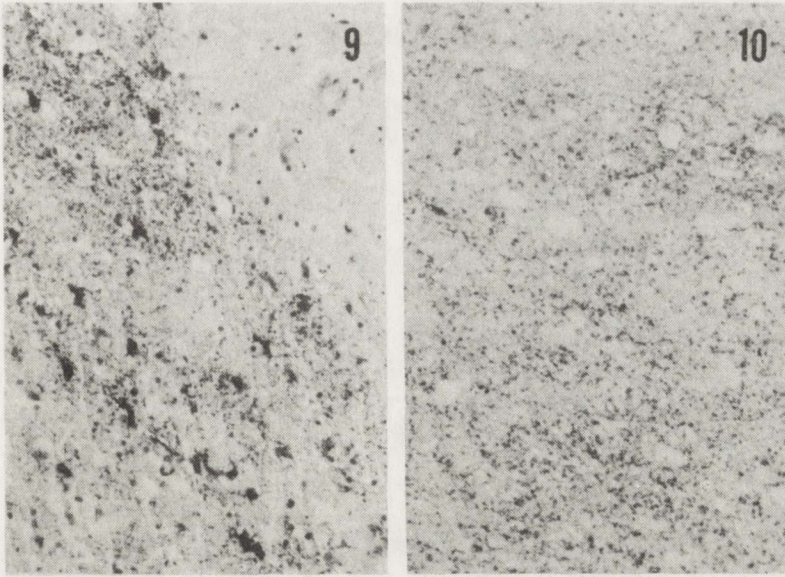


Fig. 9. Middle-aged case (55 years), 4rd day after infarct. Astrocytic proliferation and hypertrophy in white matter adjacent to necrotic focus. x 224

Fig. 10. Senile case (86 years) with the same survival time. In white matter adjacent to infarct region numerous GFAP-immunopositive particles. x 224

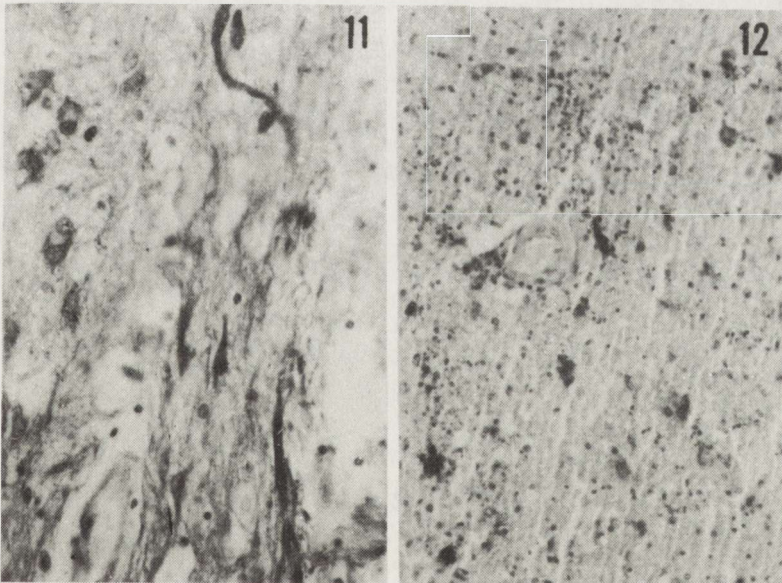


Fig. 11. Middle-aged case (45 years), 5th day after infarct. Rosenthal's fibers in white matter adjacent to cavitated necrotic tissue. x 448

Fig. 12. Senile case (86 years), 5 days of survival. A few immunoreactive astrocytes in white matter adjacent to infarct region. x 224

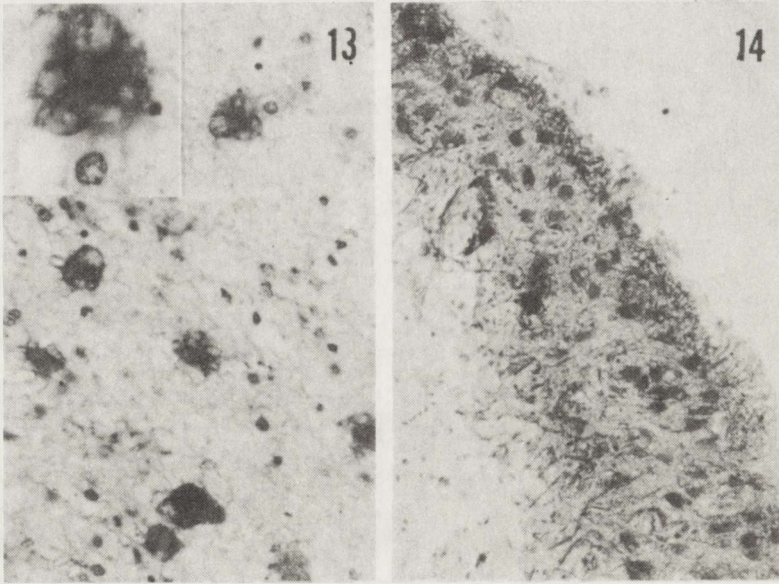


Fig. 13. Senile case (87 years), 11 days of survival. White matter adjacent to necrotic focus. Vacuolar degeneration of gemistocytes. x 448. Insert: gemistocyte with numerous vacuoles
Fig. 14. Senile case (83 years), 35 days after brain stroke. Distinct astroglial reaction in cortical molecular layer adjacent to necrotic focus. x 224

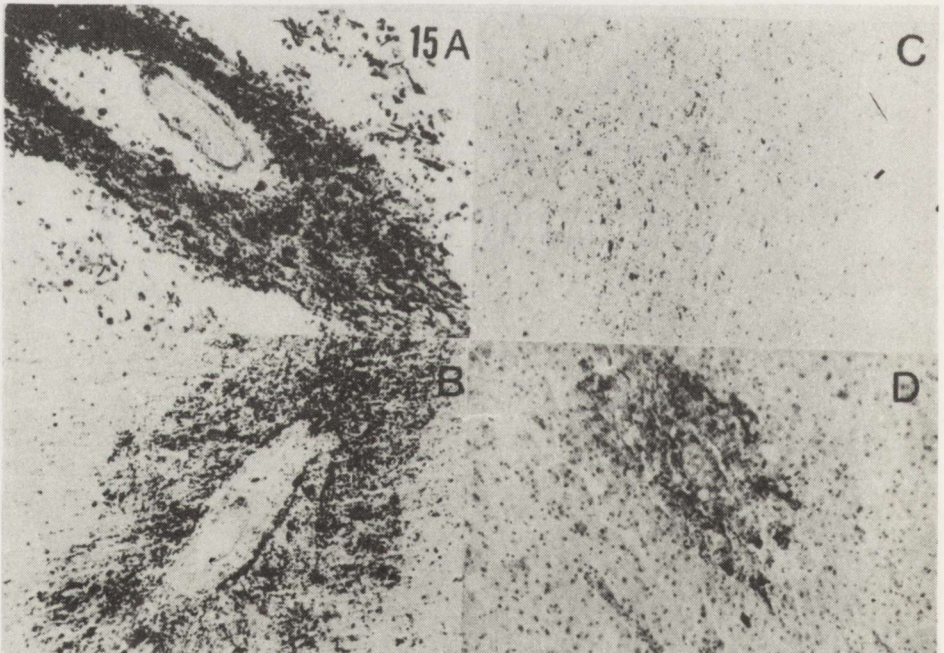


Fig. 15. Immunoreaction of astrocytes in better preserved tissue islands within necrotic foci. x 224.
A—case 49-year-old, 3rd day after infarct. *B*—case 86-year-old, 5 days after brain stroke. *C*—case 101-year-old with 6 days of survival. *D*—case 87-year-old, survived 15 days after ischemic incident

of their hypertrophic and gemistocytic forms (Fig. 3). White matter in the neighbourhood of the infarct revealed also proliferation and hypertrophy of astrocytes (Fig. 4) as well as clasmatodendrosis of their processes. In this case thick processes, immunopositive to GFAP, resembling Rosenthal's fibers were noted. In the senile case (88 years) with the same survival time, the infarct region presented spongy changes without features of tissue breakdown and astroglial cells immunoreactivity. GFAP-positive astrocytes were seen only in the adjacent better preserved cortical layers (Fig. 5). In the less damaged tissue islands within the spongy basal ganglia mainly GFAP-positive particles and a few immunoreactive astrocytes were found. White matter in the vicinity of the infarct region showed similar changes (Fig. 6). In this case poor proliferation of astrocytes was striking. Differences in the astroglial reactivity between the middle-aged and senile cases were also disclosed on the 4th day after brain stroke (Figs 7–10).

On the 5th day after ischemic incident, in the middle-aged case (45 years) infarct cavitation was found, whereas in senile case (86 years) festoonlike infarct region did not exhibit tissue breakdown. In the middle-aged case immunoreactive astrocytes and gemistocytes in the cortical molecular layer adjacent to cystic area, were rather numerous, whereas in the senile case poor astrocytic reactivity was noted. In the white matter adjacent to the infarct region, in middle-aged case, besides some gemistocytes with short irregular processes, single thick fibers, immunoreactive to GFAP (Fig. 11) resembling Rosenthal's fibers, were observed. In the senile case at the infarct border astroglial cells revealed a poor immunoreactivity (Fig. 12).

In the group of senile cases with longer survival time after brain stroke the astrocytic reactivity varied in particular cases. However, in general the surroundings of the infarcted region exhibited in longer surviving subjects more advanced glial proliferation and hypertrophy (Fig. 14). Sometimes hypertrophic astrocytes showed significant regressive changes with vacuolar degeneration (Fig. 13). Irregular thick processes resembling Rosenthal's fibers were found in one senile case on the 35th day after brain stroke. Comparison of the astrocytic reaction in the island of better preserved tissue within necrotic focus revealed its higher intensity in middle-aged than in senile cases (Fig. 15).

DISCUSSION

Results of our investigations indicate that, during the first two days after ischemic brain infarct, astroglial cell reactivity is very poor in both age groups and regressive changes predominate. As known, tissue ischemia is followed by profuse metabolic disturbances. They bring about tissue acidosis due to, i.a., accumulation of lactates (Rafałowska et al. 1978) impairing both nerve cells (Rehncrona et al. 1985) and their processes and myelin sheaths (Balentine, Green 1987). Experimental studies of Rehncrona et al. (1985) revealed that ischemia and tissue lactic acidosis lead to energy and electrophysiological

disturbances, the intensity of which is determined by intensity and duration of lactic acidosis. Astrocytes are quite resistant to tissue acidosis. Norenberg et al. (1987a) demonstrated in primary tissue culture that lactic acidosis at pH 5.0 causes irreversible changes in astrocytes after 10–30 min. An increase of hydrogen ions acts similarly as lactic acidosis (Norenberg et al. 1987b). In human ischemic brain stroke the intensity of tissue acidosis is very hard to determine. However, profuse ion changes initiating a cascade of metabolic disturbances within the infarct area and its surroundings lead to an irreversible impairment of nerve and glial cells. This was perhaps manifested in our material as a lack of astrocyte immunoreactivity during the first two days after infarct.

In the surroundings of the necrotic region, GFAP-positive astrocytes appeared on the third day after ischemic insult, they were more numerous in middle-aged than in senile cases. Experimental studies revealed a decrease of blood flow and metabolic disturbances within the infarct surroundings, however, of a lower intensity than within necrotic region (Mies et al. 1983). Such disturbances may evoke reversible structural and biochemical changes, influencing, i.a. enzymatic processes in the astrocytes, connected with the presence of creatine kinase BB-isoenzyme (Thompson et al. 1980; Yoshimine et al. 1983), protein kinase C (Norenberg et al. 1987b) or carbonic anhydrase (Cammer, Tansey 1988a, b). However, it does not explain the delayed and less intensive astrocyte reactivity in senile cases as compared with middle-aged ones. It is not known whether in a senile brain the cells synthesize a smaller quantity of enzyme, or synthesize it slower, or perhaps not the quantity of enzyme is changed, but its metabolic activity is reduced. The alterations in senile brain homeostasis may influence all these factors (Freilich, Weiss 1983). An intensive astrocytic reactivity accompanied by regressive changes of astrocyte bodies and their processes on the 11th and the 35th day after stroke in two senile cases may be an exponent of individual variations in the senile brain reactivity or aging itself.

It is presumed that there exists a relation between hypertrophy of astrocytes and microglial proliferation (Gall et al. 1979; Gage et al. 1988). In our material the microglial reaction was poor in cases of both age groups, similarly as in the majority of other cases with cerebral vascular diseases.

It should be emphasized, that thick irregular processes resembling Rosenthal's fibers were observed in 3 middle-aged cases (on 3rd, 5th and 12th days after stroke) and only in one senile case (on 35th day). Rosenthal's fibers are immunoreactive to GFAP (Johnson, Bettice 1986) and mainly contain GFAP, vimentin and 17KMW protein. The latter protein is present in normal brains (Goldman 1987).

Lack of morphometric investigations excludes precise determination of the astroglia proliferation. However, it seems that in middle-aged cases this proliferation was more pronounced. Proliferation of astrocytes occurs in many pathological conditions and is caused by various pathological factors. In recent

experimental data it is considered that brain tissue damage itself does not induce directly proliferation of the astrocytes, but *via* the synthesis of compounds stimulating proliferation. Autolytic digestion of impaired brain tissue is associated with an increase of the fibroblast growth factor (FGF) (Berry et al. 1983), what leads further to a release of plasminogen activators (Rogister et al. 1988). The latter play an important role in the process of development, in which they act as a stimulating astrocyte mitosis factor (Moonen et al. 1985). Astrocytosis also occurs in the regions of endings of nerve fibers regenerating after injury (Scheider, Denaro 1988). According to Gage et al. (1988) astrocytes synthesize and secrete the nerve growth factor (NGF) the activity of which increases in the areas of axonal outgrowth. In the deafferented areas astrocytes are immunoreactive to the epidermal growth factor (EGF), which seems to be an indicator of astrocytic reactivity (Nieto-Sampedro et al. 1988). Each of the mentioned above factors could be engaged in our cases; in the senile group perhaps their role was smaller. Decreased activity or content of various neurotransmitters in the senile brain (McGeer et al. 1977; Algeri et al. 1983, Joseph, Ruth 1983) suggest, that aging could modify the action of various biochemical compounds, and among them also the factors having influence on astrocytic reactivity.

REAKTYWNOŚĆ ASTROCYTÓW W RÓŻNYCH OKRESACH ROZWOJU ZAWAŁU MÓZGU U LUDZI W WIEKU ŚREDNIM I STARCZYM

Streszczenie

Badany materiał obejmował 13 przypadków autopsyjnych z niedokrwiennym zawałem mózgu u pacjentów w wieku 45–101 lat. Grupa w wieku średnim obejmowała 6 przypadków w wieku 45–57 lat, grupa starcza – 9 przypadków w wieku 80–101 lat. W obu grupach wieku porównano immunoreaktywność komórek astrogliowych. Dla ujawnienia kwaśnego białka włóknikowego (GFAP) zastosowano metodę immunoperoksydazy pośredniej według Sternbergera i wsp. (1970). W okresie pierwszych dwóch dni po udarze w obu grupach wieku wykazano bardzo skąpy odczyn immunocytochemiczny. Immunoreaktywne astrocyty w otoczeniu ognisk martwicy pojawiały się w przypadkach z 3-dniowym przeżyciem. Były one liczniejsze i wykazywały bardziej nasilony odczyn w przypadkach w wieku średnim niż w grupie starczej. Autorzy sugerują, że zaawansowany wiek może wpływać modyfikująco na te czynniki, które warunkują odczynowość astrogliu.

REFERENCES

1. Algeri S, Calderini G, Toffano G, Ponzio F: Neurotransmitter alteration in aging rats. In: Aging of the brain. Eds: D Samuel, S Gershon, VE Grimm, G Toffano, Raven Press, New York, 1983, pp 227–243.
2. Balentine JD, Green WB: Myelopathy induced by lactic acid. Acta Neuropathol (Berl), 1987, 73, 233–239.
3. Berry M, Maxwell WL, Logan A, Mathewson A, McConnel P, Ashhurst DE, Thomas GH: Deposition of scar tissue in the central nervous system. Acta Neurochir, 1983, Suppl 32, 31–53.

4. Cammer W, Tansey FA: Localization of glial cell antigens in the brains of young normal mice and the dysmyelinating mutant mice, jimpy and shiverer. *J Neurosci Res*, 1988 a, 20, 23–31.
5. Cammer W, Tansey FA: Carbonic anhydrase immunostaining in astrocytes in the rat cerebral cortex. *J Neurochem*, 1988 b, 50, 319–322.
6. Freilich JS, Weiss B: Altered adaptive capacity of brain catecholaminergic receptors during aging. In: *Aging of the brain*. Eds: D Samuel, S Gershon, VE Grimm, G Toffano. Raven Press, New York, 1983, 277–300.
7. Gage FH, Olejniczak P, Armstrong DM: Astrocytes are important for sprouting in the septohippocampal circuit. *Exp Neurol*, 1988, 102, 2–13.
8. Gall C, Rose G, Lynch G: Proliferative and migratory activity of glial cells in the partially deafferented hippocampus. *J Comp Neurol*, 1979, 183, 539–549.
9. Goldman JE: Isolation of 17KMW component of Rosenthal fibers. *J Neuropathol Exp Neurol*, 1987, 46, 351 (Abstr).
10. Janeczko K: Age-dependent response to injury of the cerebral hemisphere tissue of rats. A quantitative autoradiographic study. *Folia Biol (Kraków)*, 1986, 34, 3–20.
11. Janeczko K: The proliferative response of astrocytes to injury in neonatal rat brain. A combined immunocytochemical and autoradiographic study. *Brain Res*, 1988, 456, 280–285.
12. Johnson AB, Bettica A: Rosenthal fibers in Alexander's disease show glial fibrillary acidic protein (GFAP) immunoreactivity with the immunogold staining method. *J Neuropathol Exp Neurol*, 1986, 45, 349 (Abstr).
13. Joseph JA, Roth GS: Age-related alterations in dopaminergic mechanisms. In: *Aging of the brain*. Eds: D Samuel, S Gershon, VE Grimm, G Toffano. Raven Press, New York, 1983, 245–256.
14. McGeer PL, McGeer EG, Suzuki JS: Aging and extrapyramidal function. *Arch Neurol*, 1977, 34, 33–35.
15. Mies G, Auer LM, Ebhardt G, Traupe H, Heiss WD: Flow and neuronal density in tissue surrounding chronic infarction. *Stroke*, 1983, 14, 22–27.
16. Miyake T, Kitamura T, Takamatsu T, Fujita S: A quantitative analysis of human astrocytosis. *Acta Neuropathol (Berl)*, 1988, 75, 535–537.
17. Moonen G, Grau-Wagemans MR, Selak J, Lefebvre PP, Rogister B, Vassalli JI, Belin D: Plasminogen activator is a mitogen for astrocytes in developing cerebellum. *Dev Brain Res*, 1985, 20, 41–48.
18. Nieto-Sampedro M, Gomez-Pinilla F, Knauer DJ, Broderic JT: Epidermal growth factor receptor immunoreactivity in rat brain astrocytes. Response to injury. *Neurosci Lett*, 1988, 91, 276–282.
19. Norenberg MD, Mozes LW, Gregorios JB, Norenberg LO B: Effects of lactic acid on astrocytes in primary culture. *J Neuropathol Exp Neurol*, 1987 a, 46, 154–166.
20. Norenberg MD, Norenberg LO B, Neary JT: Morphologic effects of a pherbol ester on astrocytes in primary culture. *J Neuropathol Exp Neurol*, 1987 b, 46, 360 (Abstr).
21. Rafałowska J, Friedman A, Karczewska E, Nibrój-Dobosz I, Tomankiewicz Z: Ocena badań gazometrycznych oraz kwasu mlekowego w krwi tętniczej i płynie mózgowo-rdzeniowym w zawałach mózgu. *Neurol Neurochir Pol*, 1978, 12, 6, 687–697.
22. Rafałowska J, Dolińska E, Dziewulska D, Krajewski S: Human brain infarcts in middle and senile age. I. Blood brain barrier permeability in immunocytochemical studies (in Polish). *Neuropatol Pol*, 1990, 28, 1–17.
23. Rehncrona S, Rosén J, Smith ML: Effect of different degrees of brain ischemia and tissue lactic acidosis on the short-term recovery of neurophysiologic and metabolic variables. *Exp Neurol*, 1985, 87, 458–473.
24. Rogister B, Leprince P, Rettman B, Labourdette G, Sensenbrenner M, Moonen G: Brain basic fibroblast growth factor stimulates the release of plasminogen activators by newborn rat cultured astroglial cells. *Neurosci Lett*, 1988, 91, 321–326.
25. Scheider JS, Denaro FJ: Astrocytic responses to the dopaminergic neurotoxin 1-met-

- hyl-4-phenyl-1,2,3,6-tetrahydropyridine (MPTP) in cat and mouse brain. *J Neuropathol Exp Neurol*, 1988, 47, 452-458.
26. Seitelberger F: General neuropathology of the degenerative diseases of the central nervous system. In *Handbook of clinical neurology*. Eds: PJ Vinken, GW Bruyn. Elsevier, New York, 1975, vol 21, 43-72.
 27. Sternberger LA, Hardy PH, Jr, Cuculis FF, Meyer MG: The unlabelled antibody enzyme method of immunohistochemistry preparation and properties of soluble antigen-antibody complex (horseradish peroxidase-antiperoxidase) and its use in identification of spirochetes. *J Histochem Cytochem*, 1970, 18, 315-333.
 28. Thompson RJ, Kynoch PAM, Sariant J: Immunohistochemical localization of creatine-kinase-BB isoenzyme to astrocytes in human brain. *Brain Res*, 1980, 201, 423-426.
 29. Yoshimine T, Morimoto K, Homburger HA, Yanagihara T: Immunohistochemical localization of creatine kinase BB-isoenzyme in human brain: comparison with tubulin and astroprotein. *Brain Res*, 1983, 265, 101-108.

Authors' address: Department of Neurology, School of Medicine, 1A Banacha Str, 02-097 Warsaw, Poland.

MARIA DAŃBSKA¹, DANUTA MAŚLIŃSKA², TADEUSZ MAJDECKI³

PREMATURE INFANT WITH TUBEROUS SCLEROSIS. MORPHOLOGICAL AND IMMUNOHISTOCHEMICAL STUDY

^{1, 2}Laboratory of Developmental Neuropathology, Medical Research Centre, Polish Academy of Sciences, Warsaw, Poland, ³Central Railway Hospital, Warsaw, Poland

The case of a premature infant of 27-week gestation, the youngest so far reported with tuberous sclerosis is described. Rhabdomyoma of the myocardium was found. The giant, atypical cells in the majority GFAP-positive were found in periventricular matrix centers, in aggregates, and were disseminated in the cerebral white matter and in the subpial "nodules". Giant cell astrocytoma was seen in the cerebellum. The findings confirm dysontogenetic differentiation in germinal centers and maturation of atypical cells along the pathways of migration.

Key words: *Tuberous sclerosis, premature infant, giant cell astrocytoma, giant glia.*

Tuberous sclerosis (TS) a dominantly inherited neuroectodermal dysplasia is known since 1880 when Bourneville recognized it as a distinct entity. The "tubers" — subependymal, cortical or found everywhere in the brain were described as containing abnormal astrocytes or neurons with some bizarre cells difficult to differentiate as glial or nerve cells (Boremann et al. 1933). Ultrastructural and immunohistochemical methods enabled the study of dysplastic cells in TS. Many reports have been published (Poivier, Escourolle 1970; Arsenio et al. 1972; Ribadeau-Dumas et al. 1973; Stefansson, Wollman 1981; Huttenlocher, Heydemann 1984; Nardell et al. 1986), but further examination concerning their final characteristics is still required.

Premature infants with TS are of particular interest for studies on dysontogenesis in this disease. Following the paper of Chou and Chou (1989) reviewing the seven so far reported cases, we have the opportunity to present a new very young case.

CASE REPORT

It was a premature male baby born in the 27th week of gestational age, after an apparently uneventful pregnancy and with no remarkable familial anamnesis. He died on the first day of life because of respiratory and circulatory insufficiency. Perinatal brain damage was clinically suspected.

At autopsy rhabdomyomata of the myocardium were found and a generalized hyperemia of the internal organs.

The brain looked like that of a premature newborn of 27–28 weeks of developmental age. On coronal sections periventricular small hemorrhages and focal disintegration of the white matter were seen. No other macroscopic abnormalities were noted.

Formalin-fixed, paraffin-embedded tissue sections comprising three levels of the cerebral hemispheres, brain stem and cerebellum were employed for routine histological evaluation as well as for examination with various immunohistochemical cell markers and the lectin. Sections 5 μm thick were deparaffinized and dehydrated and stained with hematoxylin-eosin and cresyl violet or tested with antibodies to glial fibrillary acidic protein (GFAP, Amersham), neuron specific enolase (NSE, ICN Immuno Biologicals) and *Ricinus communis*-I agglutinin (RCA-120, Vector Laboratories). The avidin-biotin-peroxidase complex (ABC) staining technique was used (Hsu et al. 1982). For studies with RCA-1 sections were incubated overnight at 4°C in a 1:1000 dilution of lectin in phosphate buffered salt solution (PBS), pH 7.6 (Wiśniewska, Maślińska 1990).

Control procedures included replacement of lectin by its specific buffer or addition of inhibiting sugar — 0.1 M solution of lactose (Sigma Chemicals).

For studies with antibodies to cell markers sections were incubated overnight at 4°C in a 1:1000 dilution of GFAP or in a 1:200 dilution of NSE in PBS, 7.6 (Wilkinson et al. 1990).

Microscopic examination confirmed both macroscopic features: developmental age \pm 27 weeks and periventricular ecchymoses surrounded by fresh necrosis usually within nests of matrix cells. The distinct neuropathological changes not suspected macroscopically consisted in aggregates of giant cells distributed in foci, but also disseminated in the white matter (Fig. 1). Numerous giant cells were observed around the blood vessels. The cells were large, dysplastic, some were binucleated, some formed syncytial-like structures. Many of them looked like protoplasmic astrocytes hypertrophied to an unusual degree. The topography of aggregations was ubiquitous. They were most numerous in centrum semiovale, but they were also found within the periventricular matrix (Fig. 2) and in the cortical molecular layer involving the glio-pial barrier (Fig. 3). Similar large cells were seen in the cerebellum in the foliar white matter. Dysplastic giant cells formed, in the cerebellar white matter near the pontocerebellar angle, a small tumor with cytoarchitecture of giant cell astrocytoma (Fig. 4). Several cells of this tumor were bi- and trinuclear. Mitoses were not observed.

The immunohistochemical reaction for GFAP was positive in nearly all the giant cells in pathological aggregates (Figs 5, 6) and also in normal astrocytes. The intensity of the reaction was uneven. Atypical giant cells in nests within matrix centers were weakly stained, while in the white matter and subpial

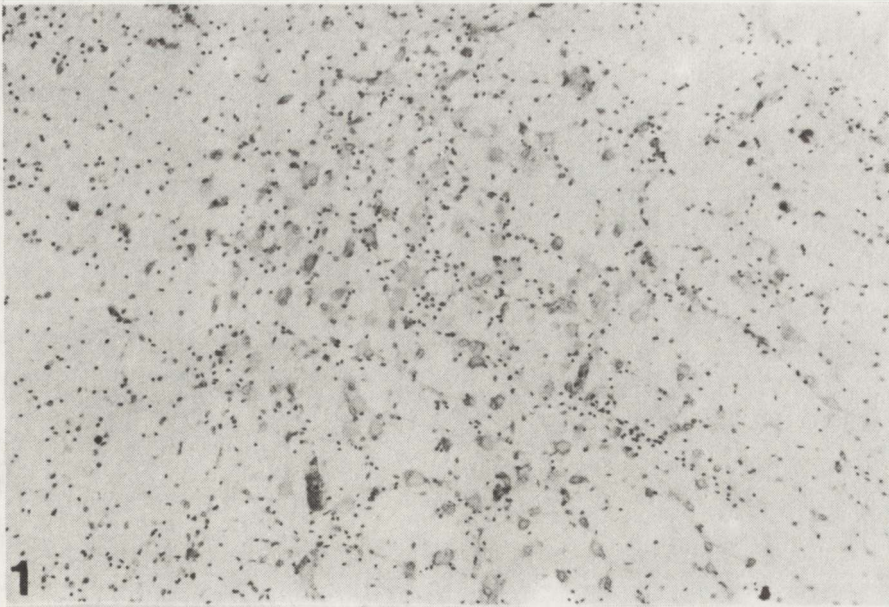


Fig. 1. Atypical cells in the hemispheric white matter. Cresyl violet. x 60

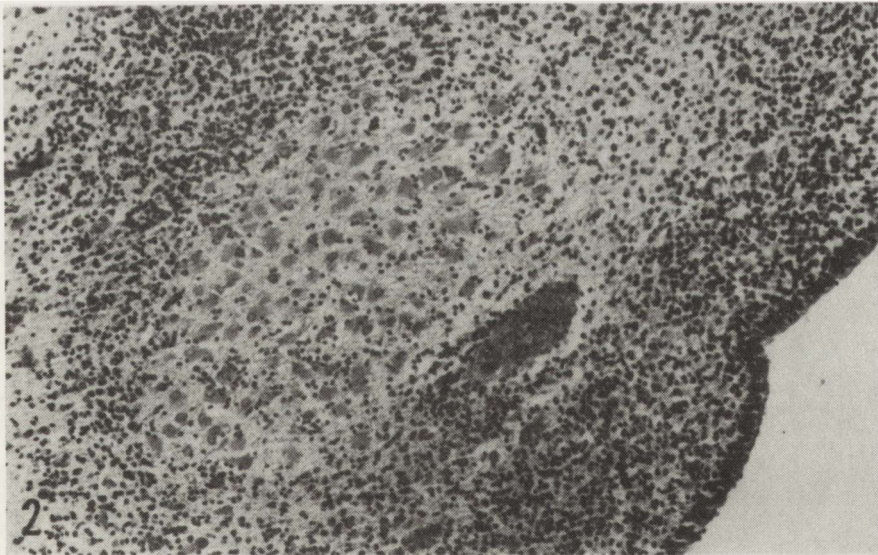


Fig. 2. Aggregation of giant cells in periventricular matrix center. HE. x 60

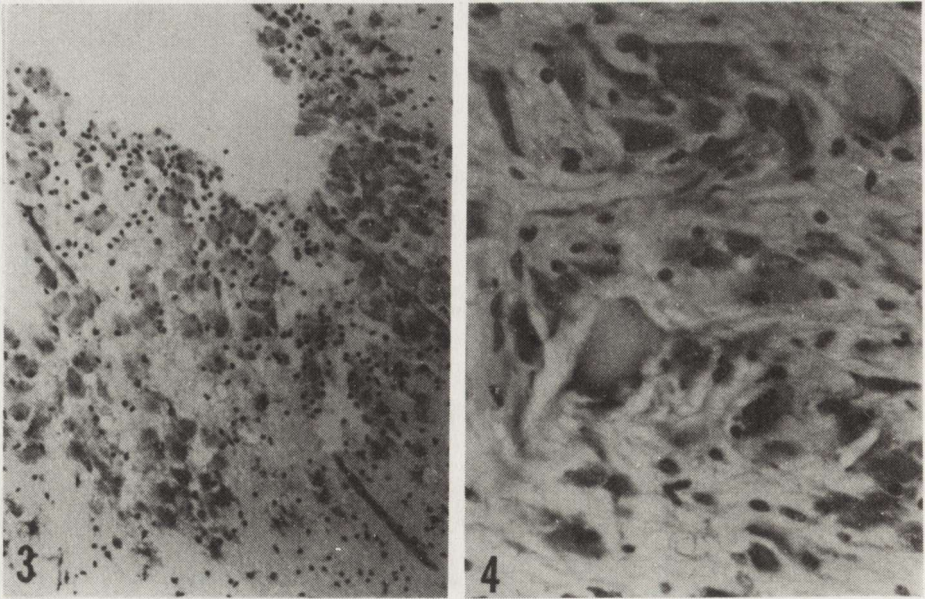


Fig. 3. Subpial nodule of atypical cells. Cresyl violet. x 100

Fig. 4. Giant cell astrocytoma in cerebellar white matter. HE. x 200

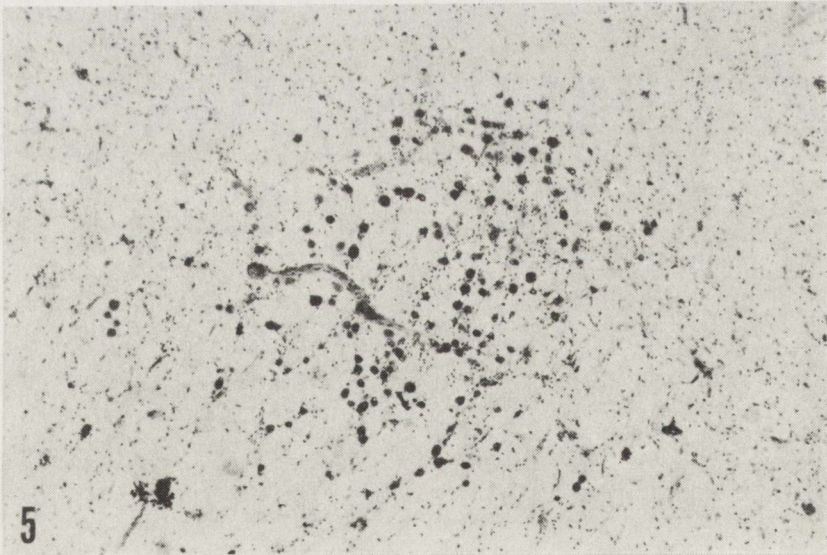


Fig. 5. GFAP-positive atypical giant cells in the white matter (parallel to Fig. 1). x 60

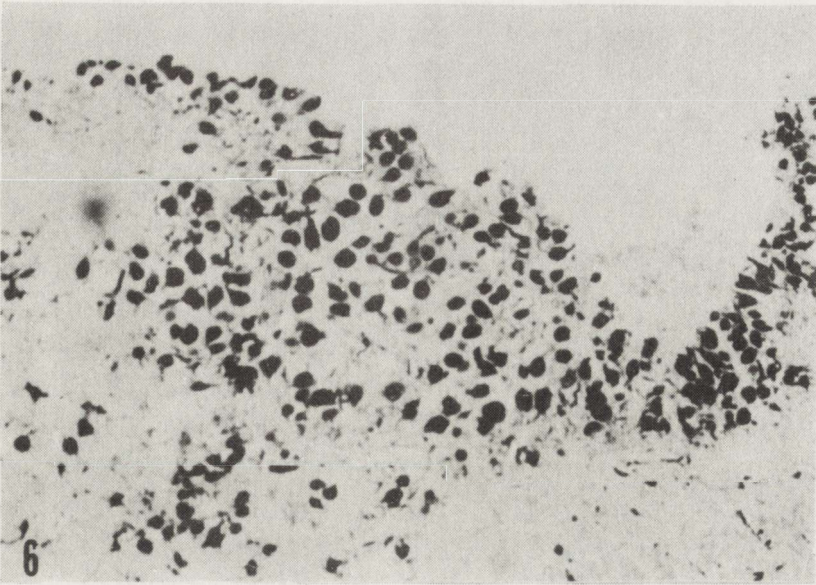


Fig. 6. GFAP-positive subpial atypical cells (parallel to Fig. 3). x 100

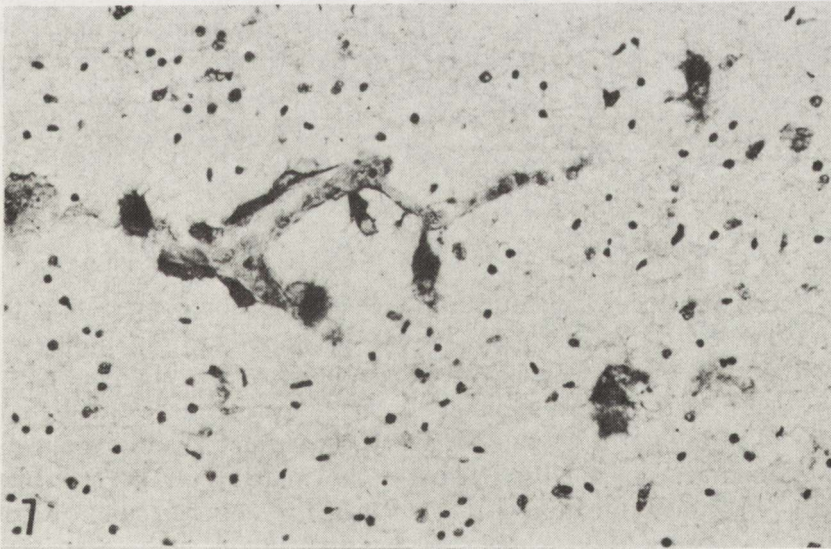


Fig. 7. GFAP-positive perivascular cells. x 200

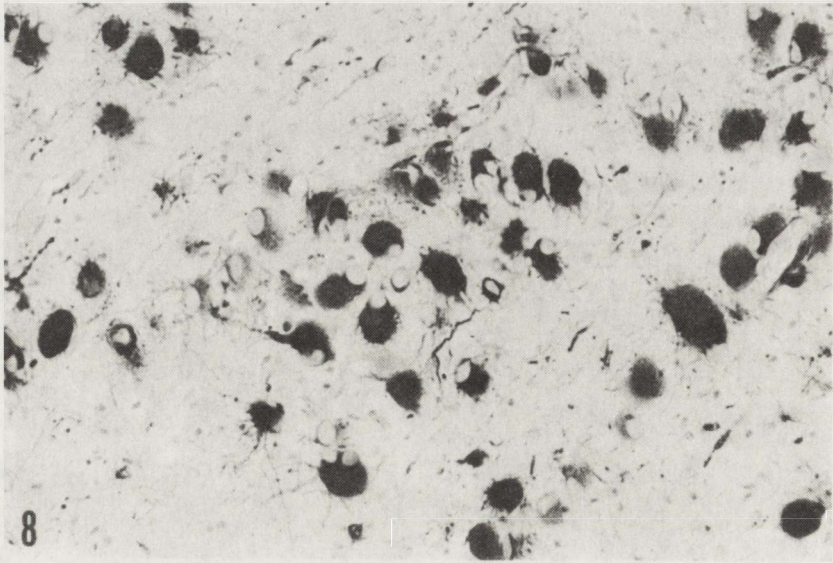


Fig. 8. GFAP-positive uneven staining in giant cells in the white matter. x 200

aggregates they were intensively but unevenly stained (Figs 7, 8). The cells with most intensive reaction were comparable to normal astrocytes. The cells forming the cerebellar tumor were also unevenly positive, but generally the tumor exhibited an intensive reaction for GFAP. The NSE reaction was positive, but rather weak in neuronal cells and it was not visible in dysplastic cells. The RCA reaction showed an abundant network of small blood vessels which was more dense in the nests of giant cells. The dysontogenic tumor in the cerebellum appeared as richly vascularized. The other elements exhibiting this reaction — microglial cells — were randomly disseminated in the nervous tissue, but greater accumulations were observed around the aggregates of giant cells.

Control procedures included replacement of primary antibodies by appropriate preimmunized serum

DISCUSSION

In our newborn delivered after 27 weeks of gestation congenital pathology was not suspected clinically and TS was diagnosed neuropathologically.

Cardiac rhabdomyoma was detected at autopsy as the first pathologic finding. This tumor is most common among otherwise rare cardiac tumors in infants (Platt et al. 1987). The occurrence of cardiac rhabdomyomata in TS cases is estimated as 5–50% (Marritt 1983; Platt et al. 1987). This great discrepancy in the estimations is related to the age of the examined patients. Cardiac rhabdomyomata often diagnosed in small infants with TS are the cause of their premature death (Thibault, Manuelidis 1970; Probst, Ohnacker 1977).

It was found in all the cases of prematurely born babies with TS (Chou, Chou 1989).

The macroscopic appearance of the central nervous system in our case did not present abnormalities. The subpial "nodules" did not reach the dimension visible on the external surface of the cortical mantle. The presence of giant atypical cells in those nodules, in aggregates, disseminated in the brain hemispheres and cerebellum allowed to diagnose the Bourneville disease.

The microscopic appearance of our case, although similar to that described in other newborn (Thibault, Manuelidis 1970; Probst, Ohnacker 1977; Sharp, Robertson 1983; Chou, Chou 1989) supplemented by immunohistochemical reactions enables to point out some special features of the youngest so far reported premature infant with TS.

GFAP was in our case positive in the majority of atypical cells, but the uneven intensity of this reaction demonstrated various levels of their differentiation. Numerous foci of giant cells of the astrocytic line were observed in matrix centers around the lateral ventricles. They were evidently less intensively stained similarly as in the case of Chou and Chou (1989). These observations confirmed that several cells in the matrix centers already display features of dysontogenesis. Notwithstanding at which level of abnormal differentiation they migrate, the GFAP reaction shows their maturation along the pathway of migration. The neuronal origin of some giant cells suggested by other authors (Arsenio et al. 1972; Stefansson, Wolfmann 1981) was not confirmed by the NSE reaction in our study. The RCA reaction was very intensive. We were able to observe rich vascularization of pathologic aggregates, particularly the dysontogenic tumor. The tumor resembled that of subependymal giant cell astrocytoma which is localized in TS cases most frequently in the anterior part of the lateral ventricle (Donegani et al. 1972). Other localizations were also described but that observed in our case seems to be rather unusual.

More frequent findings of TS in premature babies during the last twenty years suggest, that this rare disease could be encountered owing to neuropathological examination of this age group.

STWARDNIENIE GUZOWATE U NOWORODKA-WCZEŚNIAKA. BADANIE MORFOLOGICZNE I IMMUNOHISTOCHEMICZNE

Streszczenie

Noworodek-wcześniejak urodzony w 27 tygodniu życia płodowego jest najmłodszym wśród dotąd opisanych przypadków stwardnienia guzowatego. Znalaziono u niego *rabdomyoma* mięśnia sercowego. W mózgu stwierdzono olbrzymie nietypowe komórki w większości GFAP-dodatnie, zlokalizowane w okołokomorowych gniazdach macierzy, rozsiane lub w skupiskach w istocie białej oraz w podołonowych guzkach. W mózdku napotkano ognisko o typie gwiaździaka olbrzymiokomórkowego. Stwierdzone zmiany potwierdzają dane o dysontogenetycznym różnicowaniu komórek w ogniskach macierzy i o dojrzewaniu nietypowych komórek wzdłuż dróg migracji.

REFERENCES

1. Arsenio C, Alexianu M, Horvat L, Alexianu D, Petrovivi AL: Fine structure of atypical cells in tuberous sclerosis. *Acta Neuropathol (Berl)*, 1972, 21, 185-193.
2. Boremann S, Dykmans J, van Bogaert L: Etudes cliniques, genealogiques et histopathologiques sur les formes heredofamiliales de la sclerose tubereuse. *J Neurol (Brussels)*, 1933, 33, 713-746.
3. Chou TM, Chou SM: Tuberous sclerosis in the premature infant: a report of a case with immunohistochemistry on the CNS. *Clin Neuropathol*, 1989, 8, 45-52.
4. Denegani G, Grattarole FR, Wildi E: Tuberous sclerosis. In: *Handbook of clinical neurology*. Eds: PJ Vinken, GW Bruyn. Elsevier, New York, 1972, 14, 340-389.
5. Hsu SM, Raine L, Fanger H: The use of avidin-biotin complex (ABC) in immunoperoxidase technique. *J Histochem Cytochem*, 1982, 29, 577-580.
6. Huttenlocher PR, Heydemann PT: Fine structure of cortical tubers in tuberous sclerosis: A Golgi Study. *Ann Neurol*, 1984, 16, 595-602.
7. Merrit HH: *Textbook of neurology*, 3rd edition. Lee and Febigen, Philadelphia, 1983, p 444.
8. Nardell E, De Benedictis G, La Stilla G, Nicolardi G: Tuberous sclerosis: a neuropathological and immunohistochemical (PAP) study. *Clin Neuropathol*, 1986, 5, 261-266.
9. Platt LD, Devore GR, Horestein J, Pavlova Z, Kovacs B, Falk RE: Prenatal diagnosis of tuberous sclerosis: the use of fetal echocardiography. *Prenat Diagn*, 1987, 7, 407-411.
10. Poivier J, Escourelle R: Etude ultrastructurelle d'une tumeur cerebrale dans un cas de sclerose tubereuse de Bourneville. VI Congress Internationale de Neuropathologie, Mason, Paris, 1970.
11. Probst E, Ohnacker H: Sclerose tubereuse de Bourneville chez un premature. *Acta Neuropathol (Berl)*, 1977, 40, 157-161.
12. Ribadeau-Dumas JL, Poivier J, Escourelle R: Etude ultrastructurelle des lesions cerebrales de la sclerose tubereuse de Bourneville. *Acta Neuropathol (Berl)*, 1973, 25, 259-270.
13. Stefansson K, Wollmann R: Distribution of the neuronal specific protein 14-3-2 in central nervous system lesions of tuberous sclerosis. *Acta Neuropathol (Berl)*, 53, 113-117.
14. Sharp D, Robertson DM: Tuberous sclerosis in an infant of 27 weeks of gestation age. *Can J Neurol Sci*, 1983, 10, 59-62.
15. Thibault HJ, Manuelidis EE: Tuberous sclerosis in a premature infants. Report of a case and review of the literature. *Neurology*, 1970, 20, 139-146.
16. Wilkinson M, Hume R, Strange R, Bell JE: Glial and neuronal differentiation in the human fetal brain 9-23 weeks of gestation. *Neuropathol Appl Neurobiol*, 1990, 16, 193-204.
17. Wiśniewska KE, Maślińska D: Lectin histochemistry in brains with juvenile form of neuronal ceroid lipofuscinosis (Batten disease). *Acta Neuropathol (Berl)*, 1990, 80, 274-279.

Authors' address: Laboratory of Developmental Neuropathology, Medical Research Centre, Polish Academy of Sciences, 3 Pasteura Str, 02-093 Warsaw, Poland.

HALINA KROH, EDMUND RUZIKOWSKI

MULTIPLE SCHWANNOMAS OF *CAUDA EQUINA*
IN THE COURSE OF PERIPHERAL SCHWANNOMAS.
CASE REPORT

Department of Neuropathology, Medical Research Centre, Polish Academy of Sciences, Warsaw
and Department of Neurosurgery, School of Medicine, Warsaw

A case of a 60-year-old woman, who developed three schwannomas of *cauda equina* and in the past suffered of retroperitoneal neurinoma and maxillary neurinoma is reported. The discussion concerns the pure form of multiple schwannomas or their participation in von Recklinghausen disease.

Key words: *Schwannomas, multiple schwannomas.*

Description of clinical features and histology of multiple schwannomas of the cranial nerves, spinal roots and peripheral nerves is usually included in the chapters on neurofibromatosis on the ground of the rarity of multiple schwannomas in pure form without association with von Recklinghausen disease. The tumors in the case presented below seem to represent such a group of schwannomas.

CASE REPORT

A 60-year-old female was hospitalized in the Neurosurgical Department (transferred from Neurology) with chief complaint of pain in her legs spreading into the groin during rest and enhanced during walking. For 10 months she suffered of gradually progressing pins and needles sensation in the gluteo-femoral area and weakness of her left leg. The papers on her discharge from other hospitals informed that 14 years ago she had been operated due to a retroperitoneal tumor localized in the hypogastric area and 11 years ago due to the only partly excized tumor of the right maxilla. Both neoplasms were diagnosed histologically as neurinomas.

Myelography with Amipaque (performed in Department of Neurology) showed a block of contrast with round smooth outlines at the level of the lower

margin of L_1 up to the upper margin of L_4 (Figs 1 a, b). CSF examination: proteins 285 mg%, cytosis 3/1 mm^3 .

On admission there was slight motor weakness and hypesthesia of the lower left extremity, decreased pyramidal reflexes, limitation of lumbar motor function, pain, Lasseque bilateral positive.

There were neither cafe-au-lait spots, subcutaneous nodules nor other manifestations of von Recklinghausen disease.

Operation: Laminectomy L_2 - L_4 disclosed three subdural tumors adhering to the spinal roots, located dorsally and covered with arachnoidea. They were located one above the other, their cross diameter was 1 cm, longitudinal 3-, 1- and 1 cm, respectively. They were bluish, partly cystic. Two upper tumors were successfully removed, the remnants of the capsule of the third tumor, ingrown

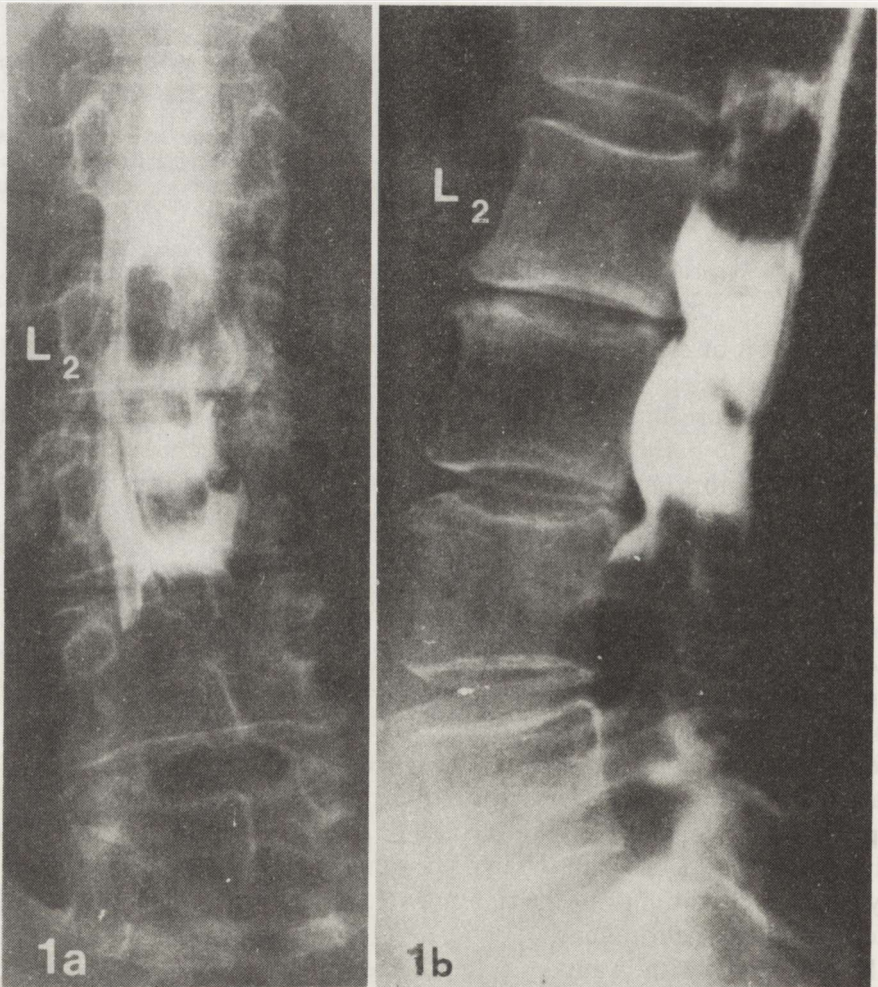


Fig. 1. Myelography with Amipaque. At the L_2 - L_4 level uneven outline of contrast and negative spots in position AP (a) and L (b)

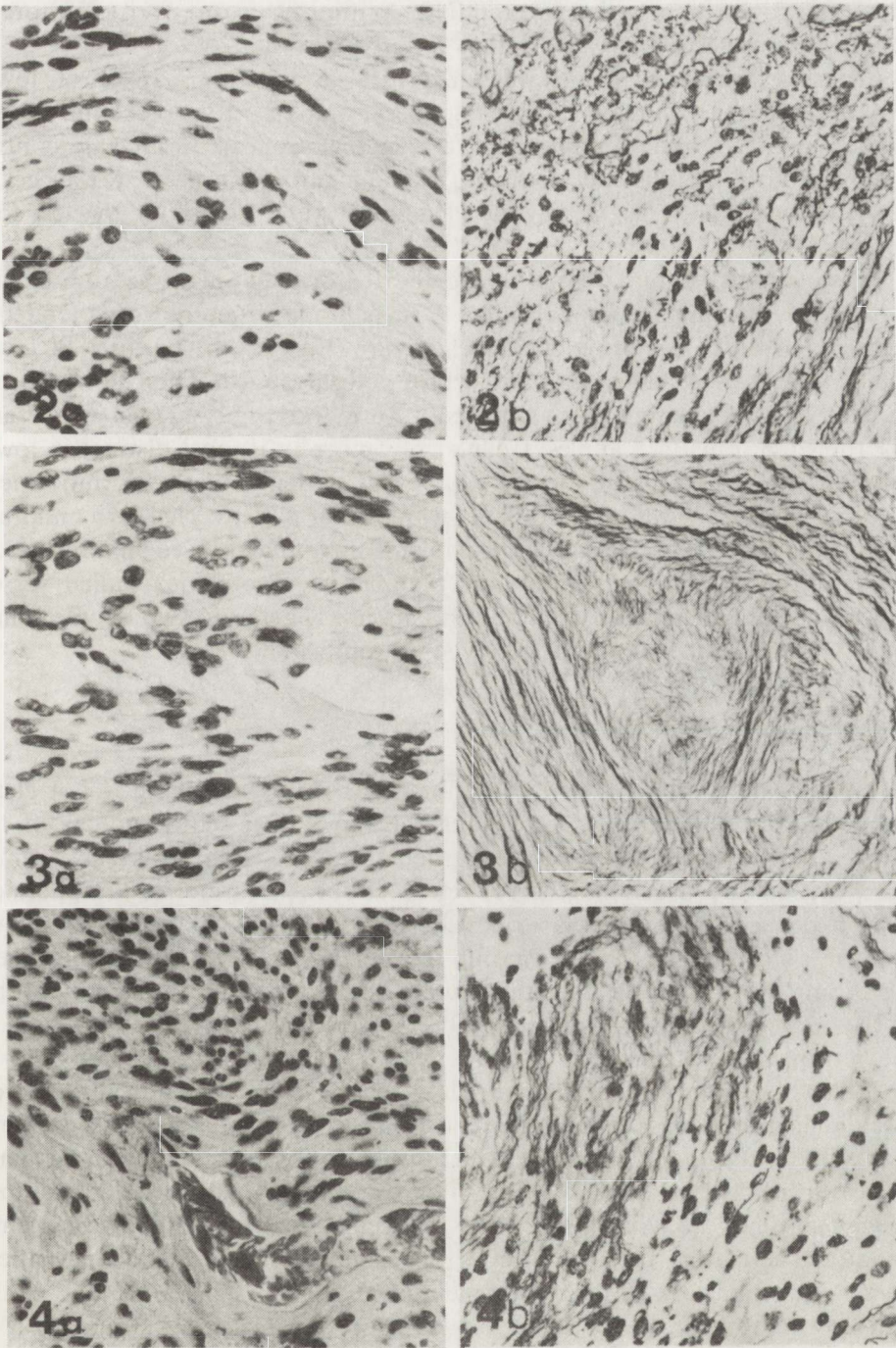


Fig. 2. Schwannoma Antoni B. *a* – loose palisade structure. HE. *b* – argyrophilic fibers. Gomori. x 100

Fig. 3. Schwannoma Antoni B. *a* – disturbed pattern. HE. *b* – area of well arranged argyrophilic fibers. Gomori. x 100

Fig. 4. Schwannoma Antoni A+B. *a* – pleomorphic area, varying density. HE. *b* – argyrophilic fibers reticular pattern. Gomori. x 100

into the root had to be left *in situ*. The continuity of one root was totally interrupted, other roots were slightly injured.

The postoperative period was uneventful except paraparesis of lower extremities for the short time following operation. After five weeks the patient walked unaided, the numbness of the legs disappeared. During control examination 18 months later there was a nodule noticed at the flexor aspect of the left forearm, 1.5 cm in diameter. Numbness and paresis of the left foot persisted.

Histological examination: Microscopic features of all three tumors are similar. The two upper tumors display loose palisade structure with a tendency to form foci and areas of reticular architecture (Figs 2 a, b, 3 a, b). The lower tumor is densely cellular but its structure is disarranged. The cell nuclei are elongated, with tapering or oval poles, have marked nuclear membrane and disordered chromatin granules. Cellular pleomorphism is most distinct in lower tumor (Figs 4 a, b). All the tumors reveal a dense mesh of thin wavy argyrophilic fibers, spread in accordance with cellular pattern. There is a multitude of thin-walled blood vessels of large diameter surrounded by edematous tissue. The lower tumor presents additionally numerous small thick-walled vessels which form conglomerates. Mitotic figures absent. Diagnosis: Two schwannomas type Antoni B, one schwannoma type Antoni A+B.

DISCUSSION

Classification of the group of tumors in the presented case is not clear. Numerous neoplasms to which belong the intraspinal schwannomas of the spinal roots, neurinoma removed earlier from the area served by ramus maxillaris of the trigeminal nerve, retroperitoneal neurinoma (autonomic?) from hypogastrium and the last one, not yet excized subcutaneous nodule on forearm, may belong to the group of tumors of von Recklinghausen. According to their localization they might be classed to the transitional form of the disease (Russel, Rubinstein 1989). We could not determine the origin of the retroperitoneal tumor.

Lately the rigorous opinions prevail as regards clinical qualification of von Recklinghausen disease. The patient must display at least a triad of symptoms like: numerous cafe-au-lait spots, numerous neurofibromas, Lisch hamartomas (Riccardi 1981; Flüeler, Bolthausen 1986) and many additional conditions including axillary freckling, CNS tumors, congenital bone deformities, intellectual handicap, hereditary changes (McCarroll 1950; Seizinger 1987). Our patient does not present any of the above mentioned clinical signs and none of the removed tumors has been diagnosed as neurofibroma.

It has been accepted that multiple schwannomas are the feature of neurofibromatosis (Minckler 1971), whereas multiple schwannomas of spinal roots are characteristic for the central form of von Recklinghausen disease (Russel, Rubinstein 1989). About 50% of cases of multiple spinal tumors are

associated with neurofibromatosis but multiple spinal schwannomas without clinical signs of the disease are not frequent and the number of published cases is about forty (Nishii et al. 1989). Even less frequent are neurinomas of maxilla and the papers concerned with schwannomas of peripheral branches of the trigeminal nerve are also scarce (David et al. 1978; Lesoin et al. 1986).

It should be stressed that in the presented case the tumors in various locations occurred every few years/between the first and the third operation 14 years elapsed/whereas in the neurofibromatosis the complex of tumors appears simultaneously and usually an earlier age.

MNOGIE NERWIAKI OGONA KOŃSKIEGO W PRZEBIEGU NERWIAKÓW NERWÓW OBWODOWYCH. OPIS PRZYPADKU

Streszczenie

Przedstawiono przypadek 60-letniej kobiety, której usunięto 3 nerwiaki ogona końskiego, a w przeszłości nerwiak pozaotrzewnowy i nerwiak szczęki górnej. Omówiono występowanie mnogich nerwiaków w postaci "czystej" i w związku z chorobą Recklinghausena.

REFERENCES

1. David DJ, Speculand B, Vernon-Roberts B, Sach RP: Malignant schwannoma of the inferior dental nerve. *Br J Plast Surg*, 1978, 31, 323-333.
2. Flüeler U, Bolthausen E: Iris hamartomata as diagnostic criterion in neurofibromatosis. *Neuropediatrics*, 1986, 183-185.
3. Lesoin F, Rousseaux M, Vilette L, Autrique A, Dhellemmes P, Pellerin P, Vaneecloo JM, Leys D, Jomin M: Neurinomas of the trigeminal nerve. *Acta Neurochir (Wien)* 1986, 82, 118-122.
4. McCarroll HR: Clinical manifestations of congenital neurofibromatosis. *J Bone Joint Surg (Am)*, 1950, 3, 601-617.
5. Minckler D: Pathology of the nervous system. Mc Graw Hill Co, 1971, vol 2, pp 2093-2112.
6. Nishii S, Hanakita J, Suwa H, Ohta F, Sakaida H: Multiple spinal neurinomas without von Recklinghausen's disease: report of three cases. *Neurol Surg (Jap)* 1989, 17, 953-957.
7. Riccardi VM: Von Recklinghausen neurofibromatosis. *New Engl J Med*, 1981, 305, 1617-1627.
8. Russel DS, Rubinstein LJ: Pathology of tumours of the nervous system. V edition, Arnold, London, Melbourne, Auckland, 1989, pp 770-775.
9. Seizinger B.: Genetic linkage of von Recklinghausen neurofibromatosis to the nerve growth factor receptor gene. *Cell*, 1987, 49, 589-594.

Author's address: Department of Neuropathology, Medical Research Centre, Polish Academy of Sciences, 3 Dworkowa Str. 00-784 Warsaw, Poland.

BARBARA GAJKOWSKA¹, DANUTA MARKIEWICZ², MARIA KOBUSZEWSKA-FARYNA²

ULTRASTRUCTURE OF HYPOTHALAMO-HYPOPHYSEAL SYSTEM OF A RAT WITH MORRIS HEPATOMA 7777 AFTER TREATMENT WITH FARMORUBICIN

¹Laboratory of Ultrastructure of the Nervous System, Medical Research Centre, Polish Academy of Sciences, Warsaw, ²Department of Pathomorphological Diagnostics, Medical Centre of Postgraduate Education, Warsaw

The effect of farmorubicin on the ultrastructure of hypothalamo-hypophyseal system of normal rat and after subcutaneous implantation of Morris hepatoma 7777 was studied. Ultrastructural changes found in some neurons of the supraoptic and paraventricular nuclei and axon terminals in hypophyseal neural lobe may indicate a decrease of synthesis and release of neurosecretory material after treatment with farmorubicin.

Key words: *Hypothalamo-hypophyseal system, farmorubicin, Morris hepatoma 7777.*

The nervous, endocrine and immunological systems play a fundamental role in the maintenance of the homeostasis of the organism. Thus, they affect processes of prophylaxis and recovery, since every disease is a disorder of internal homeostasis of the organism. The hypothalamo-hypophyseal system constitutes an anatomic structure, where exchange of information takes place and regulation of interrelations between the nervous and endocrine system, and as it has been recently suggested, between the cells of the immune system (Cross 1980; Bulloch, Pomerantz 1984; Bigotte, Olsson 1988).

Hypothalamus belongs to the few regions of the central nervous system which lack the blood-brain barrier. Transport of the substances from the blood to the surrounding nervous tissue in these regions takes place on the basis of the difference in concentration gradients.

This fact gains importance due to the growing administration of cytostatic drugs in the treatment of cancer. The blood-brain barrier in relation to many of these drugs is an effective preventive zone for the nervous tissue, but in the regions lacking this barrier the drugs permeate the brain. It seemed justified to undertake experimental studies on the effect of farmorubicin on the hypothalamo-hypophyseal system in normal animals in various stages of their development and investigate the hypothalamo-hypophyseal system of rat with

implanted Morris hepatoma 7777 following treatment with farmorubicin. Farmorubicin was administrated in doses comparable to those used in chemotherapy of malignant tumors.

MATERIAL AND METHODS

The experiment was conducted in two experimental groups:

Group I. Buffalo rats 14-day-old (5 animals) and 56-day-old (5 rats) were given a farmorubicin solution intraperitoneally, in doses of 5 mg/kg b.w. and 10 mg/kg s.w. respectively, in a series of 3 injections, at 1-week intervals. Control rats of the same age (3 rats in each group) were given an injection of 0.9% NaCl in place of the drug.

Group II. Rats aged 14 days (10 animals) and 56 days (10 rats) were implanted subcutaneously with a suspension of tissue particles of Morris 7777 hepatoma in physiological saline into the dorsal surface of the hind leg (Markiewicz 1986). Following 14 days after the implant they were treated with farmorubicin according to the dose for animals in experimental group I. Control groups consisted of 5 rats corresponding in age to experimental animals, which were given subcutaneous injections of physiological saline solution instead of the suspension of tumor tissue and farmorubicin.

One day after the last farmorubicin or 0.9 NaCl injection the rats were sacrificed by decapitation. Samples for electron microscopic studies were obtained from the supraoptic nucleus (SO) and paraventricular nucleus (PV) and from the neurohypophysis (PN) from experimental and control animals. The material was fixed in 4% glutaraldehyde in 0.2 M cacodylate buffer, pH 7.4 for 1 h, then rinsed in the same buffer for 2 h. Additional postfixation was done in 2% OsO₄ in cacodylate buffer, rinsed overnight, dehydrated in increasing concentrations of alcohol and propylene oxide and embedded in Epon 812. Ultrathin sections were cut on an LKB ultramicrotome Nova, contrasted with uranyl acetate and lead citrate and photographed in a JOEL 1200XB electron microscope.

RESULTS

Experimental group I — rats treated with farmorubicin

Supraoptic and paraventricular nuclei

The reaction of SO and PV in young and adult animals was similar, therefore, the results will be reported jointly.

Administration of farmorubicin caused distinct changes in the ultrastructure of the SO, and less pronounced ones in the PV. Many neurons of SO showed various degrees of cytoplasmic microvacuolization, with the presence of numerous neurosecretory granules and lysosomes (Fig. 1). The nuclei of these

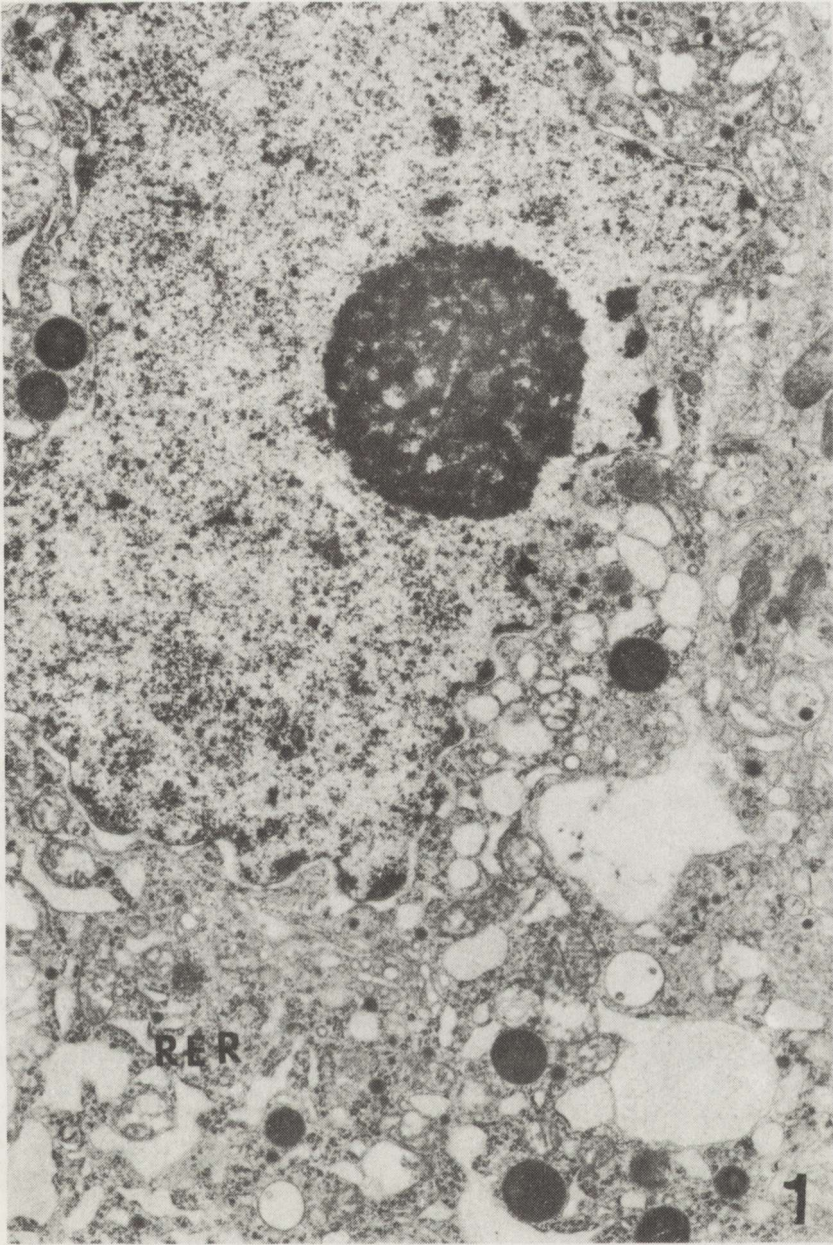


Fig. 1. Group I. SO. Normal cell nucleus with an electron dense nucleolus. In the cytoplasm neurosecretory granules, lysosomes and numerous dilated channels of granular endoplasmic reticulum (RER) forming vacuoles. x 18 000

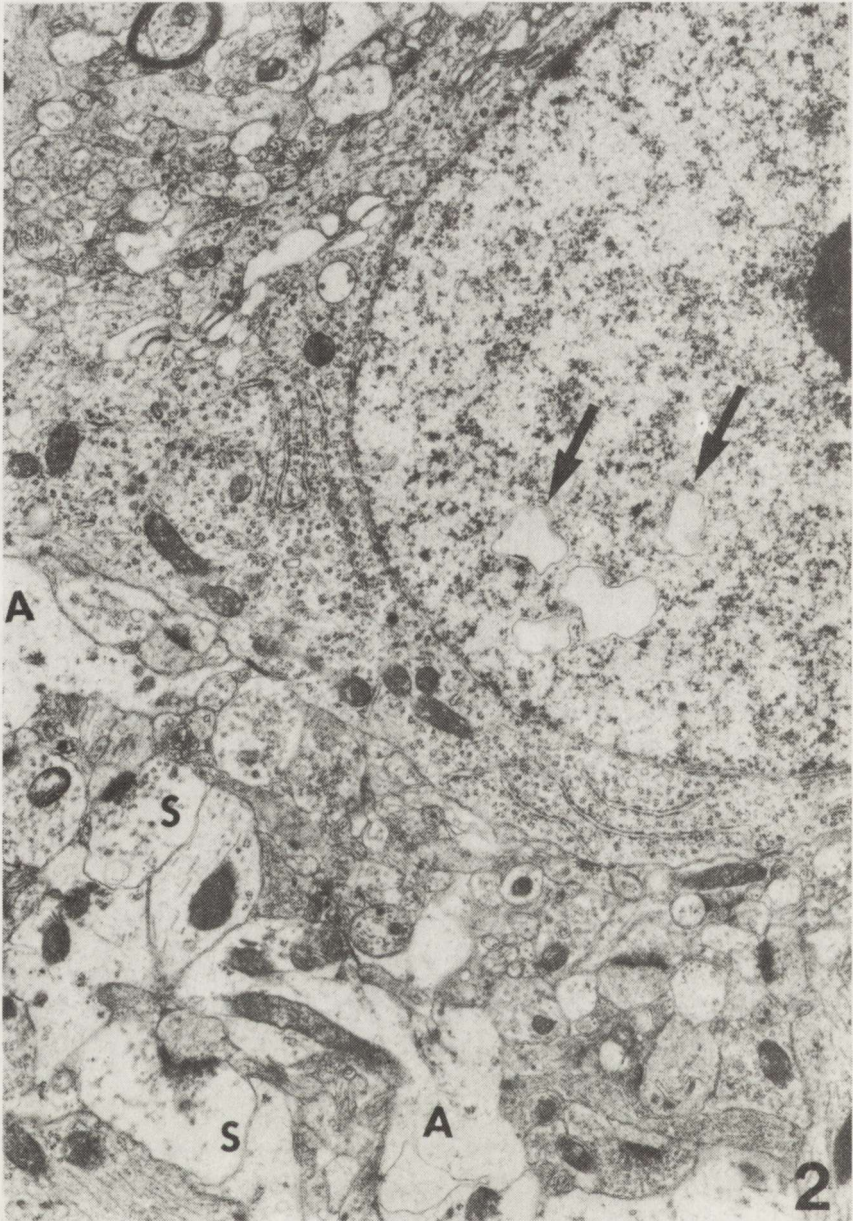


Fig. 2. Group I. SO. Intranuclear, membrane-bound vesicular structures (arrows). Normal cytoplasm. Some swollen synapses (S) and astrocytic processes (A). x 18 000

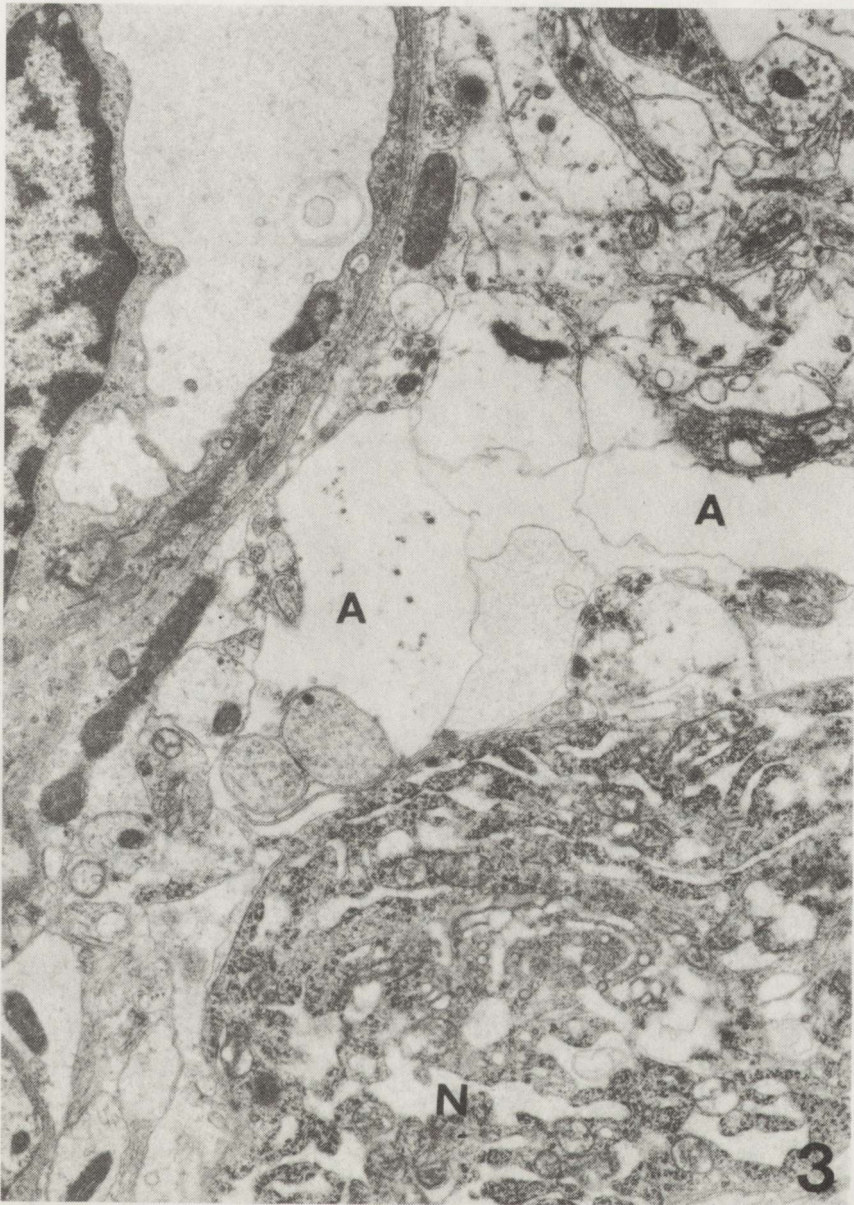


Fig. 3. Group I. SO. Swollen perivascular astrocytic processes (A) and a fragment of shrunken neuron (N). x 18 000

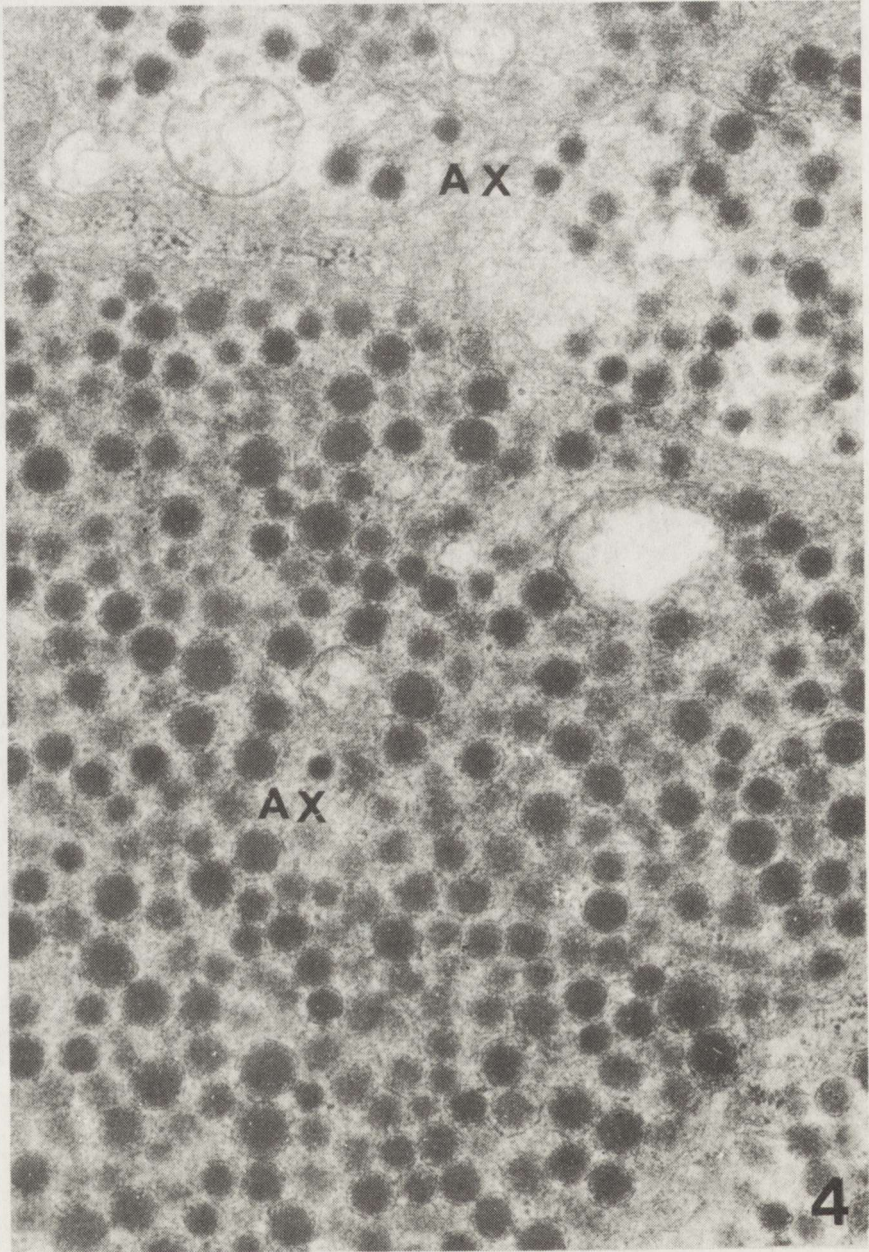


Fig. 4. Group I. Neurohypophysis. Fragments of axons (AX) containing numerous neurosecretory granules. x 36 000

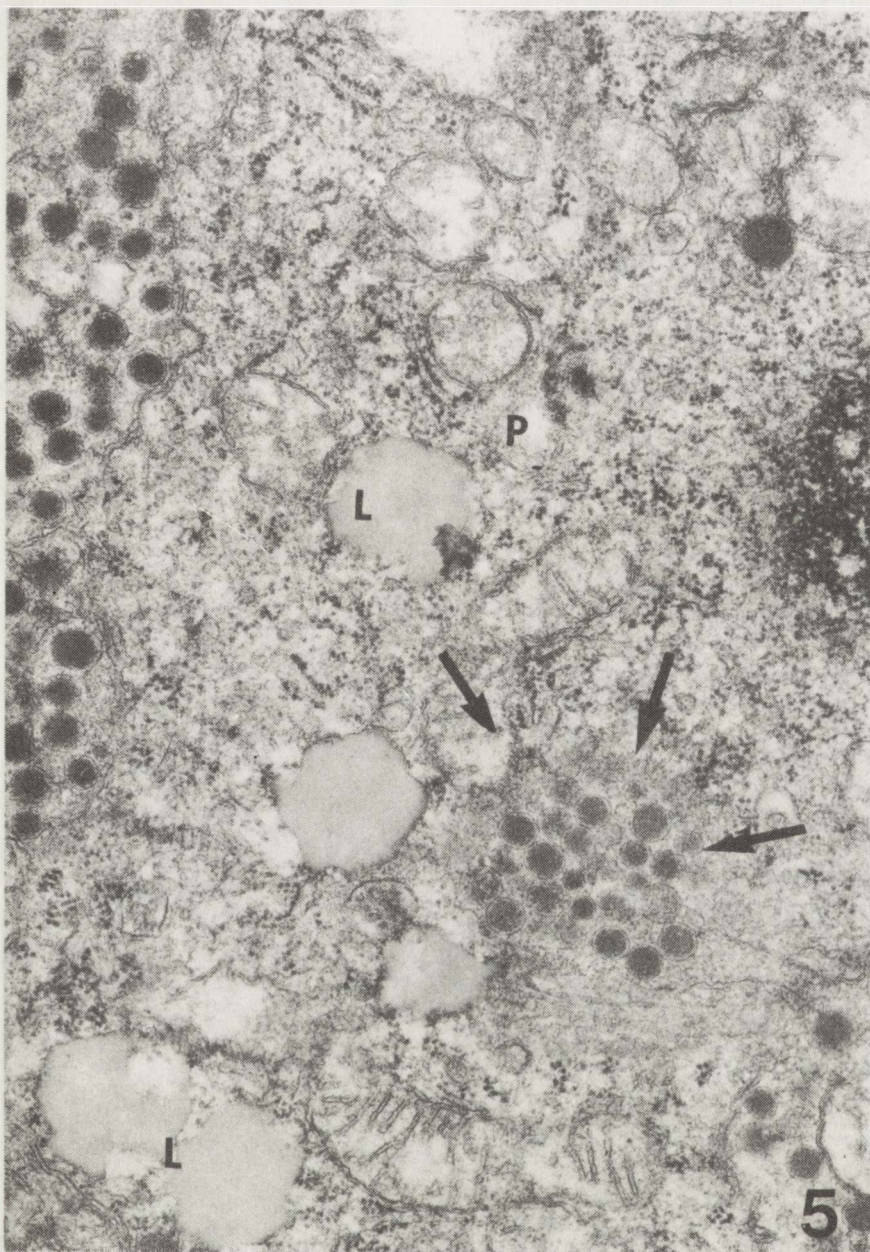


Fig. 5. Group I. Neurohypophysis. Cytoplasm of pituicyte (P) with numerous lipid bodies (L) and a fragment of axon with neurosecretory granules (arrows). x 36 000

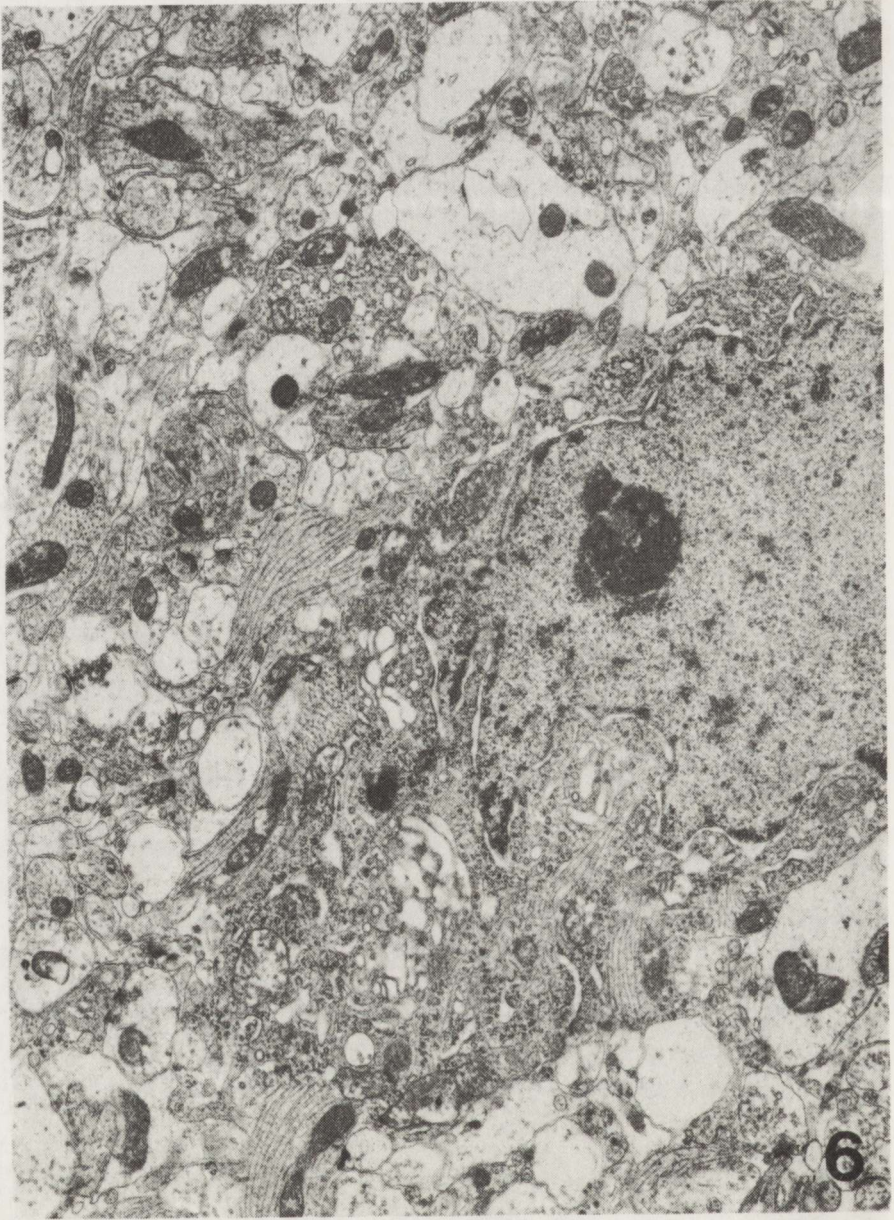


Fig. 6. Group II. SO. Shrunken neuron surrounded by swollen astrocytic processes and synapses.
x 18 000

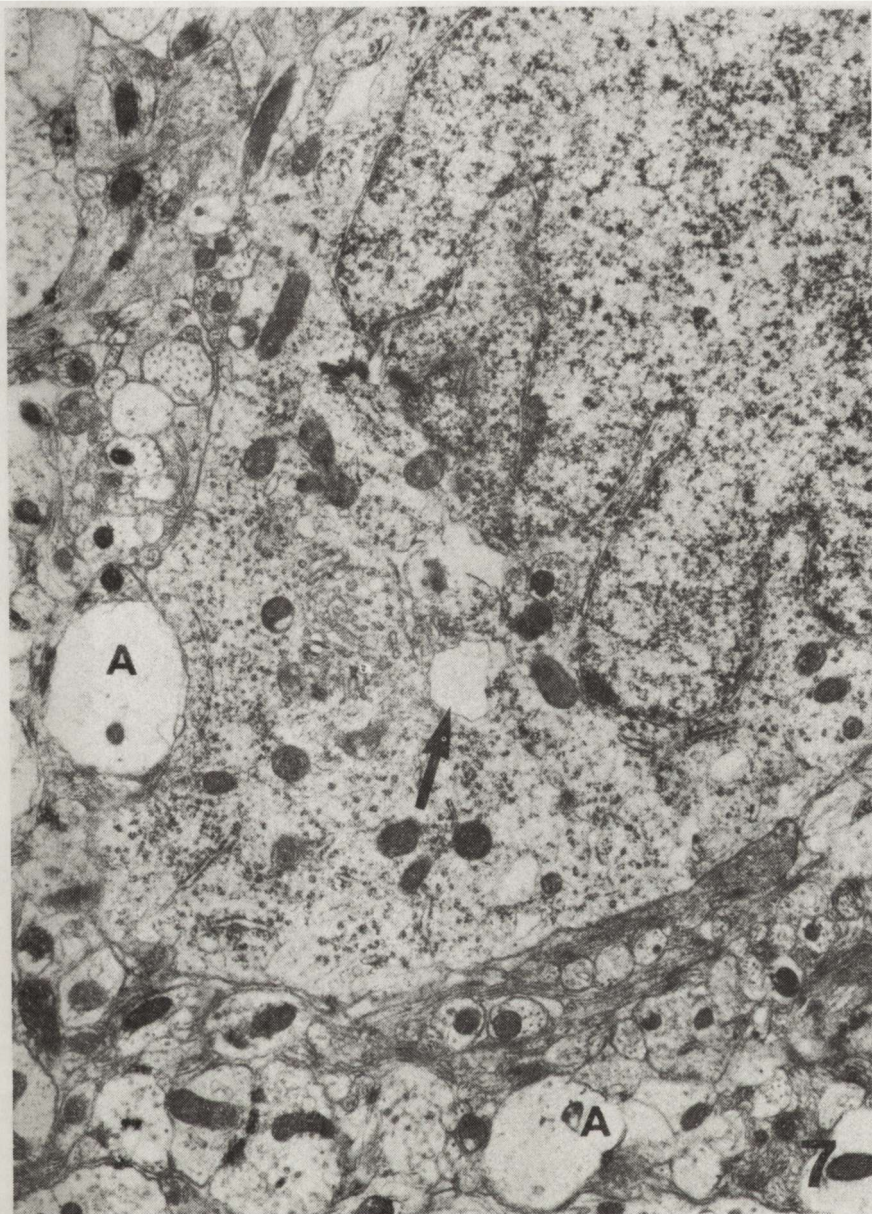


Fig. 7. Group II. PV. Numerous dilated RER channels (arrows) in the cytoplasm. Other organelles are ultrastructurally normal. Note some swollen astrocytic processes (A). x 18 000

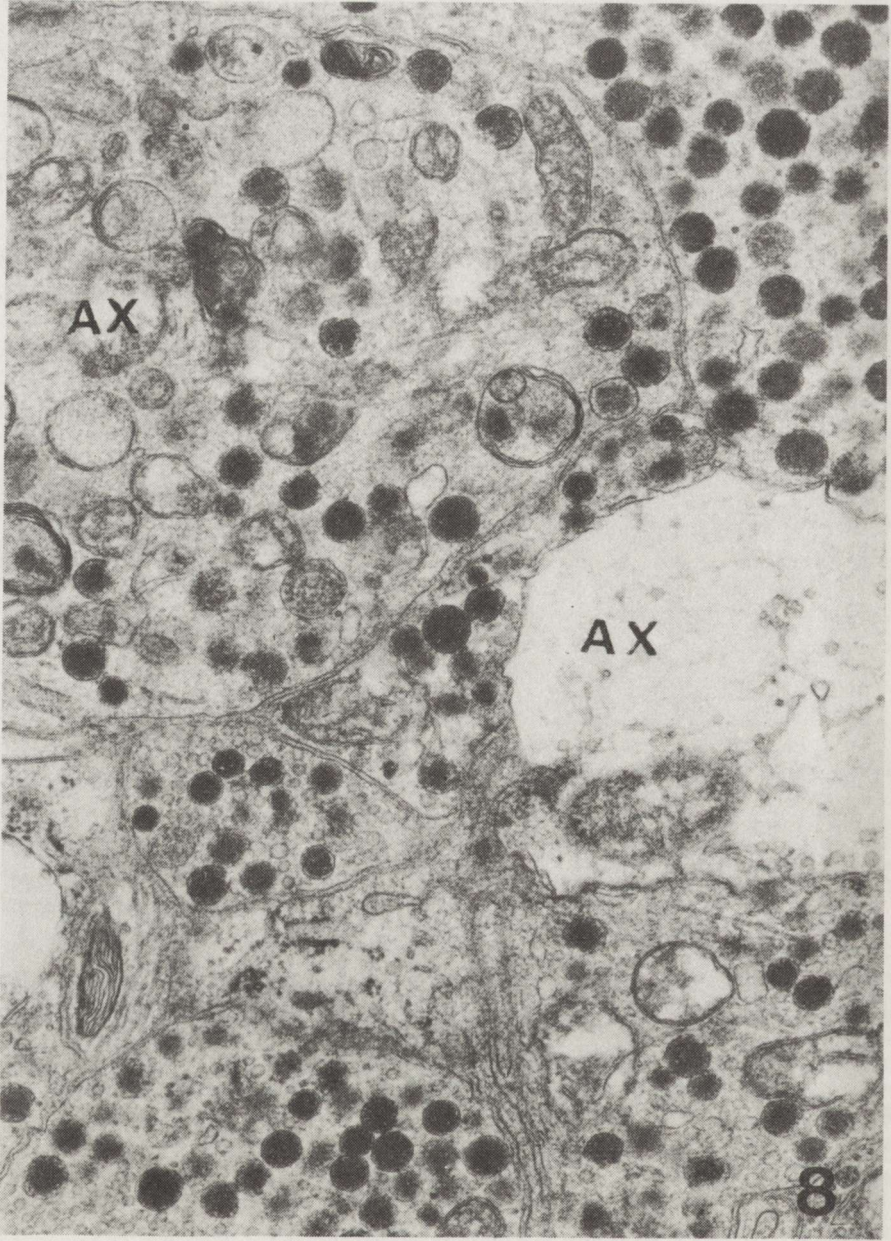


Fig. 8. Group II. Neurohypophysis. Various profiles of axons (AX) with different degrees of degeneration. x 36 000

neurons were usually irregularly shaped, with an electron-dense nucleolus and condensations of nuclear chromatin close to the nuclear envelope. Synapses and glial elements surrounding these neurons showed swelling. The remaining neurons did not display changes in ultrastructure of the cytoplasm. However, some nuclei of these neurons contained electron lucent vacuoles in the karyoplasm (Fig. 2). Synapses around these neurons were generally unchanged, although some were swollen. Around many capillaries massive swelling of astrocytic processes was noted (Fig. 3). Neurons of the PV had lobulated nuclei with deep invaginations, but their ultrastructural appearance was normal. The cytoplasm contained scanty neurosecretory granules. The remaining organelle did not display any differences as compared with controls. Neuropil of the PV did not show any changes besides the presence of single swollen astrocytic processes.

Neurohypophysis

Morphological appearance of the neural part of the hypophysis was similar in young and adult animals. In the majority of the nerve terminals there was a large number of neurosecretory granules, single mitochondria and microvesicles (Fig. 4). Only few axons had scanty neurosecretory granules, many microvesicles and electron-lucent axoplasm. All these nerve processes contained neurotubules. In all the observed nerve endings single mitochondria were swollen. Pituicytes, between the processes, usually appeared ultrastructurally normal. Only some contained more lipid droplets and, very seldom, their cytoplasm contained fragments of neurosecretory processes, which were not membrane bound (Fig. 5).

Experimental group II — rats with Morris hepatoma treated with farmorubicin

Supraoptic and paraventricular nuclei

In the SO among normal nerve cells, characterized ultrastructurally by a small amount of cytoplasmic neurosecretory granules and lobulated nuclei, neurons were found displaying various degrees of injury. They were shrunken or microvacuolated. In the surrounding neuropil numerous swollen synapses (in the presynaptic parts) and swollen astrocyte processes were encountered (Fig. 6). In the PV neurons did not differ significantly from the controls. Shrunken neurons or neurons with microvacuolization have never been observed. However, in many neurons prominent invagination of the nuclear envelope, and numerous electron lucent vacuoles in the cytoplasm were seen. A number of neurosecretory granules was markedly diminished while lysosomes were prominent (Fig. 7).

Neurohypophysis

The morphological appearance of the neurohypophysis in young and adult animals was similar. Among fibers with normal ultrastructure, accumulating a great number of neurosecretory granules, there were fibers with varying degrees of degeneration manifested by the presence of myelin figures, microvesicles, swollen mitochondria and a low number of typical neurosecretory granules. Single fibers were also present lacking neurosecretory granules in their lucent axoplasm with fragmented organelle (Fig. 8). In this experimental group pituicytes often exhibited swollen cytoplasm and an increased number of variously shaped lipid bodies.

DISCUSSION

The results of our studies indicate a diminished activity of the hypothalamo-hypophyseal system in both studied groups, that is in healthy rats following administration of the cytostatic drug – farmorubicin, and in rats with a subcutaneous implantation of Morris hepatoma 7777 treated subsequently with farmorubicin. A comparable intensity of the process of neurosecretion was noted in the hypothalamo-hypophyseal system in young as well as in adult animals.

Analysis of ultrastructural changes in the hypothalamo-hypophyseal system in rats with neoplastic disease, as done in the previous personal studies, showed stimulation of the system (Gajkowska et al. 1988). It could be due to the increased synthesis of the corticotropin releasing factor (CRF). Corticosteroids exert a well known immunosuppressive effect and participate in immunological processes of the organism. In the course of a neoplastic disease the possibility of suppressed immunological reactions should be considered (Ahlqviste 1976; McMillan et al. 1976; Hartwing 1978).

A detailed analysis of the ultrastructural features of the hypothalamo-hypophyseal system in healthy animals subjected to the effect of a cytostatic drug, revealed changes in some neurons of the studied neurosecretory nuclei. Thus, very prominent changes consisting of microvacuolization and shrinkage of the neurons were noted in the SO. On the other hand, the neurons of the PV displayed greater resistance to the effect of the cytostatic drug, however, there were usually morphological features in these neurons indicating diminished neurosecretion. The morphological appearance of the neurohypophysis indicated a decreased excretion to the blood stream of neurosecretory granules accumulating in abundance.

In neuropil of the hypothalamo-hypophyseal system, swollen synapses and swollen glial processes were frequently encountered. Similar changes had been reported in mice, after single intravenous injection of farmorubicin (Bigotte, Olsson 1988). According to these authors the changes reflected a neurotoxic effect of farmorubicin. The pharmacological mechanism of the action of

farmorubicin involves inhibition of nucleic acid synthesis. However, it should be pointed out that the majority of neurons of the PV and many neurons of the SO did not display any ultrastructural changes besides the presence of electron lucent vacuoles in the cytoplasm or karyoplasm, which should be probably related to disorders of water – electrolyte balance caused by farmorubicin.

Personal observations reveal that administration of farmorubicin to animals with implanted Morris hepatoma 7777 also caused a significant decline of neurosecretory activity of the hypothalamo-hypophyseal system. The changes noted were similar in localization and character to those after farmorubicin treatment alone, but more intensive, particularly in the SO. In the neurohypophysis, axons were observed with various degrees of degeneration and many others with normal ultrastructure, although exhibiting a diminished neurosecretion to the blood stream. In the surrounding glia free fragments of neurosecretory granules were found (not membrane bound). According to many authors pituicytes play an important role in regulation of neurosecretory granule secretion from the hypophysis, depending on the requirements of the organism and facilitate elimination of their excess (Dellemann 1973, Tweedle, Hatton 1980; Zaręba-Kowalska et al. 1983; Gajkowska 1985).

To summarize the results of the presented studies, an injurious effect of farmorubicin was noted in the hypothalamo-hypophyseal system of healthy rats and those with neoplastic disease. Morphological evaluation of the SO and PV neurons and their endings in the neurohypophysis indicates alteration and inhibition of the process of neurosecretion.

OBRAZ ULTRASTRUKTURALNY UKŁADU PODWZGÓRZOWO-PRZYSADKOWEGO SZCZURÓW Z WĄTROBIAKIEM MORRISA 7777 PO LECZENIU FARMORUBICYNĄ

Streszczenie

Badano wpływ farmorubicyny na układ podwzgórzowo-przysadkowy u zdrowych szczurów w różnych okresach ich rozwoju, oraz u szczurów z przeszczepem wątrobiaka Morrisa 7777 leczonych farmorubicyną. Analiza zmian ultrastrukturalnych w układzie podwzgórzowo-przysadkowym wykazała uszkodzające działanie farmorubicyny. Obrazy morfologiczne niektórych neuronów jądra nadwzrokowego i jądra przykomorowego oraz zakończeń ich włókien w nerwowej części przysadki wskazywały na upośledzenie i hamowanie procesu neurosekrecji.

REFERENCES

1. Ahlgviste J: Endocrine influence on lymphatic organs, immunoresponses, inflammation and autoimmunity. *Acta Endocrinol*, 1976, suppl 206, 9–136.
2. Bigotte L, Olsson Y: Distribution and toxic effects of the cytostatic epirubicin in the nervous system of the mouse after an intravenous injection. *Clin Neuropathol*, 1988, 7, 4, 148.
3. Bulloch K, Pomerantz W: Autonomic nervous system innervation of thymic – related lymphoid tissue in wild – type and nude mice. *J Comp Neurol*, 1984, 228, 57.
4. Cross R: Hypothalamic-immune interaction. *Brain Res*, 1980, 196, 79.

5. Delleman HG: Degeneration and regeneration of neurosecretory system. *Int Rev Cytol*, 1973, 36, 215-315.
6. Gajkowska B: Komplex Golgiego w stymulowanych neuronach sekrecyjnych podwzgórza szczura. *Neuropatol Pol*, 1985, 23, 445-454.
7. Gajkowska B, Markiewicz D, Kobuszewska-Faryna M: Ultrastructure of hypothalamo-hypophysial system in Buffalo rats after subcutaneous implantation of Morris hepatoma 7777. *Clin Neuropathol*, 1988, 7, 163.
8. Hartwig W: *Endokrynologia kliniczna*. PZWL, Warszawa, 1978.
9. Markiewicz D: Opracowanie modelu doświadczalnego choroby nowotworowej do badań nad uszkadzającym wpływem cytostatyków – Sprawozdanie z I etapu badań CPBR 11.5 cel 106 – 1986.
10. McMillan R, Longmire R, Jelanowsky R: The effect of corticosteroids on human IgG synthesis. *J Immunol*, 1976, 116, 1592-1595.
11. Tweedle CD, Hatton GJ: Evidence for dynamics interaction between pituicytes and neurosecretory axons in the rat. *Neuroscience*, 1980, 5, 661-667.
12. Zaręba-Kowalska A, Renkawk K, Gajkowska B: Ultrastructural study of hypophysial neural lobe of newborn rats in tissue culture. *Cell Tissue Res*, 1983, 230, 463-468.

Author's address: Laboratory of Ultrastructure of the Nervous System, Medical Research Centre, Polish Academy of Sciences, 3 Dworkowa Str, 00-784 Warsaw, Poland.



DANUTA MARKIEWICZ
1934 – 1991

After the long and persistent struggle against the emaciating disease dr Danuta Markiewicz died in Warsaw on 3rd February, 1991.

She was born on 3rd October 1934 in Głębokie, near Lublin. In 1951 she started her university studies in the Faculty of Medical Sciences, Medical Academy in Lublin. She took her MD degree in 1957.

During her studies she revealed an interest in morphological research. In 1953 she took up a job in the Department of Histology and Embryology of the Lublin Medical Academy. After she had graduated in 1957 she started working in the Neurological Department, Lublin Medical Academy under the leadership of Professor W. Stein. A deep interest both in morphological and clinical studies focused her work on the research on the morphological background of the diseases of the central nervous system. In 1962 she was accepted for doctoral studies in the Department of Neuropathology Polish Academy of Sciences, where she started the PhD thesis with Professor Ewa Osetowska. She accomplished it with great dedication, working two days out a week in Warsaw while spending the other four days as a volunteer in the Department of Neurology in Lublin. In 1965 she obtained the PhD degree conferred on her by

the Council of the Medical Faculty, Warsaw Medical Academy for her dissertation entitled: The comparative studies on the advance of atherosclerotic changes in the blood vessels of the basal ganglia in the brain with special emphasis on the globus pallidus. Prof. Ewa Osetowska was conferring her PhD degree.

In 1966 dr Danuta Markiewicz set up the Laboratory of Neuropathology in the Hospital for Nervous and Mental Diseases in Lublin. She was a head of it until 1971.

In 1971 she took over the position of the Assistant Professor in the Department of Neuropathology of the Institute of Psychiatry and Neurology in Warsaw. She was working there for 13 years, to the end of 1984. She was a chief of the Laboratory of Experimental Neuropathology. In the beginning she was working on the neuropathological changes in the mouse brain due to the audiogenic seizures, and then on the toxic influence of alcohol on human nervous system. She contributed also significantly to the ongoing research on the brain tissue transplantation. She participated actively in the studies on the experimental model of Parkinson's disease in rats and on nigrostriatal lesions due to the influence of various factors damaging substantia nigra and consequent restoration of its function by the transplantation of adrenal medullary cells. She took part in clinico-morphological demonstrations that were highly appreciated by the clinicians as a form of permanent training in the field of neuropathology. Her discrimination in the analysis of every case and her expressive presentations made her demonstrations very attractive and highly ranked by the audience.

She was highly educated both in the field of clinical neurology and neuropathology. In 1961 she passed successfully the I^o examination of neurology. In 1968 she became the II^o specialist in neurology and in 1975 – the specialist in neuropathology.

Between 1975 and 1976 she carried out a postgraduate training in the Max-Planck-Institute in Frankfurt-upon-Main with Professor Krücke. She also went through the one month training in the Institute of Neurology in Bucuresti.

Since January, 1985 she was working as a head of the Laboratory of Neuropathology in the Department of Pathomorphological Diagnostics Medical Centre of Postgradual Education in Warsaw. She was there until the end of her life. Her interests covered the neuropathological studies on the nervous tissue obtained from biopsies and autopsies taken in Bielany Hospital. She was also investigating the structural changes in the central nervous system in rats with implanted Morris hepatoma 7777. The prominent result of the studies of dr Markiewicz was the evaluation of the original experimental model of rat neoplastic disease on which she was analyzing the effect of farmorubicin therapy with the reference to the age of the animals. These results used to raise a vivid interest and recognition among the neurologists, neuropathologists, pathologists and pediatric oncologists and they are considered to be the

significant experimental achievement in relation to the oncological clinic of the childhood.

During her entire professional career she was scientifically very active. She demonstrated a scarce enthusiasm and great inquisitiveness together with scrupulosity. Because of these virtues linked to the intimate neuropathological knowledge she enjoyed a great reputation especially in the field of diagnosis of blurred and complicated cases. She took part in numerous domestic and foreign meetings and congresses. She presented 19 papers abroad while 35 were reported in Poland. She published 38 papers in Polish and international journals, one of her papers still being in press.

She was a member of the International Society of Neuropathology. She also belonged to the group of founder-members of the Polish Neuropathological Society.

She was an excellent teacher. Her lectures, conducted in a vivid and lively way, interspersed with the well chosen and accordant slides gained a big and well-earned popularity. She fervently organized postgraduate training in neuropathology for the pathologists, neurologists and neurosurgeons. To the great extent we owe her the popularization of such a type of courses among pathologists, especially those who had not been interested previously in the problems of neuropathology.

The broad-mindedness of dr Danuta Markiewicz in the field of neuropathology was supported and confirmed by her frequent contacts with the patients. Hospital activities and the constant service to the ill people was the trigger that released ideas and helped to set up neuropathological experiments. Consequently, her knowledge about the morphological basis of the nervous system diseases helped her to understand deeply the process of the illness developing in the organism of the particular patient. Therefore she was considered to be an excellent clinician. Warm-hearted and sympathetic relationships with the patients won the faith and gratefulness of numerous of them. This kind of heartnedness to the attendants manifested also itself in the everyday relations with the co-workers. She was brave, veracious, solidary and chummy, always ready to help anybody.

With respect, but also with heavy hearts we bore witness to her long lasting stubborn fight against the disease. She wanted to live not just for herself, but mainly for those near and dear, for the patients and for her research. She probably realized how important and useful her work was to everybody. In spite of the serious disease she could keep the buoyancy, hopefulness and a sense of humor.

We shall treasure her picture in our memories as a wise, brave and a warm-hearted colleague.

Jerzy Dymecki, Maria Kobuszevska-Faryna

Książki i czasopisma Ossolineum można nabywać w placówkach własnych Wydawnictwa:

- 50-106 Wrocław, Rynek 6
- 50-227 Wrocław, ul. Kleczkowska 44 (magazyn hurtowy i sprzedaż wysyłkowa)
- 80-855 Gdańsk, ul. Łągiewniki 56 (książki i muzykalia)
- 70-551 Szczecin, pl. Żołnierza Polskiego 1
- 90-447 Łódź, ul. Piotrkowska 181
- 31-110 Kraków, ul. Św. Jana 28 (sprzedaż detaliczna i hurtowa)
- 61-745 Poznań, Al. Marcinkowskiego 30 (róg 23-go Lutego)

oraz w księgarniach Ośrodka Rozpowszechniania Wydawnictw Naukowych PAN:

- 50-071 Wrocław, pl. Wolności 7, I p.
- 00-901 Warszawa, Pałac Kultury i Nauki
- 31-020 Kraków, ul. Św. Marka 22
- 61-725 Poznań, ul. Mielżyńskiego 27/29
- 40-077 Katowice, ul. Bankowa 14, paw. D, I p.
- 20-031 Lublin, pl. M. Curie-Skłodowskiej 5
- 15-082 Białystok, ul. Nowotki 13
- 90-268 Łódź, ul. Piotrkowska 48

Ponadto sprzedaż edycji ossolińskich prowadzą większe księgarnie naukowe (prywatne), w szczególności:

- 31-042 Kraków, Rynek Główny 4; 00-068 Warszawa, Krakowskie Przedmieście 7;
- 45-015 Opole, Rynek 19/20; 80-244 Gdańsk-Wrzeszcz, Grunwaldzka 111; 40-096 Katowice,
- 3 Maja 12; 31-118 Kraków, Podwale 6; 90-004 Łódź, Piotrkowska 102A; 41-200 Sosnowiec,
- Warszawska 1; 50-138 Wrocław, Kuźniczka 30/33.

Ossolineum zaprasza do współpracy księgarzy, agencje kolporterskie i odbiorców indywidualnych. Oferujemy możliwość zakupu handlowej ilości książek po cenach hurtowych bezpośrednio od Wydawnictwa (Dział Sprzedaży i Eksportu, Rynek 9, 50-106 Wrocław), na następujących warunkach: odbiór następuje własnym transportem lub przesyłką pocztową na koszt odbiorcy, a rozliczenie należności – gotówką lub czekiem potwierdzonym w banku (wpłata bezpośrednio do kasy Wydawnictwa). Przy zakupach na kwotę powyżej 10 milionów istnieje możliwość płatności przelewem, na konto Ossolineum w terminie do 14 dni od chwili otrzymania towaru. Konto: Wielkopolski Bank Kredytowy IV O/Wrocław, 359209-1078.

Zamówienia na prenumeratę czasopism w kraju należy kierować do Centrali Kolportażu Prasy i Wydawnictw, ul. Towarowa 28, 00-598 Warszawa, lub bezpośrednio do Działu Sprzedaży i Eksportu Wydawnictwa, Rynek 9, 50-106 Wrocław.

OSSOLINEUM – YOUR CHEAPEST AND MOST RELIABLE SUPPLIER OF ACADEMIC BOOKS AND PERIODICALS

Ossolineum Publishing House offers a wide spectrum of periodicals, serial publications and books covering various fields of contemporary scientific research.

For orders containing more than 10 titles (copies) a rebate of 15–20% will be granted, by purchase of 50 titles (copies) the rebate will increase to 40%. For booksellers – 50% rebate. Subscriptions – 30% rebate.

No advance payment is required.

The invoice is payable upon receipt. Individual and wholesale orders for books and periodicals published by Ossolineum, should be sent directly to the publishers. Export Department, Rynek 9, 50-106 Wrocław, Poland. Our bank account for foreign currencies: Wielkopolski Bank Kredytowy, IV O/Wrocław – 359209-1078-151-6787.

CONTENTS

A. Sawicka, U.P. Ketelsen: Cytochemistry of muscle Ca^{++} ATPase in muscular dystrophy	119
H. Drac: Morphology of peripheral nerve in some cases of congenital demyelinating polyneuropathy	133
P. P. Liberski, R. Yanagihara, C.J. Gibbs Jr., D.C. Gajdusek: Tubulovesicular structures in experimental Creutzfeldt-Jakob disease and scrapie: a putative virus or a pathological product of the disease	147
A. Taraszewska, I.B. Zelman, A. Szmielew: Development of selective neuronal loss in the rat hippocampus after injection of quinolinic acid. Light- and electron microscopic studies	157
E. Matyja, E. Kida: Effect of magnesium on quinolinic acid-induced damage of hippocampal formation <i>in vitro</i>	171
J. Rafałowska, E. Dolińska, D. Dziewulska, S. Krajewski: Astrocytic reactivity in various stages of human brain infarct in middle and senile age	181
M. Dąbbska, D. Maślińska, T. Majdecki: Premature infant with tuberous sclerosis. Morphological and immunohistochemical study	193
H. Kroh, E. Ruzikowski: Multiple Schwannomas of <i>cauda equina</i> in the course of peripheral schwannomas. Case report	201
B. Gajkowska, <u>D. Markiewicz</u> , M. Kobuszewska-Faryna: Ultrastructure of hypothalamo-hypophyseal system of a rat with Morris hepatoma 7777 after treatment with farmorubicin	207
J. Dymecki, M. Kobuszewska-Faryna: Dr Danuta Markiewicz 1934-1991	221

Indeks 36668

5
Markiewicz z poprzednio